United States
Environmental Protection
Agency

Office of Air Quality
Planning and Standards
Research Triangle Park, NC 27711

EPA-454/B-92-008
October 1992

Air

EPA

USER'S MANUAL FOR THE PLUME VISIBILITY MODEL, PLUVUE II (REVISED)

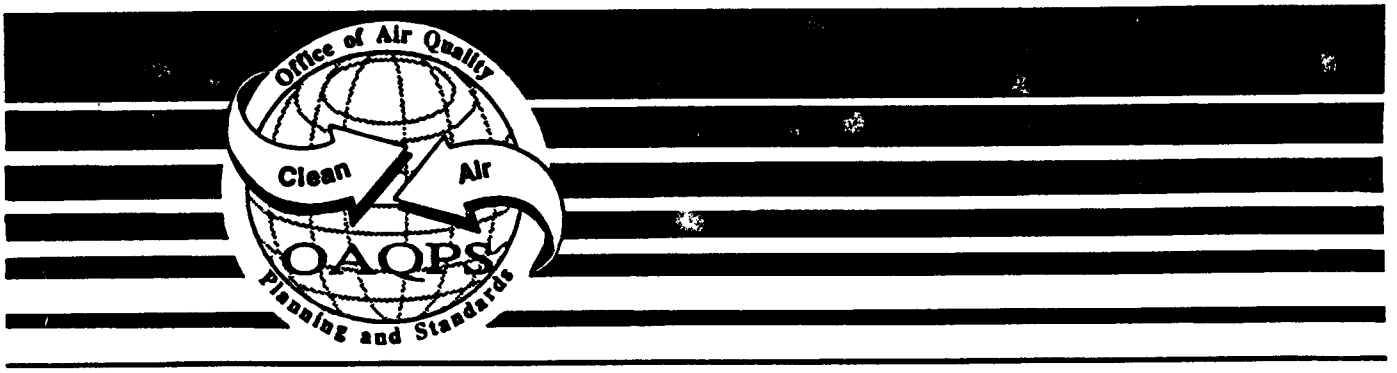

EPA-454/B-92-008

USER'S MANUAL FOR THE PLUME VISIBILITY MODEL, PLUVUE II (REVISED)

Office Of Air Quality Planning And Standards
Office Of Air And Radiation
U. S. Environmental Protection Agency
Research Triangle Park, NC 27711

October 1992

This report has been reviewed by the Office Of Air Quality Planning And Standards, U. S. Environmental Protection Agency, and has been approved for publication. Any mention of trade names or commercial products is not intended to constitute endorsement or recommendation for use.

EPA-454/B-92-008

Table of Contents

Table of Contents (Continued)

List of Tables

List of Figures

1.0 INTRODUCTION

1.1 Overview

Sources of air pollution located near Class I areas such as national parks and wilderness areas are required by the United States Environmental Protection Agency's (EPA) Prevention of Significant Deterioration (PSD) and Visibility regulations to evaluate the impact of their facility on such Class I areas. The *Workbook for Plume Visual Impact Screening and Analysis (Revised)* (EPA, 1992) recommends the use of a plume visual impact screening model (VISCREEN) for two successive levels of screening (Levels 1 and 2). A detailed plume visual impact analysis (Level 3) is conducted using the more sophisticated plume visibility model, PLUVUE II.

The PLUVUE II model described in this document refers to a restructured and revised version of the original PLUVUE II model described in the *User's Manual for the Plume Visibility Model (PLUVUE II)* (EPA, 1984a and EPA, 1984b). The model was restructured in order to improve the user interface and computing requirements and revised to remove several errors in the original PLUVUE II code. The PLUVUE II algorithm is basically the same algorithm as developed in 1984, except for some changes to correct computer coding errors and to use "lookup" tables for the calculation of the phase functions. Also, a program has been designed to assist the user with the application of the PLUVUE II visibility model on a personal computer by allowing the user to prepare an input file, select or create a library of Mie calculations to reduce computational time, and run the PLUVUE II model. This program is referred to as the RUNPLUVU visibility modeling system. In addition, this user's guide, which duplicates many of the sections contained in the original (EPA, 1984a) user's guide, has been transferred to WordPerfect 5.1 for easy downloading from the EPA's Technology Transfer SCRAM bulletin board.

The objective of the PLUVUE II model is to calculate visual range reduction and atmospheric discoloration caused by plumes consisting of primary particles, nitrogen oxides, and sulfur oxides emitted by a single emission source. Primary emissions of sulfur dioxide (SO_2) and nitric oxide (NO) do not scatter or absorb light and therefore do not cause visibility impairment. However, these emissions are converted in the atmosphere to secondary species that do scatter or absorb light and thus have the potential to cause visibility impairment. SO_2 emissions are converted to sulfate ($SO_4^=$) aerosols. These aerosols are generally formed or grow to a size (0.1 to 1.0 μm) that is effective in scattering light. NO emissions are converted to nitrogen dioxide (NO_2) gas, which is effective in absorbing light. In turn, NO_2 is converted to nitric acid vapor (HNO_3), which in turn neither absorbs nor scatters light. In some situations, nitric acid may form ammonium nitrate or organic nitrate aerosol, which scatters light. However, in many nonurban plumes, nitrate probably remains as HNO_3 vapor without visual effects. Eventually, all primary particles, secondary aerosols, and gases in a plume are removed from the atmosphere as a result of surface deposition and precipitation

scavenging. PLUVUE II is designed to predict the transport, atmospheric diffusion, chemical conversion, optical effects, and surface deposition of point and area source emissions.

The PLUVUE II model uses a Gaussian formulation for transport and dispersion. The spectral radiance $I(\lambda)$ (i.e., the intensity of light) at 39 visible wavelengths ($0.36 < \lambda < 0.75$ μm) is calculated for views with and without the plume. The changes in the spectrum are used to calculate various parameters that predict the perceptibility of the plume and contrast reduction caused by the plume (Latimer et al., 1978). The four key perception parameters for predicting visual impact are:

- reduction in visual range;
- contrast of the plume against a viewing background at the 0.55 μm wavelength;
- blue-red ratio of the plume; and
- color change perception parameter $\Delta E(L^*a^*b^*)$.

1.2 Limitations of the System

The plume visibility model PLUVUE II was evaluated with the 1981 VISTTA data base which was collected in the vicinity of the Kincaid Generating Station near Springfield, Illinois, and the Magma Copper Smelter near San Manuel, Arizona. Details of the model evaluation results are given in Seigneur et al. (1983).

For applications to distant Class I areas (more than 50 km from the emission source), the model is less accurate because of mesoscale wind speed, wind direction, and stability variations. Thus, the use of a Gaussian-based model for downwind distances greater than 50 km to predict visual effects is probably a conservative approach; however, this has not yet been demonstrated conclusively. Visual impacts for horizontal lines of sight are inversely proportional to the vertical extent of plume mixing. This vertical extent of plume mixing is defined by the vertical plume dispersion parameter (σ_z) and, at farther distances downwind, by the mixing depth. Thus, errors in predicting vertical plume dimensions will carry throughout the calculations of plume visibility impacts. However, until field measurements of mesoscale plume transport and diffusion are carried out, and until better models based on these data are developed and verified, the EPA does not know of a better approach to model plume dispersion for the purposes of plume visual impact analysis.

Other limitations are basic to the chemical mechanism used in PLUVUE II to predict the conversion of sulfur and nitrogen oxides. Although this mechanism is a reasonable approximation for most applications in nonurban areas, it is not valid for applications in photochemical (urban) atmospheres or for sources of significant quantities of reactive

hydrocarbons. For such applications, photochemical plume models or regional models should be used.

Other approximations are used in the atmospheric optics calculations and are discussed in Latimer et al. (1978). These approximations probably do not introduce significant errors in most situations; however, this has not yet been demonstrated. Terrain viewing backgrounds are idealized as white, gray, and black objects. The background atmosphere is treated as two layers; a homogeneous, surface mixed layer and a relatively clean upper-atmosphere layer. Diffusion radiation is calculated by integrating an angle-dependent radiance field according to the algorithm of Isaacs (1981). Errors in predicting diffuse-radiation intensities may adversely affect the accuracy of spectral radiance calculations, but not necessarily the accuracy of calculations of plume contrast, color differences, and reduction in visual range. In PLUVUE II, the calculated visual impact of a plume is quantified using coloration, color difference, and contrast parameters that are related to human visual perception.

1.3 User's Guide Organization

A technical overview of PLUVUE II, PLUIN2 (algorithm which allows the user to edit PLUVUE II input files), and MIETBL (algorithm which allows the user to create Mie library files as input to PLUVUE II) is presented in Section 2.0. Detailed RUNPLUVU user instructions including the basic computer requirements, detailed operating instructions, and a Level-3 plume visibility example are presented in Section 3.0. The references are given in Section 4.0.

2.0 TECHNICAL OVERVIEW

The PLUVUE II visibility modeling system combines three different algorithms: PLUVUE II, PLUIN2, and MIETBL into one algorithm called RUNPLUVU. The user of RUNPLUVU may edit PLUVUE II input files (PLUIN2 portion of RUNPLUVU), select or create Mie library files as input to PLUVUE II (MIETBL portion of RUNPLUVU), and run the PLUVUE II visibility algorithm:

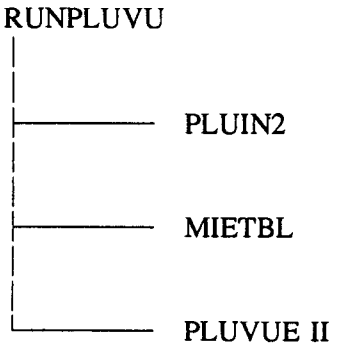

This section gives a detailed overview of the technical aspects of each routine. The PLUVUE II technical discussion is derived primarily from EPA (1984a). Section 2.1 presents in detail the PLUVUE II pollutant transport, diffusion, and removal processes; atmospheric chemistry; aerosol size distribution; atmospheric optics; geometry of the plume, observer, and sun; and how visibility impairment is quantified. Section 2.1 also discusses the most recent modifications made to the PLUVUE-II algorithm and the required input data. A description of PLUIN2 is provided in Section 2.2. Section 2.3 presents in detail a description of MIETBL including a discussion of Mie scattering theory, how Mie calculations are performed within MIETBL, and the accuracy of the Mie calculation methodology. A comparison of the revised PLUVUE II with the original PLUVUE II algorithm is given in Section 2.4 and the Appendix.

2.1 PLUVUE II

The modeling of visibility impairment requires mathematical descriptions for the following physical and chemical atmospheric processes in succession:

- Emissions;
- Atmospheric transport, diffusion, and removal;
- Chemical and physical reactions and transformations of precursors in the atmosphere;

- Light scattering and absorption characteristics of the resultant aerosol; and

- Radiative transfer through the aerosol along different lines of sight.

2.1.1 Pollutant Transport, Diffusion, and Removal

There are two scales that are of interest in visibility impairment calculations. They require two different types of models:

- A near-source plume model designed to predict the incremental impact of one emission source (such as a power plant or smelter).

- A regional model designed to predict, over time periods of several days, the impacts of several emissions sources within a region whose spatial scale is in the range of 1000 km.

Calculation of near-source visual impacts, which is the design objective of PLUVUE II, requires a basic model that accurately predicts the spatial distribution of pollutants and the chemical conversion of NO to NO_2 and SO_x and NO_x to sulfates and nitrates. The plume model must be capable of handling the spatial scale from emissions at the source to at least 100 km downwind. Because the regional-scale problem may be caused by the long-range transport of pollutants over a spatial scale of 1000 km, an air quality model is needed that can account for multiple sources and for temporal variations in mixing heights, dispersion parameters, emission rates, reaction rates, and wind speed and direction. This second type of model, a regional visibility model, is beyond the scope of this user's manual. PLUVUE II is a near-source plume visibility model.

Initial Dilution in a Buoyant Plume

Modeling of the initial dilution of a plume from the top of the stack to the point of final plume rise is important when modeling the conversion of nitric oxide (NO) to nitrogen dioxide (NO_2) in a power plant plume because of the quick quenching of the thermal oxidant of NO. The rate of this reaction is second order with respect to NO concentrations; therefore, the rate is fastest in the initial stages of plume dilution. It is also important to account for the initial dilution of buoyant releases because the rate of dilution caused by the turbulent entrainment of ambient air by a rising plume parcel can be considerably greater than that indicated by diffusion coefficients based on measurements for nonbuoyant releases (e.g., Pasquill-Gifford σ_y, σ_z). Thus, initial plume dilution during plume rise should be taken into account to calculate accurately both plume dilution and atmospheric chemistry.

Briggs (1969) suggested that the characteristic plume radius (R_p) increases linearly with the height of the plume above the stack and can be represented as follows:

$$R_p = 0.5\ (\Delta h) \quad . \tag{1}$$

Briggs described the plume rise (Δh), as a function of downwind distance (the "2/3 power law"), as follows:

$$\Delta h = 1.6\ F^{1/3} x^{2/3} u^{-1} \quad , \tag{2}$$

where F is the buoyancy flux, x is the downwind distance, and u is the wind speed. For initial dilution, we can assume that the plume is circular in cross section and has a Gaussian profile. We can also assume that the radius of the plume is the distance from the plume centerline to the point at which the plume concentration is 10 percent of the centerline concentrations. Thus, we have

$$R_p = 2.15\ \sigma_y = 2.15\ \sigma_z \quad , \tag{3}$$

where σ_y is the horizontal dispersion coefficient and σ_z is the vertical dispersion coefficient. The concentration (χ) of a given species at the centerline of the plume can be calculated by a modified Gaussian model that can be represented as

$$\chi = \frac{Q}{2\pi \sigma_y \sigma_z V} \quad , \tag{4}$$

where V is the velocity of the parcel, which has a horizontal component (the wind speed u) and a vertical component w, which can be calculated by differentiating Equation (2). Thus

$$w = \frac{dz}{dt} = \frac{2}{3}\ 1.6\ F^{1/3} u^{-1/3} t^{-1/3} \quad , \tag{5}$$

where t is the time traveled. With this formulation, time-dependent plume temperature and NO concentrations can be calculated for accurately predicting the thermal oxidation of NO during plume rise.

Combining Equations (1), (3), and (4), the initial dilution of plume material, after the plume has reached its final height, is calculated as follows:

$$\chi = \frac{2.94\ Q}{(\Delta h)^2 u} \quad , \tag{6}$$

where Q is the emission rate.

Thus, plume material is assumed to be at least as dilute as that shown by Equation (6). For emissions sources having more than one stack, it is assumed that there is an overlap of plumes from individual stacks. For cases in which the initial dilution during plume rise is

greater than the standard Gaussian formula would predict at the downwind distance of final plume rise, a virtual point-source offset is introduced so that dilution at this distance is at least as much as that shown in Equation (6).

Plume Rise

The final plume rise in PLUVUE II is calculated using the modified plume rise formulas of Briggs (1969, 1971, 1972) defined as follows:

For unstable or neutral atmospheric conditions, the downwind distance of final plume rise is $x_f = 3.5\ x^*$, where

$$x^* = \begin{cases} 14\ F^{5/8}, & \text{if } F < 55\ m^4 s^{-3} \\ 34\ F^{2/5}, & \text{if } F > 55\ m^4 s^{-3} \end{cases} \quad . \tag{7}$$

The final plume rise under these conditions is

$$\Delta h = 1.6\ F^{1/3}(3.5\ x^*)^{2/3} u^{-1} \quad . \tag{8}$$

For stable atmospheric conditions, the downwind distance of final plume rise is $x_f = \pi\ u\ s^{-1/2}$, where the stability parameter s is defined as follows:

$$s = g\ \frac{\delta\theta/\delta z}{T} \quad , \tag{9}$$

where g is the gravitational acceleration, $\delta\theta/\delta z$ is the potential temperature gradient, and T is the temperature.

The plume rise for stable atmospheric conditions is

$$\Delta h = \text{minimum of} \begin{cases} 2.6(F/(us))^{1/3} \\ 5\ F^{1/4} s^{-3/8} \end{cases} \quad . \tag{10}$$

The buoyancy flux (F) in the above equations is calculated on the basis of the flue gas volumetric flow rate per stack (V′), flue gas and ambient temperature in degrees Kelvin (T_{stack}, $T_{ambient}$), and gravitational acceleration, as follows:

$$F = \frac{gV'}{\pi}\left(1 - \frac{T_{ambient}}{T_{stack}}\right) \quad . \tag{11}$$

Gaussian Plume Diffusion

After the plume has achieved its final height (about 1 km downwind), plume concentrations for uniform wind fields can be adequately predicted using a Gaussian model if the wind speed u at plume height H (or $h_s + \Delta h$, where h_s is the stack height) and the rate of diffusion are known for the particular situation so that diffusion coefficients (σ_y, σ_z) can be selected:

$$\chi = \frac{Q}{2\pi\sigma_y\sigma_z u} \exp\left[-\frac{1}{2}\left(\frac{y}{\sigma_y}\right)^2\right]\left\{\exp\left[-\frac{1}{2}\left(\frac{H+z}{\sigma_z}\right)^2\right] + \exp\left[-\frac{1}{2}\left(\frac{H-z}{\sigma_z}\right)^2\right]\right\} \quad . \tag{12}$$

Equation (12) is appropriate for a conservative species and can be modified to be appropriate for a nonconservative species by changing the source term Q.

It is necessary for calculating plume visual impact to integrate, along the line of sight, the plume extinction coefficient, the magnitude of which depends on primary and secondary particulate and nitrogen dioxide concentrations. Equation (12) can be integrated (Ensor et al., 1973) in the cross-wind direction y, from $y = -\infty$ to $y = +\infty$, to obtain the optical thickness of the plume:

$$\tau_{py} = \int_{-\infty}^{+\infty} b_{ext}\, dy = \frac{Q'(x)}{(2\pi)^{1/2}\sigma_z u}\left\{\exp\left[-\frac{1}{2}\left(\frac{H+z}{\sigma_z}\right)^2\right] + \exp\left[-\frac{1}{2}\left(\frac{H-z}{\sigma_z}\right)^2\right]\right\} \quad , \tag{13}$$

where b_{ext} is the incremental increase in extinction coefficient in the plume and Q′ is the flux of the plume extinction coefficient over the entire plume cross section at downwind distance x. In the vertical direction z, from $z = 0$ to $z = +\infty$, the plume optical thickness is

$$\tau_{pz} = \int_{0}^{\infty} b_{ext}\, dz = \frac{Q'(x)}{(2\pi)^{1/2}\sigma_y u} \exp\left[-\frac{1}{2}\left(\frac{y}{\sigma_y}\right)^2\right] \quad . \tag{14}$$

Observer-Plume Orientation

The magnitude of the visual impact of a plume depends on the orientation of the observer with respect to the plume because the plume optical thickness will vary depending on this orientation. Figure 1 shows plan and elevation views of an observer and a plume and indicates that the sight path distance through the constituents of the plume is a function of angles α and β. The optical thickness for most combinations of angles α and β can be approximated as follows:

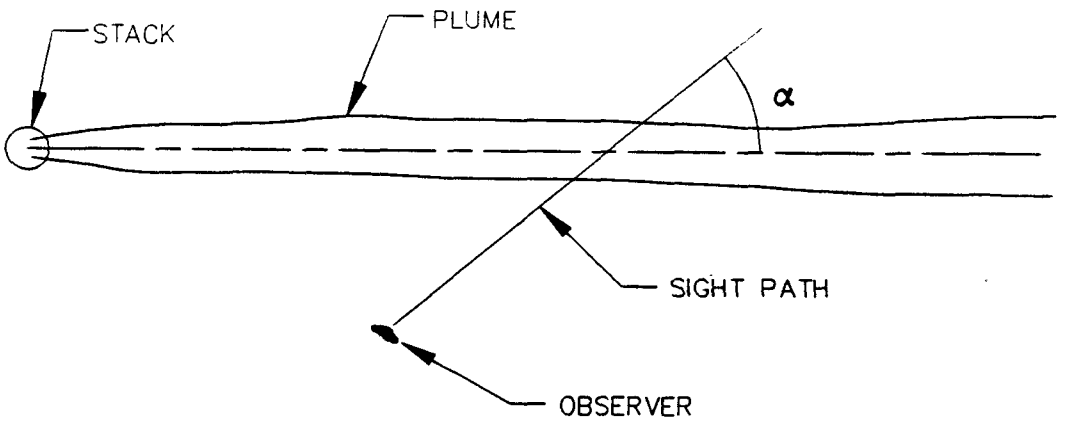

(A) PLAN VIEW

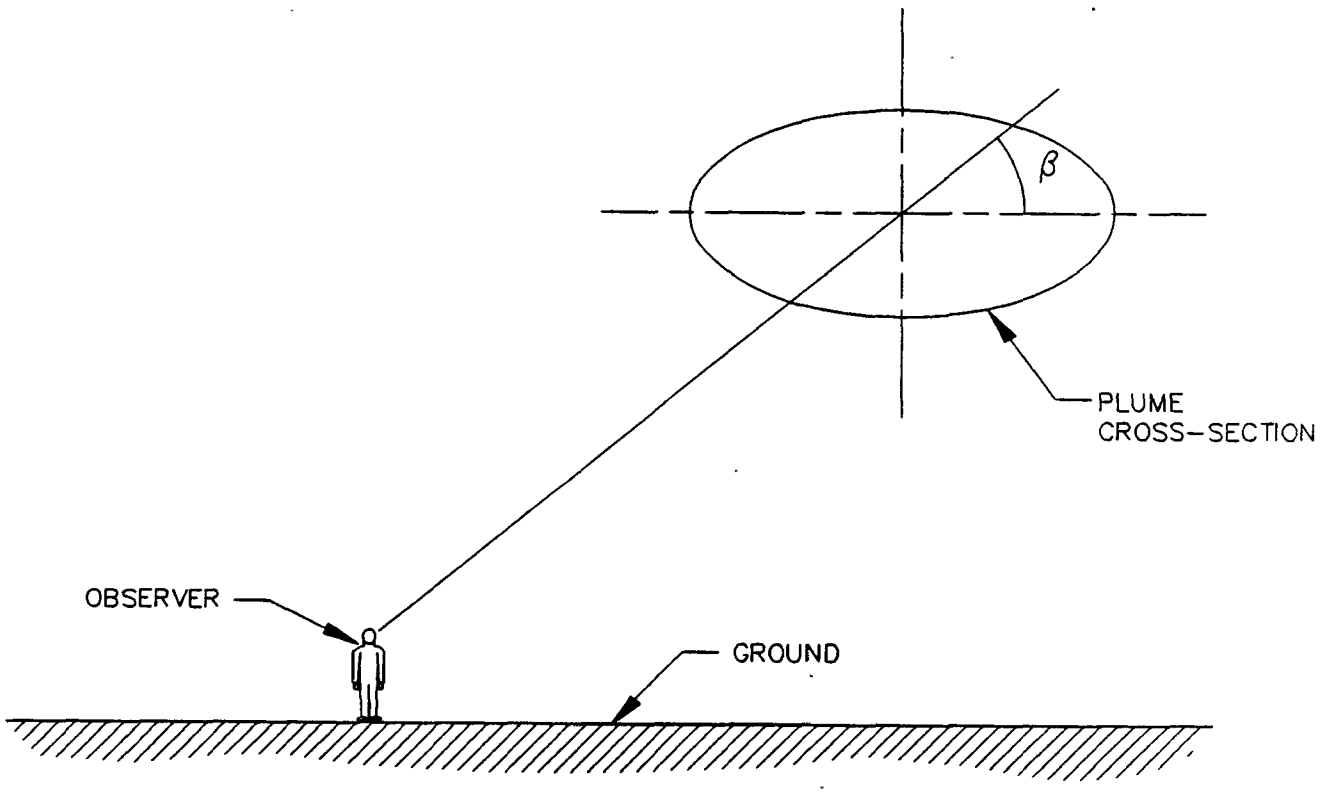

(B) ELEVATION VIEW

Figure 1. Gaussian plume visual impact model: observer-plume geometry.

$$\tau_p(\alpha,\beta) = \frac{1}{\sin\ \alpha}\left[(\tau_{py}\cos\ \beta)^2 + (\tau_{pz}\sin\ \beta)^2\right]^{1/2} \quad . \tag{15}$$

Figure 1 suggests that plume optical thickness is greater for horizontal sight paths than vertical ones, particularly during stable conditions when the plume cross section is flattened.

Limited Mixing

When vertical diffusion is limited by a stable capping layer, Equation (12) is no longer valid, and a Gaussian formulation, with terms for reflection from the top of the mixed layer (at altitude H_m), is used. Let H' be the height of the virtual source positioned above the top of the mixed layer: $H' = 2\ H_m - H$.

The Gaussian formulation for limited mixing is

$$\chi = \frac{Q}{2\pi\ \sigma_y\sigma_z\ u}\exp\left[-\frac{1}{2}\left(\frac{y}{\sigma_y}\right)^2\right]\left\{\exp\left[-\frac{1}{2}\left(\frac{H+z}{\sigma_z}\right)^2\right] + \exp\left[-\frac{1}{2}\left(\frac{H-z}{\sigma_z}\right)^2\right] + \right. \tag{16}$$
$$\left. \exp\left[-\frac{1}{2}\left(\frac{H'-z}{\sigma_z}\right)^2\right] + \exp\left[-\frac{1}{2}\left(\frac{H'+z}{\sigma_z}\right)^2\right]\right\} \quad .$$

In this instance of limited mixing, the plume material eventually becomes uniformly mixed in the vertical direction for $0 < z < H_m$. In the limit, the concentration is expressed as follows:

$$\chi = \frac{Q}{(2\pi)^{1/2}\sigma_y u H_m}\exp\left[-\frac{1}{2}\left(\frac{y}{\sigma_y}\right)^2\right] \quad . \tag{17}$$

The calculation of plume optical thickness in the y-direction becomes simply

$$\tau_{py} = \frac{Q'(x)}{uH_m} \quad . \tag{18}$$

Surface Deposition

Surface deposition is calculated by integrating the plume concentrations at the ground and multiplying by a deposition velocity, V_d, that characterizes gas and particulate surface depletion:

$$-\frac{dQ}{dx} = V_d \int \chi \, dy \quad . \tag{19}$$

Since nocturnal ground-based stable layers shield a plume from the ground at night, surface deposition is effectively zero at night. This is handled in the model using a flag keyed to the time of day at which the plume parcel is at a given downwind distance.

Power Law Wind Profile Extrapolation of Surface Winds

PLUVUE II is designed to use either wind speed aloft or surface wind speed (commonly measured at 10 m above the surface). The power law extrapolation presented in the *User's Manual for a Single-Source (CRSTER) Model* (EPA, 1977) is used. The surface wind speed is extrapolated to stack height for the plume rise calculation, and the surface wind speed is extrapolated to the final plume height for Gaussian concentration calculations*. The power law extrapolation is as follows:

$$u = u_0(z/10)^p \quad , \tag{20}$$

where u = wind speed at altitude z (ms^{-1}) and u_0 = surface wind speed (ms^{-1}). The profile exponent p is a function of stability and has the following values for urban classification*:

Pasquill Stability Class		Wind Speed Profile Exponent (p)
A	Extremely unstable	0.10
B	Moderately unstable	0.15
C	Slightly unstable	0.20
D	Neutral	0.25
E	Slightly stable	0.30
F	Moderately stable	0.30

2.1.2 Atmospheric Chemistry

The conversion of emission of nitric oxide (NO) and sulfur dioxide (SO_2) to nitrogen dioxide (NO_2) gas and sulfate (SO_4) aerosol, species responsible for visual effects, must be calculated in the visibility model.

---

* This is not consistent with current EPA regulatory models. The PLUVUE II algorithm was not modified because of the potential effect on the model performance.

The rate of chemical conversion of these primary emissions to secondary species responsible for visual impact is dependent on the concentration of the reacting species and ultraviolet (UV) solar flux. Thus, conversion rates are dependent on both plume dilution and time of day. A plume parcel at a given downwind distance has a specific gas, time of emission, and history of UV irradiation, which can affect the amount of NO_2 and SO_4 in the plume at a given time. Thus, the chemical conversion in each plume parcel must be treated separately, taking into account these factors.

PLUVUE II is structured to take a "snapshot" of a plume at a given time. In PLUVUE II, the chemical conversion is calculated for each plume parcel, observed at a given distance, in a Lagrangian manner; i.e., the reaction rates are calculated at each of several discrete downwind distances and times from the point of emission to the downwind distance at which the plume parcel is observed. Thus, the age of a plume parcel observed at downwind distance x_{obs} is x_{obs}/u, where u is the wind speed. The time (t) at which a plume parcel is at a given downwind distance (x) related to the time of observation (t_{obs}) is as follows:

$$t = t_{obs} - \frac{x_{obs} - x}{u} \quad . \tag{21}$$

The UV flux is calculated as a function of time that a plume parcel is at a given downwind distance x from the solar zenith angle (i.e., the angle between direct solar rays and the normal to the earth's surface). The zenith angle is calculated on the basis of the latitude, longitude, date, and time using a subroutine developed by Schere and Demerjian (1977).

The rate of chemical conversion is also dependent on the location of the plume parcel within the plume. PLUVUE II makes calculations at the following altitudes within the plume (y = 0): at the plume centerline (z = H) and at $z = H \pm n\,\sigma_z$, where n = 1 and 2.

Conversion of NO to NO_2

Nitrogen dioxide gas can cause a yellow-brown discoloration of the atmosphere. Although some discoloration is a result of wavelength-dependent light scattering caused by submicron aerosol, the dominant colorant of power plant plumes is NO_2, which causes a yellow-brown discoloration that may be apparent at significant distances downwind of large coal-fired power plants, particularly in areas where the background visual range is excellent.

Very little NO_2 is emitted directly from combustion sources. However, colorless nitric oxide is formed by the thermal oxidation of atmospheric nitrogen at the high temperatures experienced in the combustion zone (the boiler in a power plant) and the oxidation of nitrogen that may be present in the fuel. Chemical reactions in the atmosphere can form sufficient NO_2 from NO to cause atmospheric discoloration. Available measurements of NO

and NO_2 concentrations in power plant plumes in non-urban areas suggest that the conversion of NO to NO_2 can be calculated from a simple set of three reactions.*

The first of these is the thermal oxidation of NO to NO_2:

$$2NO + O_2 \rightarrow 2NO_2 \quad . \tag{22}$$

The reaction is termolecular, but bimolecular with respect to NO; it is therefore very fast at high concentrations of NO but slow at the lower concentrations that exist in the atmosphere or in a plume. The reaction rate for Equation (22), based on Baulch et al. (1973) is

$$\frac{d[NO_2]}{dt} = \left[4.015 \times 10^{-12} \exp\left(\frac{1046}{RT}\right)\right] [NO]^2[O_2] \quad (in\ ppm/s) \quad , \tag{23}$$

where R is the universal gas constant and T is the absolute temperature.

The reaction with ozone also affects the conversion of NO to NO_2:

$$NO + O_3 \xrightarrow{K_r} NO_2 + O_2 \quad . \tag{24}$$

The reaction is fast, with a rate (Leighton, 1961; Davis et al., 1974; Niki, 1974) at 25°C of

$$\frac{d[NO_2]}{dt} = 0.44\ [NO][O_3] \quad (in\ ppm/s) \quad . \tag{25}$$

This reaction time accounts for the ozone depletion measured within power plant plumes and is important because ozone concentrations can be high even in nonurban regions. Measured ozone concentrations in nonurban areas of the western United States range from 0.02 to 0.08 ppm.

Whereas the thermal oxidation rate in the reaction shown in Equation (23) decreases as the plume mixes (because the NO concentration decreases), the formation of nitrogen dioxide via Equation (24) is enhanced as the plume mixes because additional ozone from the atmosphere is mixed into the plume, allowing Equation (24) to proceed. When there are no reactions converting NO_2 to NO (e.g., at night), Equation (24) proceeds until all of the NO in the plume is converted to NO_2 or until the ozone concentration in the plume drops to zero. Therefore, the rate of conversion of NO to NO_2 via Equation (24) is limited by the rate of the plume mixing that provides the necessary atmospheric ozone.

---

* In urban areas, a complete photochemical mechanism should be applied to calculate NO_2 concentrations. Also, it should be noted that NO_2 is destroyed by reaction with the hydroxyl radical (OH·), as discussed in the next subsection.

To complete the set of chemical reaction mechanisms, we must consider the photolysis of NO_2. When sunlight illuminates a plume containing nitrogen dioxide, short wavelength light and ultraviolet radiation are absorbed by the NO_2. As noted above, absorption of the shorter wavelength light produces the characteristic yellow-brown color associated with NO_2. Absorption of the more energetic ultraviolet light (UV) results in dissociation of the NO_2 molecule:

$$NO_2 + h\nu \xrightarrow{K_d} NO + O \quad , \tag{26}$$

$$O + O_2 \rightarrow O_3 \quad . \tag{27}$$

Leighton (1961) gave the rate of the reaction presented in Equation (26) as

$$\frac{d[NO_2]}{dt} = -K_d\,[NO_2] \quad (in\ ppm/s) \quad , \tag{28}$$

where K_d depends on the amount of light incident on the nitrogen dioxide. Davis et al. (1974) gave the following expression for K_d as a function of the solar zenith angle Z_s:

$$K_d = 1 \times 10^{-2} \exp\left(- \frac{0.38}{\cos Z_s} \right) \quad (in\ s^{-1}) \quad . \tag{29}$$

With this set of chemical reactions, the chemical conversion of NO to NO_2 in the atmosphere can be calculated from background pollutant concentrations and from plume NO_x increments using the technique suggested by Latimer and Samuelsen (1975) and White (1977). Making the steady-state approximation, we have

$$[NO_2] = \frac{K_r}{K_d}\,[NO][O_3] \quad , \tag{30}$$

where

$$[NO] = [NO_x] - [NO_2] \tag{31}$$

and

$$[O_3] = [O_3]_b - \left([NO_2] - [NO_2]_t - [NO_2]_b \right) \quad . \tag{32}$$

$[NO_2]_t$ signifies the concentration of NO_2 formed via the termolecular reaction presented in Equation (22) and $[NO_2]_b$ signifies background concentrations. Substituting Equations (31) and (32) into Equation (30) we can solve for the concentration of NO_2 using the standard quadratic equation in the form of $(y = (-b \pm \sqrt{b^2 - 4ac}\,) / 2a)$ where $y = [NO_2]$. The positive root of the quadratic was found to be physically unreasonable; therefore, the quadratic was solved using the negative root as follows:

$$[NO_2] = 0.5 \left\{ [NO_x] + [O_3]_b + [NO_2]_t + [NO_2]_b + \frac{K_d}{K_r} - \right.$$
$$\left. \left[\left([NO_x] + [O_3]_b + [NO_2]_t + [NO_2]_b + \frac{K_d}{K_r} \right)^2 - 4[NO_x] \left([O_3]_b + [NO_2]_t + [NO_2]_b \right) \right]^{1/2} \right\} \quad (33)$$

Conversion of SO_2 to $SO_4^=$

It is critical to calculate the conversion of SO_2 emissions to sulfate ($SO_4^=$) aerosol, because the latter can effectively scatter light and cause reductions in visual range. The usual approach is to assume that sulfur dioxide (SO_2) gas is converted to sulfate ($SO_4^=$) aerosol at some constant rate; this approach employs a user-input value of a pseudo-first-order rate constant whose value is empirically determined.

There is considerable variation, however, in such measured SO_2-to-$SO_4^=$ conversion rates, which range from a few tenths of a percent to several percent per hour. Much of this variance in SO_2-to-$SO_4^=$ conversion observed in the field measurement programs in recent years can be explained using a model that accounts for the reactions of plume SO_2 and NO_2 with the hydroxyl (OH·) radical. This chemical mechanism is incorporated in PLUVUE II. In clean background areas, the gas-phase oxidation of SO_2 and NO_2 to sulfate aerosol and nitrate (nitric acid vapor) is due primarily to the reaction of these species with OH·. Previous assessments of homogeneous (gas-phase) oxidation of SO_2 to sulfate estimated the proportion assignable to the reaction with hydroxyl between about 75 percent in clean atmospheres (Calvert et al., 1978; Altshuller, 1979) and as low as 40 percent in polluted urban air (Isaksen et al., 1978), but more recent estimates place these values much higher. Kinetic models forming the basis of the early estimates used the value of 1.3×10^{-12} $cm^3mol^{-1}s^{-1}$ for the rate constant of reaction for HO_2 and CH_3O_2 with NO. More recently, however, this rate has been measured at 8.1×10^{-12} $cm^3mol^{-1}s^{-1}$ (Hampson and Garvin, 1978). This larger rate constant lowers the expected concentration of these peroxy radicals by a factor of 6 and, in turn, greatly reduces the SO_2 conversion resulting from reactions with these radicals. When recalculated using the new rate constant, the fraction of SO_2-to-sulfate conversion that results from reaction with the hydroxyl radical is approximately 95 percent for clean atmospheres and 70 percent for the extremely polluted case.

These estimates are supported by the work of Miller (1978), who found that the SO_2 oxidation rate was not dependent on the absolute concentrations of hydrocarbons and nitrogen oxides but on the ratio of nonmethane hydrocarbon to nitrogen oxides.

The rate of sulfate (and nitric acid) formation can be estimated by calculating the steady-state concentration of OH· within a plume. This steady-state plume OH· concentration is calculated by balancing the rate of OH· production with the rate of OH· destruction.

With the assumption of steady-state concentrations of O(¹D) and OH· in the plume, plume pseudo-first-order SO_2-to-SO_4 and NO_2-to-HNO_3 conversion rates can be calculated as follows:*

$$-\frac{1}{[SO_2]}\frac{d[SO_2]}{dt} = K_{37}[OH\cdot] \quad , \tag{34}$$

$$-\frac{1}{[NO_2]}\frac{d[NO_2]}{dt} = K_{38}[OH\cdot] \quad , \tag{35}$$

where $K_{37} = 2.0 \times 10^6$ ppm^{-1} min^{-1} and $K_{38} = 1.4 \times 10^4$ ppm^{-1} min^{-1}.

Plume OH· concentrations are reduced below background tropospheric values for two reasons:

- Plume ozone (O_3) concentrations are reduced below background values because of the reaction $NO + O_3 \rightarrow NO_2 + O_2$ (Eq. 24).
- Plume concentration of NO_2 and SO_2 are high, thus reducing steady-state OH· concentrations.

It should be pointed out that at night there is no production of OH· from ozone photolysis; also, in early morning and later afternoon and in winter, OH· production is diminished because ultraviolet flux decreases as solar zenith angles approach 90°. Thus, sulfate and nitrate are not formed at night and are formed only very slowly in concentrated plumes. Nitrate is expected to remain as HNO_3 vapor and without visual effects until it is eventually deposited. Ammonium nitrate could exist in aerosol form; however, sulfate competes for available atmospheric ammonia.

2.1.3 Aerosol Size Distribution

The aerosol size distribution is characterized by a series of aerosol modes, each having a log-normal distribution of mass (or volume). Each of the following modes is treated separately in PLUVUE II:

---

* The user is given the option in PLUVUE II of supplementing the SO_2-to-$SO_4^=$ conversion rate calculated on the basis of steady-state plume OH· concentrations with a user-input pseudo-first-order rate constant, which can be varied as a function of downwind distance.

- Background accumulation mode (submicron) aerosol (typically having a mass median diameter of about 0.3 μm and a geometric standard deviation of 2).

- Background coarse mode (> 1 μm) aerosol (typically having a mass median diameter of about 6 μm and a geometric standard deviation of 2).

- Background carbonaceous aerosol (typically having a mass median diameter of about 0.1 μm and a geometric standard deviation of 2).

- Plume primary particulate aerosol (e.g., fly ash emissions).

- Plume secondary sulfate ($SO_4^=$) aerosol (typically having a mass median diameter of 0.1 to 0.3 μm and a geometric standard deviation of 2).

- Plume carbonaceous aerosol (typically having a mass median diameter of 0.1 μm and a geometric standard deviation of 2).

The expression developed by Winkler (1973) is used to calculate the amount of liquid water associated with submicron background and plume sulfate aerosol as a function of relative humidity.

Secondary aerosol is assumed to form in the submicron plume secondary aerosol mode. A time delay equal to the time between successive downwind distances is introduced to account for coagulation and condensation time delays.

2.1.4 Atmospheric Optics

In the atmospheric optics component of the plume visibility model, the light scattering and absorption properties of the aerosol and the resultant light intensity (spectral radiance) for various illumination and viewing situations are computed.

Calculation of the Scattering and Absorption Properties

After the concentrations of the pollutants are specified by the transport and chemistry subroutines, their radiative properties must be determined. For NO_2, the absorption at a particular wavelength is a tabulated function (Nixon, 1940) multiplied by the concentration. For aerosols, however, the procedure is more complicated.

In general, a particle's ability to scatter and absorb radiation at a particular frequency is a function of size, composition, shape, and relative humidity. The flexibility to specify the size distribution of both primary and secondary particles was desired. Therefore, the effect of particle size on the wavelength dependence of the extinction coefficient and the phase

function, the solution of Maxwell's equations for scattering by a sphere, and the so-called Mie equations were used in PLUVUE II. These calculations are appropriate for atmospheric aerosol; comparisons of Mie calculations, with empirical correlations of scattering-to-mass, indicate substantial agreement. The Mie calculations are input to the PLUVUE II model using the MIETBL algorithm which is discussed in detail in Section 2.3.

Calculation of Light Intensity

The light intensity, or radiance (watts/m^2/steradian) at a particular location in the atmosphere is a function of the direction of observation Ω and the wavelength λ. Calculation of the light intensity in a medium follows from the radiative transfer equation. This equation is a conservation of energy statement that accounts for the light added to the line of sight by scattering and the light lost because of absorption and scattering. Approximations and solution techniques applicable to planetary atmospheres have been discussed by Hansen and Travis (1974) and Irvine (1975).

To compute the spectral light intensity at the observer, we sum (integrate) the scattered and absorbed light over the path, r, associated with the line of sight Ω. The resultant general expression for the background sky intensity at a particular wavelength is

$$I_b(\Omega) = \int_0^{\tau_\infty} \frac{\omega(\tau)}{4\pi} \int_{\Omega'=4\pi} I(\Omega',\tau')\, p(\Omega' \rightarrow \Omega,\tau')\, d\Omega'\, e^{-\tau'}\, d\tau' \quad , \tag{36}$$

where

τ	=	the optical depth ($\tau \equiv \int_0^r b_{ext}\, dr$, where b_{ext} is the extinction coefficient),
ω	=	the albedo for single scattering ($\omega \equiv b_{scat}/b_{ext}$ where b_{scat} is the scattering coefficient),
$p(\Omega' \rightarrow \Omega)$	=	the scattering distribution function for the angle $\Omega' \rightarrow \Omega$, and
I	=	the spectral intensity at τ' from direct and diffuse solar radiation.

The intensity seen by an observer in direction Ω of a background viewing object of intensity I_o at distance R is

$$I_{obj}(\Omega) = I_o(\Omega)e^{-\tau_R} + \int_0^{\tau_R} \frac{\omega(\tau')}{4\pi} \int_{\Omega'=4\pi} I(\Omega',\tau)\, p(\Omega' + \Omega,\tau')\, d\Omega'\, e^{-\tau'}\, d\tau' \quad . \tag{37}$$

Equations (36) and (37) then completely describe the spectral intensity of the sky and a background object. Once these two quantities are known, the visual effects of the intervening atmosphere can be quantified. In evaluating Equations (36) and (37), we encounter two main

difficulties: first, the quantity in the integral is a fairly complicated function, and accurate specification is tedious. Second, the atmosphere is inherently inhomogeneous; thus, the radiative properties of ω and p are somewhat complicated functions of r and Ω. The following approximations are therefore made in PLUVUE II:

- Plane parallel atmosphere
- Two homogeneous layers
- Average solar flux approximation

The equation for the background intensity at the surface becomes, for a given viewing direction:

$$I_b(\Omega) = I_{sky}(\Omega)\, e^{-\tau_L} + F_s \int_0^{\tau_L} \frac{\omega(\tau')}{4\pi}\, e^{-\tau_s/\mu_s}\, P(\Omega'_s \rightarrow \Omega, \tau')\, e^{-\tau'} d\tau' + \int_0^{\tau_L} \frac{\omega(\tau')}{4\pi} \int_{\Omega'=4\pi} I(\Omega', \tau')\, P(\Omega' \rightarrow \Omega, \tau)\, d\Omega'\, e^{-\tau'} d\tau' \quad . \tag{38}$$

The radiance impinging on the top of the planetary boundary layer, $I_{sky}(\Omega)$, is calculated from average properties of the upper atmospheric layer:

$$I_{sky}(\Omega) = \frac{\overline{\omega_\infty}}{4\pi}\, \overline{P_\infty}(\theta_s)\, F_s \int_{\tau_L}^{\tau_\infty} e^{-\tau_s/\mu_s}\, e^{-\tau'}\, d\tau' \quad , \tag{39}$$

where $\overline{\omega}_\infty$ and $\overline{P}(\theta_s)$ are average albedo and phase functions, respectively, and τ_L is the optical depth of the planetary boundary layer. The atmosphere is then assumed to be composed of two layers of homogeneous properties, i.e., an upper atmospheric layer and a planetary boundary layer.

In Equation (38), the first term represents the light that travels directly from the object to the observer, the second term is integrated along the line of sight and represents the light that has been scattered once from the sunlight's angle of incidence into the line of sight (single-scattering term), and the third term represents the light that has been scattered at least once before being scattered into the line of sight (multiple-scattering term).

The first term is calculated from the values of the background object radiance or sky radiance at the top of the boundary layer and extinction coefficient. The background object radiance, $I_o(\Omega)$, is calculated from the optical depth and from the molecular and aerosol scattering phase functions. Since the sky radiance, $I_{sky}(\Omega)$ is given by Equation (39), it depends on the aerosol concentration, the size distributions, and the scattering angle.

For the second term, one assumes spatially averaged albedo $\overline{\omega}$ and phase functions $P(\theta_s)$ for the planetary boundary layer. Equation (37) may be rewritten as follows:

$$I_{obj}(\Omega) = I_o(\Omega)\, e^{-\tau_R} + F_s \frac{\overline{\omega}}{4\pi} P(\theta_s) \int_o^{\tau_R} e^{-\tau_z/\mu_s}\, e^{-\tau'}\, d\tau' + G(\Omega,\tau_R) \quad , \tag{40}$$

where θ_s is the single-scattering angle and $G(\Omega,\tau_R)$ is the multiple-scattering term. The second term is calculated from the values of the extinction coefficient along the line of sight. Similarly, Equation (38) is rewritten as follows:

$$I_b(\Omega) = I_{sky}(\Omega)\, e^{-\tau_L} + F_s \frac{\overline{\omega}}{4\pi} P(\theta_s) \int_o^{\tau_L} e^{-\tau_z/\mu_s}\, e^{-\tau'}\, d\tau' + G(\Omega,\tau_\infty) \quad . \tag{41}$$

The radiance of a plume with a background object is calculated in three steps, as shown schematically in Figure 2. First, the background radiance incident on the plume, $I_1(\Omega)$, is calculated according to Equation (42):

$$I_1(\Omega) = I_o(\Omega)\, e^{-\tau_1} + F_s \frac{\overline{\omega}}{4\pi} P(\theta_s) \int_o^{\tau_1} e^{-\tau_z/\mu_s}\, e^{-\tau'}\, d\tau' + G(\Omega,\tau_1) \quad , \tag{42}$$

where τ_1 is the optical depth between the background object and the observer.

The radiance leaving the plume, $I_2(\Omega)$, is calculated from $I_1(\Omega)$ and the scattering and absorption of light in the plume:

$$I_2(\Omega) = I_1(\Omega)\, e^{-\tau_p} + F_s \frac{\overline{\omega_p}}{4\pi} P(\theta_s) \int_o^{\tau_p} e^{-\tau_z/\mu_s}\, e^{-\tau'}\, d\tau' + G(\Omega,\tau_p) \quad , \tag{43}$$

where τ_p is the optical depth of the plume along the line of sight, and $\overline{\omega}_p$ is the plume albedo. These variables are calculated from the plume gas and particle scattering and absorption coefficients. The integration of these coefficients is carried out by assuming that the plume is Gaussian (Latimer and Samuelsen, 1978).

The plume radiance at the observer location, $I_p(\Omega)$, is then calculated from $I_2(\Omega)$ according to Equation (44):

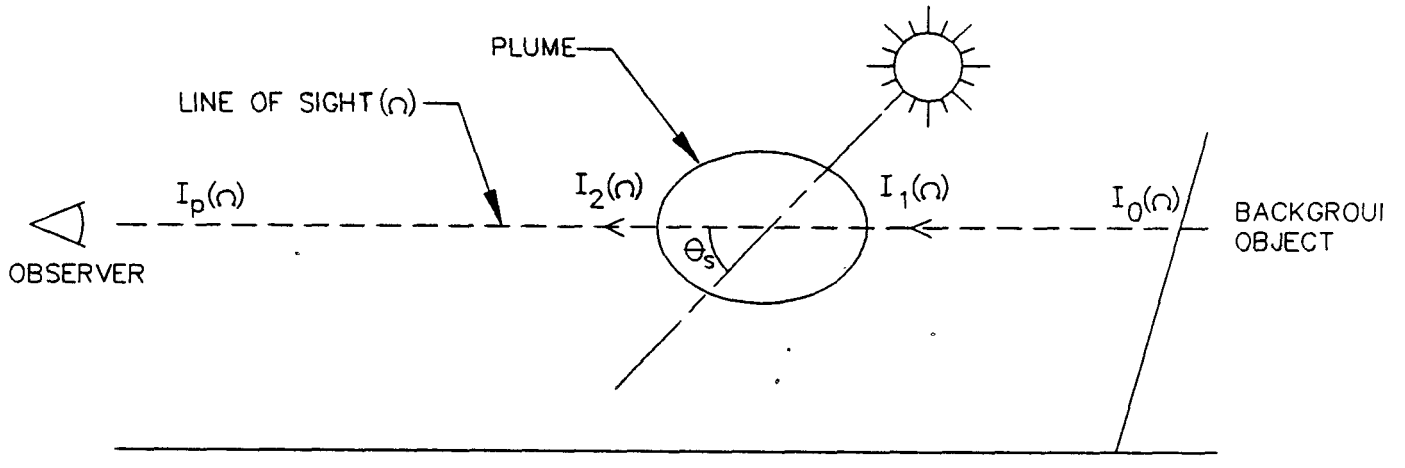

Figure 2. Schematic representation of the plume radiance calculations.

$$I_p(\Omega) = I_2(\Omega)\, e^{-\tau_2} + F_s \frac{\overline{\omega}}{4\pi} P(\theta_s) \int_o^{\tau_2} e^{-\tau_s/\mu_s}\, e^{\tau-\tau'}\, d\tau' + G(\Omega,\tau_2) \quad , \tag{44}$$

where τ_2 is the optical depth between the plume and the observer.

The contrast of the plume can then be calculated from the plume and background radiances as follows:

$$c = \frac{I_p(\Omega) - I_{obj}(\Omega)}{I_{obj}(\Omega)} \quad . \tag{45}$$

In calculating the radiances, the multiple-scattering term requires the integration of the angle-dependent sky radiance over all angles and over the optical depth. The calculation is performed in two steps that are summarized as follows.

First, the scattered intensity source function is calculated according to the algorithm of Isaacs (1981). The formulation is based on a two-stream approximation to the radiative transfer equation and employs the Rayleigh and Henyey-Greenstein phase functions for molecular and aerosol scattering, respectively. The phase functions are calculated according to Mie theory. Then, the multiple-scattering term is calculated by integrating over Ω' and τ'. This approach allows an anisotropic description of the multiple-scattering term that is computationally reasonable.

Thus, the background intensity and the intensity in the direction of an object at distance R from the observer can be computed given the following inputs:

- Background radiative properties (e.g., size distribution visual range),
- Solar zenith angle,
- Scattering angle,
- Viewed object intensity,
- Direction of observation, and
- Planetary boundary layer height.

The plume is treated as a homogeneous layer with a given optical thickness and mean properties $\overline{\omega}_{plume}$ and $\overline{p}_{plume}(\theta)$. It is also assumed that the plume does not affect the solar radiation illumination (an optically thin plume).

Spectral radiance, or light intensity $I(\lambda)$, is calculated for 39 wavelengths spanning the visible spectrum (0.36 μm < λ < 0.74 μm, in 0.01 μm increments).

2.1.5 Geometry of Plume, Observer, and Sun

For performing as many as four different types of optics calculations at selected points along the plume trajectory, PLUVUE has two modes: plume-based and observer-based calculations. The calculations for plume transport, diffusion, and chemistry are identical for calculations in both modes. The major difference between the two types of calculations is the orientation of the position of the viewer to the source and the plume.

Plume-based calculations are repeated for several combinations of plume-observer-sun geometries. Because of the repetitions, these plume-based calculations are more time consuming and produce more printed output than the observer-based calculations, which are performed for only the specific line-of-sight orientations corresponding to the given observer position, the portions of the plume being observed, and the specific position of the sun relative to these lines of sight.

There are four types of optics calculations: (1) horizontal views through the plume with a sky viewing background; (2) nonhorizontal views through the plume with a sky viewing background; (3) horizontal views through the plume with white, gray, and black viewing backgrounds; and (4) horizontal views along the axis of the plume with a sky viewing background.

Figure 3 illustrates the geometry of the plume-based optics calculations of horizontal views through the plume. This figure depicts schematically the variety of distances from the observer to the plume and the variety of horizontal azimuthal angles between the line of sight and the plume trajectory.* Calculations for all these geometries are repeated for up to six different scattering angles.

Figure 4 shows the geometry for the optics calculation for horizontal views perpendicular to the plume with white, gray, and black viewing backgrounds. For each point on the plume trajectory and each scattering angle, the calculations are executed for a range of distances from the observer to the background object, starting at the plume centerline and ending at 80 percent of the background visual range. The distances, from the observer to the plume, range from 2 percent to 80 percent of the background visual range.

Figure 5 illustrates the configuration used for the plume-based calculation for views along the axis of the plume. The calculations are made from the second through the final downwind distances. At each point, the observer is looking toward the emissions source with a sky background. The calculations are made for views through plume segments defined by the particular point of analysis, as well as successive analysis points upwind. The

---

* These azimuthal angles are measured from the plume centerline to the line of sight such that the angles range from 0° to 90°.

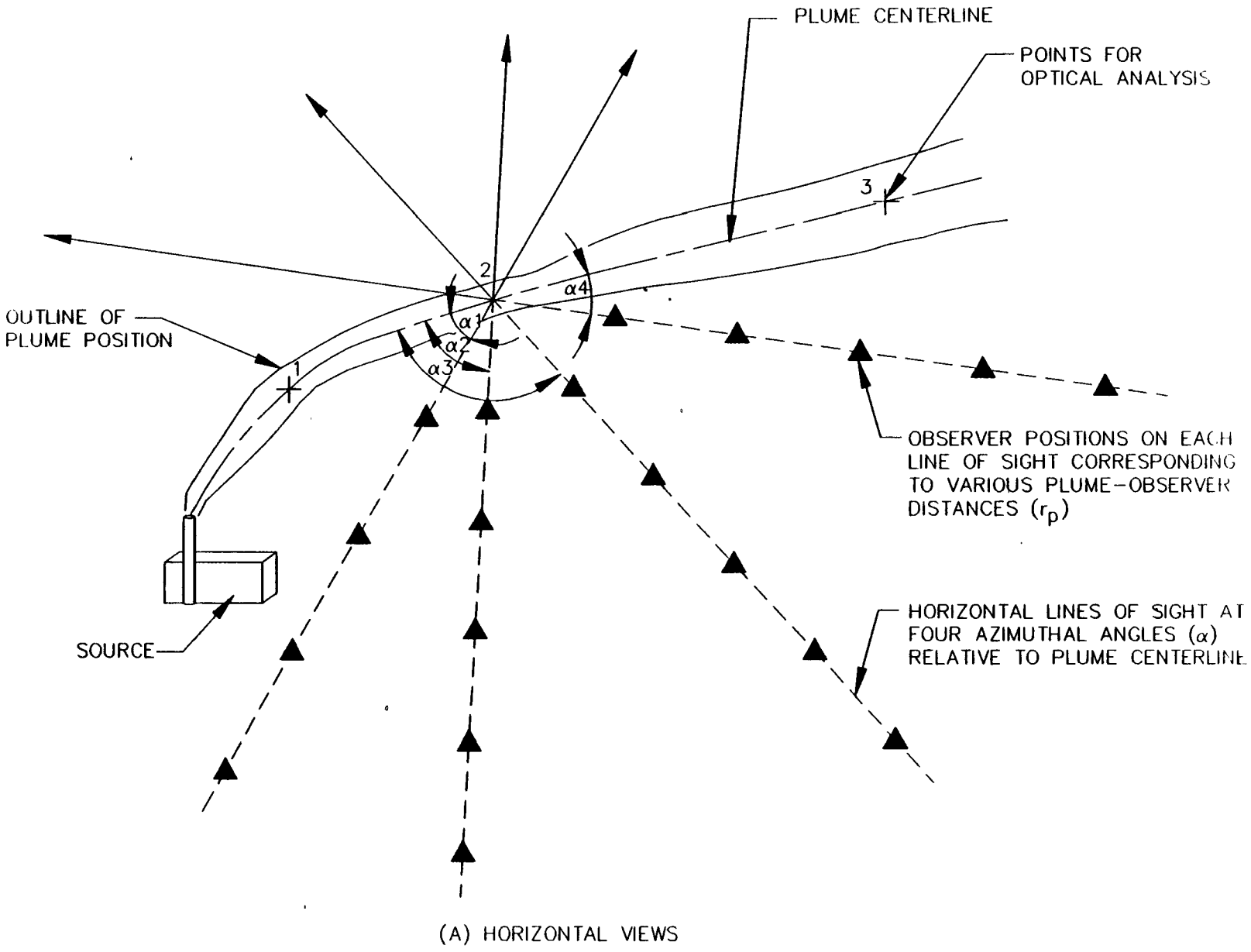

Figure 3. **Geometries for plume-based calculations with a sky background.**

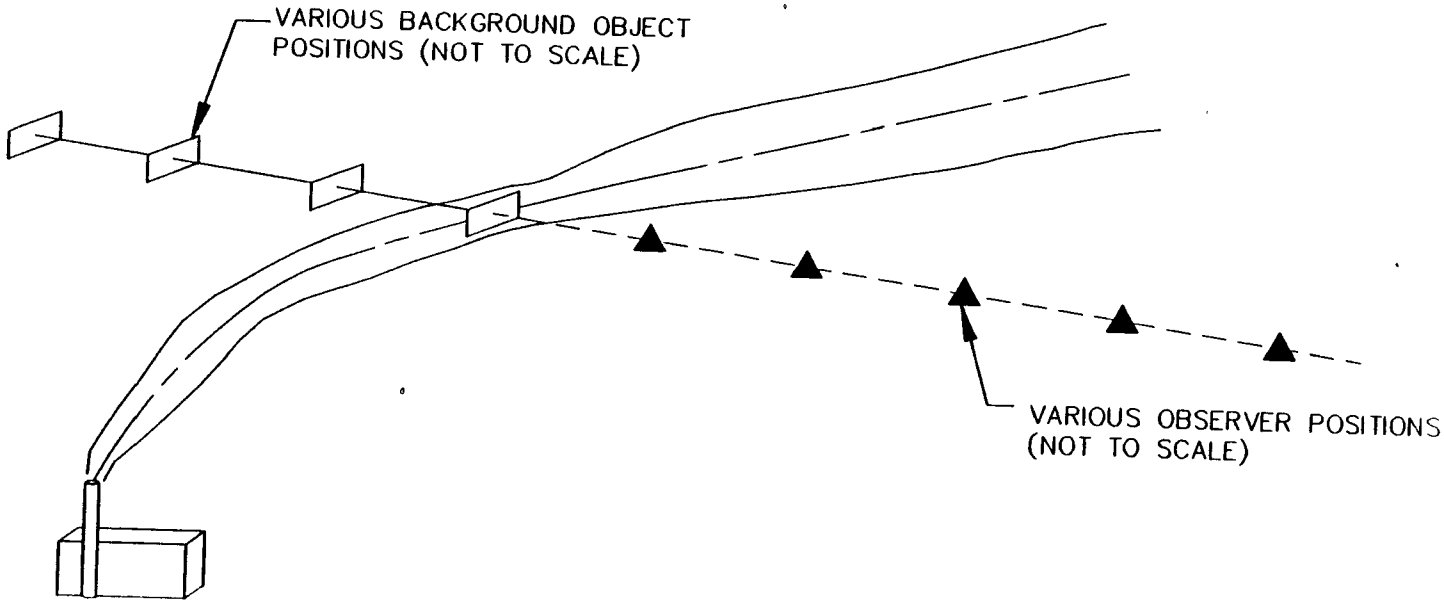

Figure 4. Geometries for plume-based calculations for viewing of white, gray, and black objects for horizontal views perpendicular to the plume.

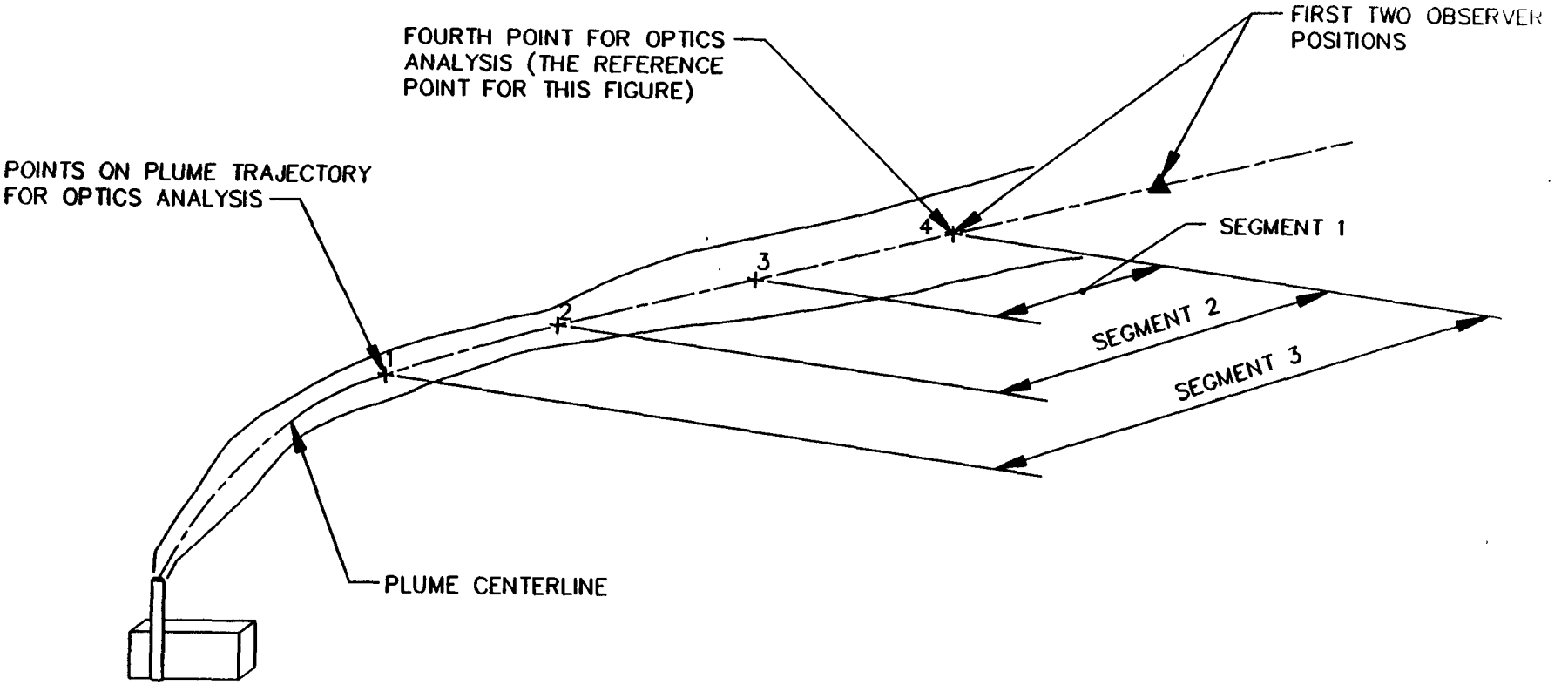

Figure 5. Geometries for plume-based calculations for horizontal views along the axis of the plume.

calculations are repeated for observer positions at a range of distances from the downwind point at which the plume segment is assumed to end.

The observer-based geometry used for views through the plume center with a clear sky background is shown in Figure 6. At each point of analysis along the plume trajectory, the optics calculation is made for only one scattering angle, one plume-observer distance, and one azimuthal angle specific for the source position, observer position, wind direction, date, and time of day used as input. For calculations with white, gray, and black viewing backgrounds, the geometries are the same as those for horizontal views with a sky background (Figure 7), with the addition of the specific background object distance, along each line of sight, from the observer through the points on the plume trajectory.

Figure 7 is a plan view of the geometry for an observer-based calculation for views along the plume. At each analysis point along the plume trajectory, the centerline concentration is integrated along a segment on the line of sight that would correspond to a Gaussian distribution. The line of sight is always horizontal. The calculation is performed for a clear sky background and for white, gray, and black viewing objects at the specific distance for each line of sight.

It should be noted that if the distance (r_p) and azimuthal angle (α) are such that the observer is within the plume, the total plume optical thickness along the line of sight is reduced accordingly. The calculated distance r_p is the distance between the observer and the centroid of plume material viewed by the observer.

2.1.6 Quantifying Visibility Impairment

Visibility impairment may be quantified once the spectral light intensity or radiance $I(\lambda)$ has been calculated for the specific lines of sight of an observer at a given location in an atmosphere with known aerosol and pollutant concentrations. Visibility impairment--including reduction in visual range, the perceptibility of plumes and haze layers, and atmospheric discoloration--is caused by changes in light intensity as a result of light scattering and absorption in the atmosphere.

Some parameters which may be used to characterize the visibility effects of the plume are listed:

- Visual Range Reduction

  This parameter is the percentage reduction in visual range (the farthest distance one can see a large, black object) caused by the plume material. This parameter can be interpreted to indicate the haziness or loss of contrast of viewed landscape features caused by plume material.

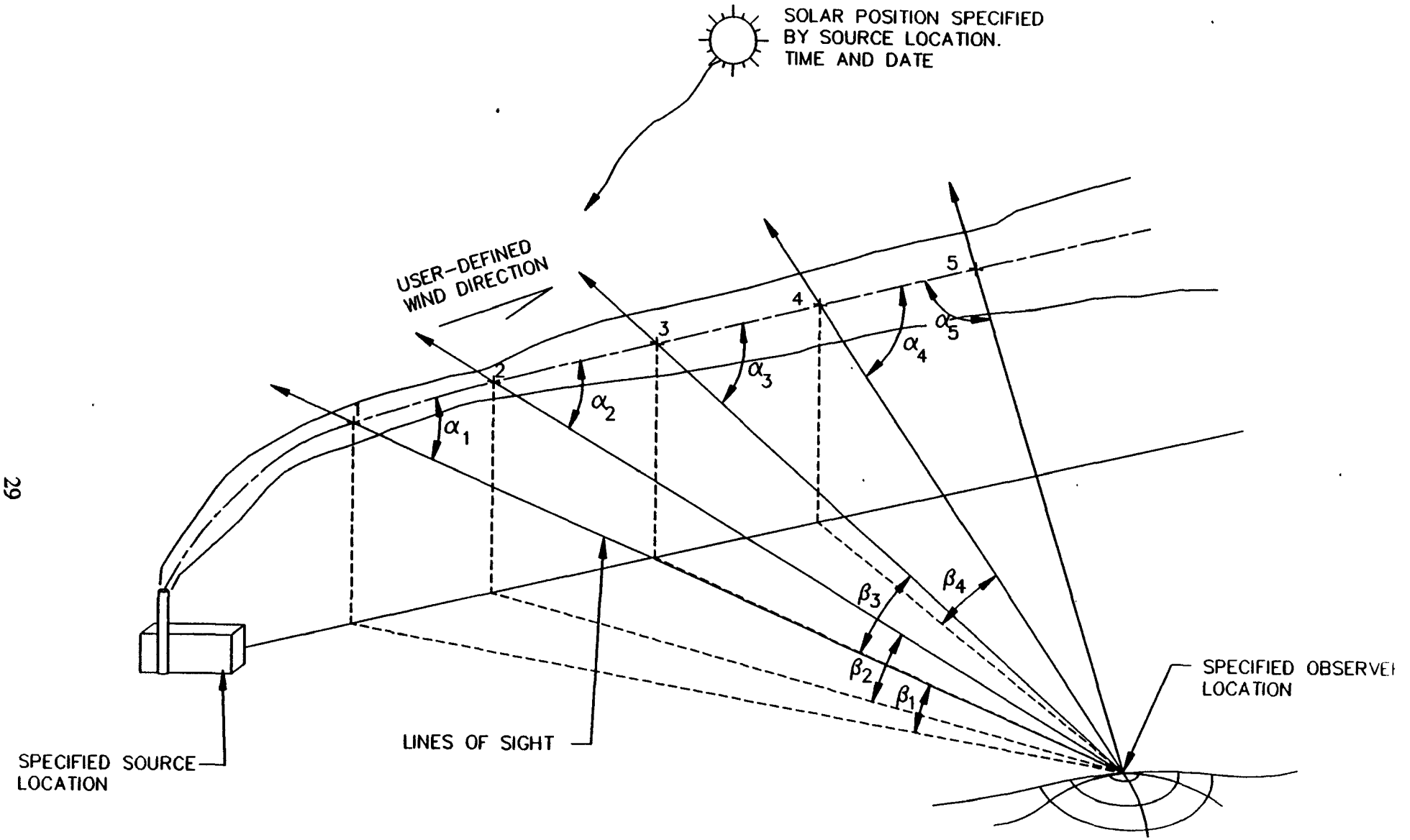

Figure 6. Geometry used for observer-based calculations for nonhorizontal views through the plume for clear-sky backgrounds.

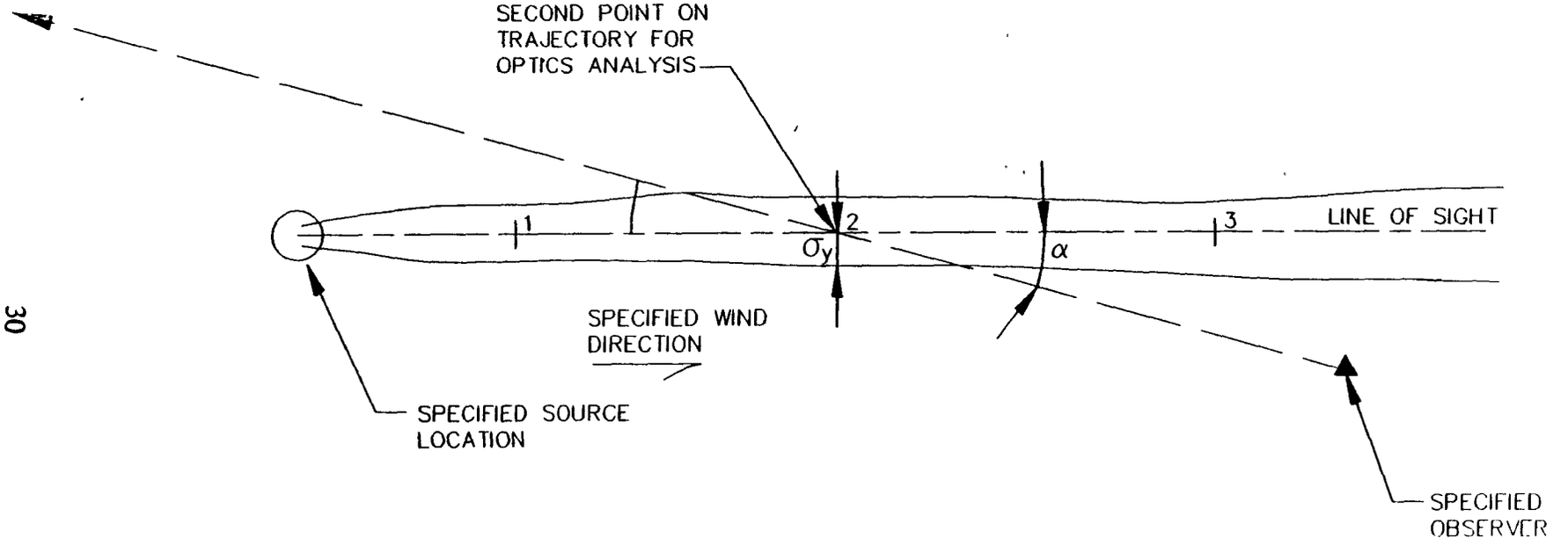

Figure 7. Plan view of geometry for observer-based calculations for views along the plume.

- Plume Contrast

  This parameter is the relative brightness of a plume compared to a viewing background. A contrast that is positive indicates a relatively bright plume and a negative contrast indicates a dark plume. Contrasts with absolute values greater than 0.02 are generally perceptible. A two percent contrast is used to define visual range. Plume contrast calculations in PLUVUE II are done at one wavelength, 0.55 μm, which is a green color in the middle of the visible spectrum, which extends from 0.4 μm (blue) to 0.7 μm (red).

- Blue-Red Ratio

  This parameter indicates the relative coloration of a plume relative to its viewing background. Blue-red ratios less than one indicate relatively yellow, red, or brown plumes. Blue-red ratios greater than one indicate plumes that are whiter, grayer, or bluer than the viewing background. Blue-red ratios less than 0.9 or greater than 1.1 would be indicative of perceptible plumes.

- Color Contrast Parameter (ΔE)

  The color contrast parameter or ΔE is probably the best single indicator of the perceptibility of a plume due both to its contrast and its color with respect to a viewing background. ΔE is calculated for the entire visible spectrum and indicates how different the brightness and color of plume and background are. The larger the value of ΔE, the greater the perceptibility of the plume. Under ideal viewing conditions, when the viewing background is uniform and the plume is sharp-edged, a just perceptible ΔE would be one; for cases of plumes with diffuse edges, a just perceptible ΔE threshold would be greater than one, perhaps two (EPA, 1988).

2.1.7 Code Modifications

In 1989 (SAI, 1989), the PLUVUE II model was revised to include an interpolated scheme to calculate the phase functions which significantly decreased the execution time of the PLUVUE II computer code. The development of an interpolative scheme to calculate phase functions needed in the visibility model was performed by Richards and Hammarstrand (1988). The phase function calculation uses "lookup" tables which contain the phase functions for different particle size distributions. Further details concerning the phase function calculations are given in Section 2.3.

Details concerning the most recent modifications to the PLUVUE II algorithm are as follows:

- Under Pasquill-Gifford stability class A conditions, PLUVUE II was found to produce numerical overflows. Diagnostic checks indicated that the interpolation formula based on a series of logarithms to calculate σ_y and σ_z in PLUVUE II have a relatively large degree of error (especially for values of σ_z). In order to avoid the numerical overflows caused by the logarithmic equations, the subroutines used to calculate σ_y and σ_z in ISC2 (EPA, 1992) were substituted for the original PLUVUE II subroutines.

- The optical depth (called TAUP3) in subroutine PLMOBJ becomes negative and produces light amplification rather than attenuation along a line of sight when the observer and the object lies close to the plume. Initially PLUVUE II insures that the plume lies in the foreground of an object for the case where the azimuthal angle for the plume line of sight is 90°. However, this check was not conducted by PLUVUE II for angles other than 90° when the plume moves away from the observer and the distance to the object remains the same. As a result, the plume-observer distance (RP) exceeded the observer-object distance (RO). When this occurs, a negative optical depth (TAUP3) is estimated, which in turns results in light being amplified along the line of sight rather than being attenuated. Code has been added to PLUVUE II to check if RO is less than RP. If this occurs, then the following message is printed "You have placed the plume behind the background - stopped processing" and the program stops.

- When the scattering angle approaches the solar zenith angle near 45°, a PLUVUE II code check to avoid an inverse cosine argument outside the range (-1, 1) terminated many of the optical computations. Due to the conversion from radians to degrees plus other numerical manipulations, the distance calculations produce slight numerical arguments greater than 1.0 to the inverse cosine function. The numerical excesses were found to be of the order of less than one percent (-1.01, 1.01). As a result, for excesses less than two percent (1.000000 to 1.020000), the argument is now truncated to 1.00000 so that the estimates continue to be made. For excesses greater than two percent, should they occur, the optical estimations are stopped.

- The stability class supplied for intermediate distances seemed to be ignored by PLUVUE II. It was decided that the ability to change stability class with downwind distance should not be allowed; therefore, the option was disabled in PLUVUE II by setting NXSTAB to NX2+1 and INEW to I. NXSTAB (the index for downwind distance where stability changes from I (stability index) to INEW (secondary stability index)) and INEW are no longer input to PLUVUE II.

- The PLUVUE II model incorrectly predicted impacts for lines of sight with terrain background. It was discovered that there were errors in the PLUVUE II model when calculating the effects of multiple scattering because two of the three multiple scattering integral terms were missing from the algorithm. The corrected integral terms have been incorporated in the revised version of PLUVUE II.

In addition to the code modifications listed above, a number of cosmetic changes have been made to the code. Headers have been added to all subroutines. Unused variables and arrays, along with commented out statements, have been eliminated.

2.1.8 Input Data

The input data needed to run PLUVUE II are contained in one file of 80 byte, card-image records. As is discussed in Sections 2.2 and 3.2, the RUNPLUVU visibility modeling system allows the user to interactively edit the PLUVUE II input file. The PLUVUE II input data include the following parameters:

- Wind speed aloft or at the 10-m level
- Stability category
- Lapse rate
- Height of the planetary boundary layer (mixing depth)
- Relative humidity
- SO_2, NO_x, and particulate emissions rates
- Flue gas flow rate, exit velocity, and exit temperature
- Flue gas oxygen content
- Ambient air temperature at stack height
- Ambient background NO_x NO_2, O_3, and SO_2 concentrations
- Properties (including density, mass median radius, and geometric standard deviation) of background and emitted aerosols in accumulation (0.1-1.0 μm), coarse (1.0-10.0 μm), and carbonaceous aerosol size modes
- Coarse mode background aerosol concentration
- Background visual range or background sulfate and nitrate concentration
- Deposition velocities for SO_2, NO_x, coarse mode aerosol, and accumulation mode aerosol
- UTM coordinates of the source location
- Elevation of the source location
- UTM coordinates and elevation of the observer location for an observer-based analysis
- UTM zone for the site and observer locations
- Time, day, month, year, and time zone for the time and date of the simulation
- For an observer-based run, terrain elevation at the points along the plume trajectory at which the analysis will be performed
- For an observer-based run with white, gray, and black viewing backgrounds, the distances from the observer to the terrain that will be observed behind the plume
- For an observer-based run, the wind direction

The input data file also has numerous switches or flags to allow the user to select the particular subset of the complete model that is required. Table 1 lists the input parameters with formats, summary descriptions, and suggested values for some of the input parameters.

TABLE 1

DATA REQUIREMENTS FOR PLUVUE II

Card No.	Format	Variables	Description
1	A40	FILE1	Mie library filename
2	A40	FILE2	Binary output file #1
3	A40	FILE3	Binary output file #2
4	6A4	PLANT	Name of source
5	F5.1	U	Wind speed (mph)
	I5	I*	Stability index
	F5.2	ALAPSE	Ambient temperature lapse rate (°F/1000 ft)
6	I2	IUSFC*	Index for height for U (=1 for 7 m, 0 for effective stack height)
7	F10.0	YINITL*	Initial plume y-dimension for area source (m)
	F10.0	ZINITL*	Initial plume z-dimension for area source (m)
8	F10.1	HPBLM	Mixing depth (m)
9	F10.3	RH	Relative humidity (percent)
10	I5	IDIS*	Flag indicating diffusion parameters to be used for stability index I ("1" for TVA, "0" for Pasquill-Gifford-Turner values, "9" for user input values)
11	I2	IFLG1*	Flag for optics calculation of horizontal views with sky background*
	I2	IFLG2*	Flag for optics calculation with nonhorizontal views and sky background*
	I2	IFLG3*	Flag for optics calculation for white, gray, and black background*
	I2	IFLG4*	Flag for optics calculation along the plume centerline*
	I2	NX2	Index indicating the number of downwind distances desired (2 < NX2 < 16)

TABLE 1 (Continued)

DATA REQUIREMENTS FOR PLUVUE II

Card No.	Format	Variables	Description
	I2	NT1*	Starting index for the scattering angles used in the generic calculation (set to 1 when executing only observed-based calculations)
	I2	NT2*	Ending index for the scattering angles used in the plume-based calculation (set to 7 when executing only observer-based calculations)
	I2	NZF*	Index for the number of altitudes for visual impact calculations: "1" for plume centerline only, "2" for plume centerline and ground level downwind
	I2	NX3	Number of downwind points selected for optical size calculations (Recommended value is 0)
	I2	NX4	Number of downwind points selected for optical size calculations (Recommended value is 0)
	I2	NX5	Number of downwind points selected for optical size calculations (Recommended value is 0)
12	I2	IDILU*	Switch for printout of table for initial plume rise data
	I2	I1HFAU	Number of hundred points to use in generating vertical scans (Recommended value is 0)
	I2	I1DFAU	Number of tens and units of points to use in generating vertical scans (Recommended value is 0)
	I2	I2FAU	Stepping interval for printout of vertical scan (Recommended value is 0)
	I2	I3FAU	Option to select individual channel plots (Recommended value is 0)
	I2	I4FAU	FORTRAN output unit number (Recommended value is 0)
13	8F10.0	DIST(1)* I=1, NX2	Downwind distances for visibility impact calculations (2 < NX2 < 16) (2 cards for NX2 > 8)
14	8F10.0	DIST(1)(cont.)	
15	F10.2	QSO2	Total SO_2 emissions rate from all stacks in tons per day
	F10.2	QNOX	Total NO_x emissions rate from all stacks in tons per day

TABLE 1 (Continued)

DATA REQUIREMENTS FOR PLUVUE II

Card No.	Format	Variables	Description
	F10.2	QPART	Total primary particulate emissions rates from all stacks in tons per day
16	F10.1	FLOW	Flue gas flow rate (cfm) per stack
	F10.1	FGTEMP	Flue gas exit temperature (°F)
	F10.1	FGO2	Flue gas oxygen concentration (mole percent) [3]***
	F10.2	WMAX	Flue gas stack exit velocity (m/s)
17	F5.1	UNITS	Number of stacks
	F5.1	HSTACK	Stack height (feet)
18	F10.1	TAMB	Ambient temperature (°F)
19	F10.3	AMBNOX	Ambient [NO_x] in ppm [0]
	F10.3	AMBNO2	Ambient [NO_2] in ppm [0]
	F10.3	03AMB	Ambient [0_3] in ppm [0.04]
	F10.3	AMBSO2	Ambient [SO_2] in ppm [0]
20	F10.3	ROVA	Mass median radius (μm) for background accumulation mode aerosol [0.16]
	F10.3	ROVC	Mass median radius (μm) for background coarse mode aerosol [3.0]
	F10.3	ROVS	Mass median radius (μm) for plume secondary aerosol [0.10]
	F10.3	ROVP	Mass median radius (μm) of emitted primary particulate [1.0]

TABLE 1 (Continued)

DATA REQUIREMENTS FOR PLUVUE II

Card No.	Format	Variables	Description
21	F10.3	SIGA	Geometric standard deviation of background accumulation mode aerosol radius [2.0]
	F10.3	SIGC	Geometric standard deviation of background coarse mode aerosol radius [2.2]
	F10.3	SIGS	Geometric standard deviation of plume secondary aerosol radius [2.0]
	F10.3	SIGP	Geometric standard deviation of plume primary aerosol radius [2.0]
22	F10.3	DENA	Particle density (g/cm^3) of background accumulation mode aerosol [1.5]
	F10.3	DENC	Particle density (g/cm^3) of background coarse mode aerosol [2.5]
	F10.3	DENS	Particle density (g/cm^3) of plume secondary aerosol [1.5]
	F10.3	DENP	Particle density (g/cm^3) of emitted primary particulate [2.5]
23	F10.3	ROVCAR	Mass median radius (μm) for carbonaceous aerosol [0.05]
	F10.3	SIGCAR	Geometric standard deviation of carbonaceous aerosol radius [2.0]
	F10.3	DENCAR	Particle density (g/cm^3) of carbonaceous aerosol [2.0]
	F10.3	FRACTC	Carbonaceous aerosol fraction of plume primary aerosol [0.0]
	F10.3	AMBCAR	Background atmospheric carbonaceous aerosol ($\mu g/m^3$) [0.0]
24	F10.3	RFRSO4	Real part of index of refraction for accumulation mode aerosol [1.5]
	F10.3	RFISO4	Imaginary part of index of refraction for accumulation mode aerosol [0.0]
	F10.3	RFRCOR	Real part of index of refraction for background coarse mode aerosol [1.5]

TABLE 1 (Continued)

DATA REQUIREMENTS FOR PLUVUE II

Card No.	Format	Variables	Description
	F10.3	RFICOR	Imaginary part of index of refraction for background coarse mode aerosol [0.0]
25	F10.3	RFRPRM	Real part of index of refraction for emitted primary aerosol [1.5]
	F10.3	RFIPRM	Imaginary part of index of refraction for emitted primary aerosol [0.0]
	F10.3	RFRCAR	Real part of index or refraction for carbonaceous aerosol [2.0]
	F10.3	RFICAR	Imaginary part of index of refraction for carbonaceous aerosol [1.0]
26	F10.3	CORAMB	Ambient coarse mode aerosol concentration ($\mu g/m^3$)
27	I5	INTYP*	Switch for next card (=1 for $AMBSO_4$ and $AMBNO_3$, $\neq$ 1 for RVAMB)
28a (INTYP=1)	F10.3	AMBSO4	Ambient background sulfate mass concentration ($\mu g/m^3$)
	F10.3	AMBNO3	Ambient background nitrate mass concentration ($\mu g/m^3$)
28b(INTYP≠1)	F10.3	RVAMB	Ambient background visual range (km)
29	F5.2	VDSO2	SO_2 deposition velocity (cm/sec) [1]
	F5.2	VDNOX	NO_x deposition velocity (cm/sec) [1]
	F5.2	VDCOR	Coarse mode aerosol deposition velocity (cm/sec) [0.1]
	F5.2	VDSUB	Accumulation mode aerosol deposition velocity (cm/sec) [0.1]
30	I5	ICON*	Index for SO_2-to-$SO_4^=$ conversion rate added to rate predicted from OH chemistry. ICON = 0 for conversion rate, set constant with distance from source. ICON = 1 for separate values for each point of analysis downwind of the source [0]
31	F10.7	RSO2C*	Rate constant for SO_2-to-$SO_4^=$ conversion to be added to prediction from OH chemistry (%/hr) [0.0]

TABLE 1 (Continued)

DATA REQUIREMENTS FOR PLUVUE II

Card No.	Format	Variables	Description
A-1** (If ICON = 1)	8F10.7	RSO2(NX)+ NX=1,8	SO_2-to-$SO_4^=$ conversion rates to be added to predictions from OH chemistry at each point of analysis on plume (%/hr)
A-2** (continuation of A-1)	8F10.7	RSO2(NX),+ NX=9,NX2	(Continuation as needed)
32	I5	NC1+	Index to control type of calculations. NC1=1 for plume-based calculations, 2 for observer based calculations only
	I5	NC2+	Index to control calculations NC2=1 for plume-based calculations only, 2 for observer-based calculations
A-3** (If NC1=1)	612	NPP+	Indices for controlling the subset of results (from plume-based calculations of horizontal views with sky, white, gray and black backgrounds) to be written to a file for later use by the VISPLOT program for generating plots. NPP controls the distance from the observer to the plume for sky background [3]
		NAP+	Index for selecting the horizontal azimuthal angle α between the line of sight and the plume trajectory for plots of results for sky backgrounds [4]
		NTP+	Index for selecting the scattering angle of plume-based data to be plotted
		NZP+	Index for selecting the level of the line of sight through the plume for plume-based data to be plotted [3]
		I01P+	Index for selecting the distance from the observer to the background object for the plume-based data to be plotted
		IPP+	Index for selecting the distance from the observer to the plume for plume-based plot data with background object views
A-3** (If NC2=2)	F10.1	XOBS	UTM x-coordinate of observer position (km) for observer-based calculations
	F10.1	YOBS	UTM y-coordinate of observer position (km)
	F10.1	ZOBS	Elevation (ft MSL) of observer position

TABLE 1 (Continued)

DATA REQUIREMENTS FOR PLUVUE II

Card No.	Format	Variables	Description
33	F10.1	XSTACK	UTM x-coordinate of source (km)
	F10.1	YSTACK	UTM y-coordinate of source (km)
	F10.1	ZSTACK	Elevation of source location (ft MSL)
34	I5	IZONE	UTM grid zone number within which source is located
	I5	IMO	Number of month for date of simulation
	I5	IDAY	Day of month for date of simulation
	F5.0	TIME	Time of day (24-hr clock)
	F5.0	TZONE*	Time zone number
	I5	IYEAR	Year for date of simulation
A-4** (If NC2=2)	8F10.1	TER(NX),* NX=1,8	Elevation of terrain at the selected points downwind of the source along the plume trajectory (ft MSL) (for observer-based calculation)
A-5** (If NC2=2)	8F10.1	TER (NX), NX=9,NX2	(Continuation as needed)
A-6** (If NC2=2)	8F10.1	ROBJCT(NAZ), NAZ=1,8*	Distances in kilometers from observer to background terrain for observer azimuths of 15°, 30°, 45°, 60°, 75°, 90°, 105°, 120°
A-7** (continuation of A-4)	8F10.1	ROBJCT(NAZ), NAZ=9,16	Distances for azimuths of 135°, 150°, 165°, 180°, 195°, 210°, 225°, 240°
A-8** (continuation of A-5)	8F10.1	ROBJCT(NAZ), NAZ=17,24	Distances for azimuths of 255°, 270°, 285°, 300°, 315°, 330°, 345°, 360°
A-9** (If NC2=2)	F10.1	WIND*	Wind direction azimuth (degrees from North)
A-10** (If IDIS=9)	F5.1	SY*	Dispersion parameters in meters,

TABLE 1 (Continued)

DATA REQUIREMENTS FOR PLUVUE II

Card No.	Format	Variables	Description
(to A-10** + NX2)	F5.1	SZ+	one card for each distance

---

* "0" if table is not desired, "1" if desired.

** "A-n" refers to cards that are optional. They are inserted only when values of prior flags or indices are set to require additional input data, e.g., when ICON=1, cards A-1 and A-2 are required.

*** Suggested values for some of the input parameters are shown in brackets.

+ More details given in Section 2.1.8.

Some of the options listed in Table 1 are further described below:

The parameter IUSFC is simply a flag to allow the wind speed to be input at the effective stack height (IUSFC = 0) or at the common 10-m instrument height (IUSFC = 1).

IFLG1 is a flag that allows the user to select or skip the calculation of visibility impairment of the plume for horizontal views with a clear sky background. IFLG2 allows the user to select or skip the calculation of visibility impairment for nonhorizontal views and clear sky background. IFLG3 allows the user to select or skip the calculation of visibility impairment calculations of the plume as seen in front of white, gray, and black backgrounds. IFLG4 allows the user to select or skip the visibility impairment calculation for an observer looking straight down the centerline of various segments of the plume or for an observer looking across the plume at a small acute angle to the plume centerline. For all of these, a value of 1 executes the calculations and a value of 0 branches around them.

NZF is a switch that indicates whether the visibility impairment calculations will be made for the plume centerline altitude only (NZF = 1) or for both the plume centerline and ground level (NZF = 2).

IDILU is a switch that controls the printing of the table of initial plume rise data. If IDILU = 0, the table is not printed, and if IDILU = 1, it is printed.

INTYP is a switch that allows the user to calculate the background visual range (INTYP = 1) from user-input background coarse mode aerosol concentrations and background sulfate and nitrate concentrations. If INTYP $\neq$ 1, the user inputs the background visual range and the background coarse mode aerosol concentration, and the model computes the background accumulation mode aerosol concentration that would be needed to cause the given visual range.

ICON is a switch that allows the user to select the conversion rate of SO_2 to $SO_4^=$, in addition to the rate calculated by the OH· model, as a constant with distance from the source (ICON = 0) or as a separate value for each point of analysis downwind from the source (ICON = 1). These conversion rates are in units of percent per hour. RSO2C gives the constant conversion rate for all points on the plume trajectory, while RSO2 gives the downwind-distance-dependent conversion rates for each point of analysis.

The parameters NC1 and NC2 are used to control whether the visibility impairment calculations are done for a plume-based scheme, an observer-based scheme, or both. NC1 set to 1 executes the plume-based calculations and NC2 set to 2 calculates the observer-based calculations. If NC1 is set to 1 and NC2 is set to 2, both types of calculations will be made. If NC1 is set to 1 and NC2 is set to 1, only the plume-based calculations will be made. Finally, if NC1 is set to 2 and NC2 is set to 2, only the observer-based calculations will be made.

The stability index I specifies the stability category for the plume dispersion parameters: I = 1 for stability A, I = 2 for stability B, I = 3 for stability C, etc.

NT1 and NT2 assign the starting and ending indices for the scattering angle array used for the plume-based visibility impairment calculations. With NT1 = 1 and NT2 = 7, the default scattering angles (22°, 45°, 90°, 135°, 158°, and 180°) are used. These angles are taken from the array TT, which has 0°, 22°, 45°, 90°, 135°, 158°, and 180° as its first seven elements. NT1 is one less than the actual starting index of TT, while NT2 corresponds to the actual ending index of TT. For a run with calculations for 90° only, set NT1 to 3 and NT2 to 4. For a run with calculations for 90° 135°, 158°, and 180°, set NT1 to 3 and NT2 to 7.

The index NX2 defines the number of points downwind along the plume trajectory where visibility impairment calculations will be made. The value of NX2 should be at least 2, but not greater than 16.

The array DIST specifies the distance downwind from the source along the plume trajectory of each point where visibility impairment calculations will be made. The units for this array are kilometers. For accurate prediction of the oxidation of NO_x to NO_2, it is important to use downwind distances that are close together and near the source. The first downwind distance must be 1 km; 2.5 km, 5 km, and 10 km are recommended for the succeeding three distances. The user is free to select the remaining points according to the needs of the situation.

YINITL and ZINITL are used for area sources and define the initial lateral and vertical dimensions of the plume. For emissions from stacks, both YINITL and ZINITL should be set to zero. The units for these two variables are meters.

When plume-based calculations are complete, a subset of the results must be selected for output to a binary file which may be used for further analysis such as plotting. The six indices listed on card A-3 determine the subset of results that will be written to the binary file. NPP selects the distance from the observer to the plume in the following manner:

NPP	Distance from Observer to Plume (fraction of background visual range)
1	0.02
2	0.05
3	0.10
4	0.20
5	0.50
6	0.80

NAP determines the horizontal azimuthal angle alpha between the plume centerline and the line of sight for a sky background:

NAP	Alpha (degrees)
1	30°
2	45°
3	60°
4	90°

NTP selects the scattering angle between the direct solar beam and the line of sight from the point of analysis to the observer. The value of NTP must be greater than or equal to NT1 and less than or equal to (NT2-1). The values of NTP for each of the six scattering angles are shown below:

NTP	Scattering Angle (degrees)
1	22°
2	45°
3	90°
4	135°
5	158°
6	180°

NZP selects the results for calculations of views through the center of the plume or views at ground level across the plume trajectory. The values of NZP are limited by the value of NZF (card no. 8). If NZF = 1, the calculations are done only for views through the plume centerline, and NZP must be set to 3. If NZF = 2, NZP may be set to 3 for values from calculations for views through the plume centerline, or NZP may be set to 6 for values from calculations for views at the surface through the plume trajectory. The index IPP selects the distance from the observer to the plume for plotting results of the calculations for views with white, gray, and black objects behind the plume. The values of IPP correspond to the distances shown below:

IPP	Distance from Observer to Plume (fraction of background visual range)
1	0.02
2	0.05
3	0.10
4	0.20
5	0.50
6	0.80

IO1P is used to select the distance from the observer through the plume to the white, gray, and black background objects behind the plume. The value of IO1P is limited by the value of IPP because the object background can be no farther than a distance equivalent to 80 percent of the background visual range from the observer. If IPP = 1, the range of values of IO1P is shown below:

IO1P	Distance from Observer to Object (fraction of background visual range)
1	0.02
2	0.05
3	0.10
4	0.20
5	0.50
6	0.80

When IPP = 2, the values IO1P available are as follows:

IO1P	Distance from Observer to Object
1	0.05
2	0.10
3	0.20
4	0.50
5	0.80

When IPP = 3, IO1P is limited to one of the following values:

IO1P	Distance
1	0.10
2	0.20
3	0.50
4	0.80

When IPP = 4, IO1P is limited to these three values:

IO1P	Distance
1	0.20
2	0.50
3	0.80

When IPP = 5, IO1P is limited to only two values:

IO1P	Distance
1	0.50
2	0.80

When IPP = 6, IO1P must be set to 1, which corresponds to a distance from the observer to the background object of 0.80 of the background visual range. These six indices do not place any restrictions on the calculations made by PLUVUE II, but they provide a means of selecting the desired subset of results to be saved for plotting.

The UTM coordinates and elevations for observer and source locations and the UTM grid zone numbers are taken from standard USGS maps. TZONE is the number of the time zone, with the Greenwich Meridian defined as 0. Values of TZONE are shown below:

Time Zone	Standard Time	Daylight Time
Eastern	5	4
Central	6	5
Mountain	7	6
Pacific	8	7

The array TER gives the elevation of terrain at each point downwind for the visibility analysis. For the purpose of calculating plume-observer-sun geometry only, the plume centerline is assumed to rise above any terrain higher than the source elevation in order to maintain the same effective height above the terrain for all points downwind. If the terrain is flat or if it is desirable to maintain the same plume elevation at all points, use zero for all TER values. The model will then set all terrain elevations to the elevation of the source location.

The ROBJT array allows the user to define the distances from the observer to the background terrain. These distances are read in for observer azimuths of from 15° to 360° in

15° increments. The distances are measured in kilometers by creating a terrain profile for each azimuth and determining the point at which the line of sight intersects the terrain. The observer-based calculations can be performed without measuring these values by setting all elements of the ROBJT array to zero. The background object distance will then be set to the observer-to-plume distance for each line of sight. WIND is the direction from which the wind is blowing, expressed in degrees.

For user-defined values of plume dispersion parameters (IDIS = 9), SY and SZ are read for each downwind distance. SY is the plume concentration horizontal standard deviation and SZ is the plume concentration vertical standard deviation in meters.

2.2 PLUIN2

The PLUIN2 computer algorithm (Richards and Hammarstrand, 1988) prepares data files of the format required for input to the revised PLUVUE II visibility model. PLUIN2 is designed to be "user friendly" and has the purpose of simplifying and speeding up the process of preparing input files to PLUVUE II. PLUIN2 is useful for both the user new to PLUVUE II, who desires assistance understanding the required inputs and does not wish to learn the details of the required data formats, as well as the experienced user who frequently prepares PLUVUE II input files and finds that PLUIN2 can shorten the time required for the work.

PLUIN2 is executed within RUNPLUVU when the user wishes to modify an existing PLUVUE II input file. As is discussed in Section 3.2, the user must supply the name of an existing input data file. This file can be either one which was previously prepared and is to be modified, or the data file (TEST.INP) supplied with the RUNPLUVU system diskette. The user will be asked the filename which contains the revisions (the filename can be the same as the input filename) which will then automatically be used as the input file to PLUVUE II. While modifying a file using the PLUIN2 portion of RUNPLUVU, the user will be issued a series of prompts describing the information represented by each quantity in the input data file and its current value. If the current value is satisfactory, it can be accepted with a carriage return. If not, a new value may be entered. If only a few data values in the input file are to be changed, it is possible to branch to the location of the data to be changed, enter the new values, and then branch to the end of the PLUIN2 portion of RUNPLUVU. It is possible to branch to any input data at any time while modifying a data file, so it is easy to review and alter data. Further details concerning branching and the use of PLUIN2 within RUNPLUVU are given in Section 3.2.

2.3 MIETBL

2.3.1 Scattering Theory

The following general discussion of scattering of solar radiation is primarily from Wallace and Hobbs (1977). The fraction of parallel beam radiation that is scattered when passing downward through a layer of infinitesimal thickness dz is described as

$$ds_\lambda \equiv \frac{dE_\lambda}{E_\lambda} = K A \sec \phi \, dz \tag{46}$$

where K is a dimensionless coefficient, A is the cross-sectional area that the particles in a unit volume present to the beam of incident radiation, and ϕ is the zenith angle. If all the particles which the beam encounters in its passage through the differential layer were projected onto a plane perpendicular to the incident beam, the product A sec ϕ dz would represent the fractional area occupied by the particles. Thus, K plays the role of a scattering area coefficient which measures the ratio of the effective scattering cross section of the particles to their geometric cross section. On any given occasion a variety of particle shapes and a whole spectrum of particle sizes are likely to be present simultaneously. For the idealized case of scattering by spherical particles of uniform radius r, the scattering coefficient K can be prescribed on the basis of theory. It is convenient to express K as a function of a dimensionless size parameter $\alpha = 2\pi r/\lambda$, which is a measure of the size of the particles in comparison to the wavelength of the incident radiation. Figure 8 shows a plot of α as a function of r and λ.

The scattering area coefficient K depends not only upon the size parameter but also upon the index of refraction of the particles responsible for the scattering. Figure 9 shows K as a function of α for two widely differing refractive indices.

For the special case of $\alpha << 1$ (the extreme left-hand side of Figure 9), Rayleigh showed that, for a given value of refractive index, $K \propto \alpha^4$ and the scattered radiation is evenly divided between the forward and backward hemispheres. It can be seen from Figure 8 that the scattering of solar radiation by air molecules falls within this so-called Rayleigh scattering regime.

When α is greater than about 50 (the value of the abscissa at the extreme right-hand side of Figure 9), $K \approx 2$ and the angular distribution of scattered radiation can be described by the principles of geometric optics.

For intermediate values of the size parameter between about 0.1 and 50, the scattering phenomenon must be described by Mie (e.g. Gustav Mie, a German physicist who carried out fundamental studies on the theory of electromagnetic scattering and kinetic theory). Within this so-called Mie regime, K exhibits the oscillatory behavior as shown in Figure 9. The angular distribution of scattered radiation is very complicated and varies rapidly with α,

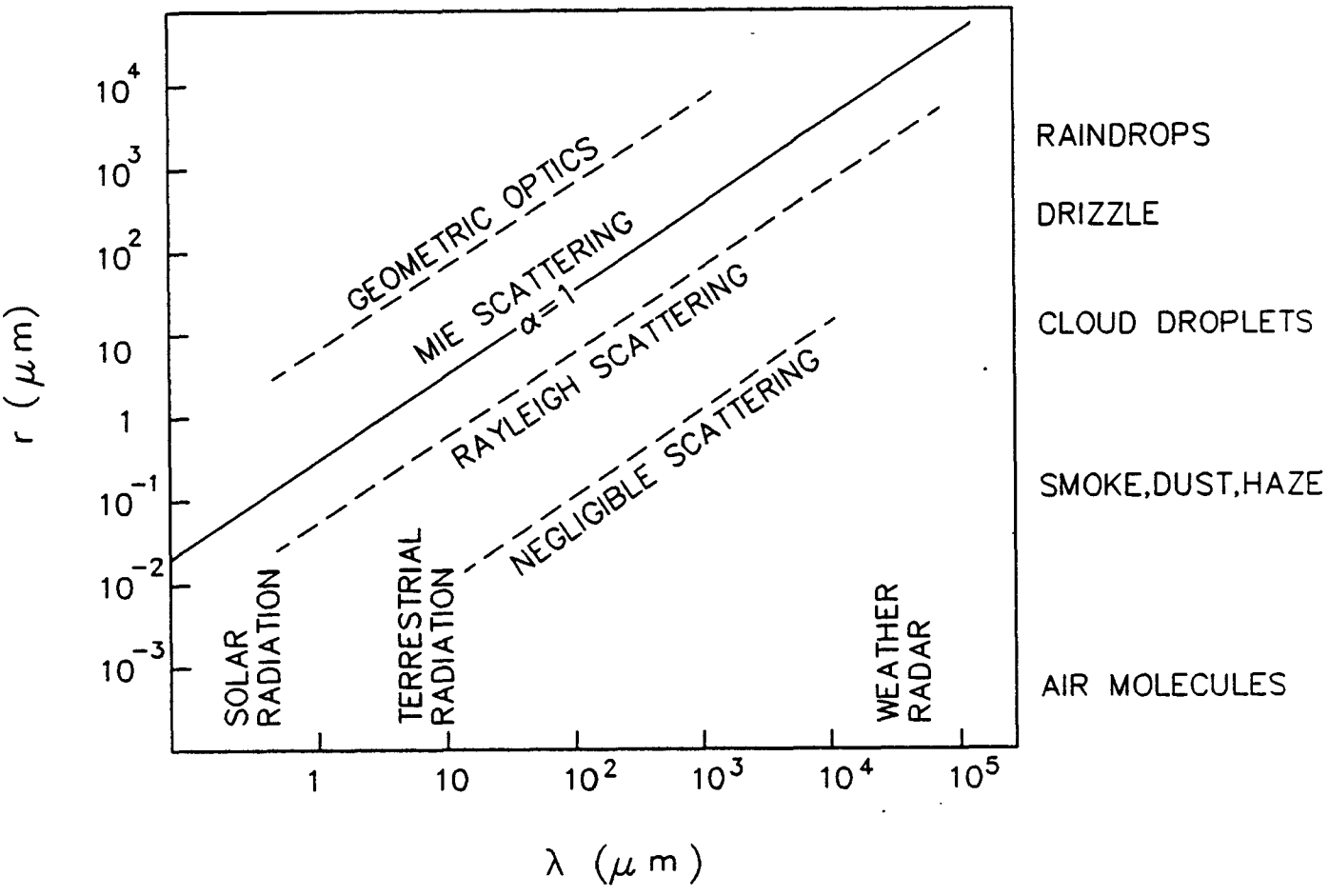

Figure 8. Size parameter α as a function of wavelength of the incident radiation and particle radius (Wallace and Hobbs, 1977).

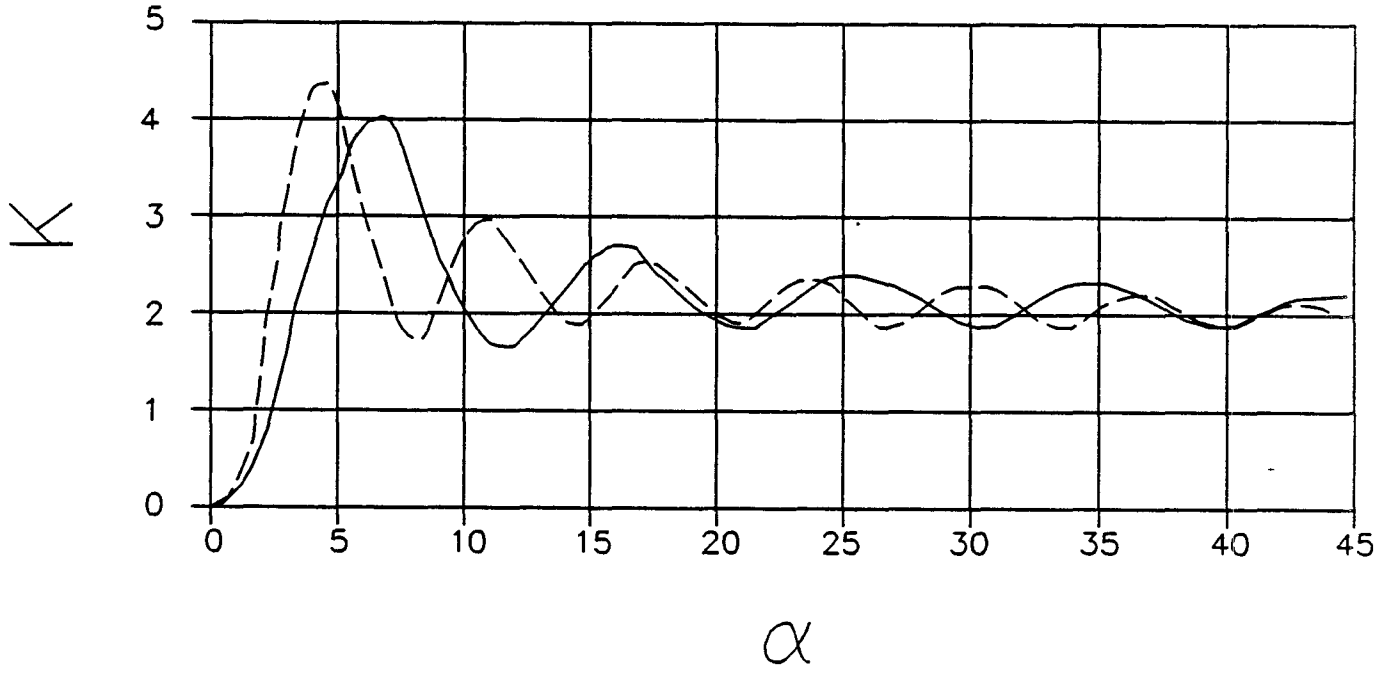

Figure 9. Scattering area coefficient K as a function of size parameter α for refractive indices of 1.330 (___) and 1.486 (- - -) (Wallace and Hobbs, 1977).

with forward scattering predominating over back scattering. The scattering of sunlight by particles of haze, smoke, smog, and dust usually falls within the Mie regime. If the particles are rather uniform in size, the scattered sunlight may be either bluish or reddish in hue, depending upon whether $\delta K/\delta\alpha$ is positive or negative a the wavelengths of visible light. Usually such particles exhibit a spectrum of sizes wide enough to span several maxima and minima in the plot of $K(\alpha)$, thus rendering the scattered light neutral or whitish in color.

2.3.2 Mie Calculations

There are only two quantities which need to be known about an isotropic, homogeneous sphere in order to calculate all of its light scattering properties: the relative index of refraction (m-ik), where m is the real and ik is the imaginary portion of the index of refraction, and the size parameter (α). The relative index of refraction is the index of refraction of the particle divided by the (real) index of refraction m_o of the medium in which it is imbedded. Since the index of refraction of the particle may have a real part, which, for example, describes the bending of light at its surface, and an imaginary part, which describes the absorption, the relative index of refraction will, in general, be complex. It is possible for m to be less than unity; and when there is no absorption, k is equal to zero.

The size parameter α is given by

$$\alpha = \frac{2\,\pi\,r}{\lambda} = \frac{2\,\pi\,r\,m_o}{\lambda_o} \quad , \tag{47}$$

where r is the particle radius, λ is the wavelength of light in the medium, and λ_o is the wavelength of light in a vacuum.

Let I_o be the irradiance of collimated light falling on the sphere (measured in units of energy per area), and I be the irradiance of scattered light measured in units at a large distance b from the sphere. In general, the directions of the incident and scattered light define a plane. If the incident light is plane polarized so that the electric vector is perpendicular to this plane, all of the scattered light will also be plane polarized with the electric vector perpendicular to the plane. The relation between the intensities is given by

$$I_r = \frac{i_1}{k^2\,b^2}\,I_{or} \quad , \tag{48}$$

where i_1 is a dimensionless quantity calculated from the Mie equations, and $k = 2\pi/\lambda$. Here the subscript r specifies the polarization, and is the last letter of perpendicular. The angle θ through which the light has been scattered does not appear in Equation (48), but i_1 is a function of this angle. It is customary to choose $\theta = 0°$ for the unscattered beam, and $\theta = 180°$ for light which is scattered directly backwards. As mentioned earlier, i_1 also depends on the relative refractive index and α, but on no other variables.

If the incident light is polarized parallel with the plane, all of the scattered light is also polarized parallel, and a similar relation is written

$$I_l = \frac{i_2}{k^2 b^2} I_{al} \quad , \tag{49}$$

where the subscript l is the last letter of parallel. If the incident light is unpolarized, then we may regard it as being made up of equal parts of the above two polarizations and obtain

$$I = \frac{i_1 + i_2}{2 k^2 b^2} I_o \quad . \tag{50}$$

Since i_1 and i_2 are in general not equal and the scattered light of the two polarizations have various phase differences, the scattered light is, in general, elliptically polarized. For most work, the three relations just given provide all the information on intensities and polarization that is desired. However, the MIETBL algorithm also calculates the phase difference δ between the parallel and perpendicular scattered radiation, where δ is positive if the parallel electric field lags the perpendicular field. Anyone interested in this phase difference should refer to page 36 of van de Hulst (1957).

In general, four numbers are necessary and sufficient to specify the polarization of a beam of light, and the four Stokes parameters are convenient for this purpose. Chandrasekhar (1950) gives an excellent introduction to these parameters and their properties (see pages 24 to 36), and it is recommended that anyone interested in more than unpolarized light should read these pages.

The irradiance of the scattered light is strictly proportional to the intensity of the incident light. Therefore, the total amount of energy scattered can be represented as a constant times the intensity of the incident light. This constant, which is called the scattering cross section, has the dimensions of area, and can be thought of as the area which would intercept a quantity of light equal to that which is scattered.

Since Equation (50) gives the intensity of light scattered in any direction, it is possible to integrate it over all directions and find the total amount of light scattered, and hence the scattered cross section C_{sca}. The result is

$$C_{sca} = \frac{\pi}{k^2} \int_0^{\pi} (i_1 + i_2) \sin \theta \, d\theta \quad . \tag{51}$$

A dimensionless quantity Q_{sca} can be obtained by dividing Q_{sca} by the cross section of the sphere

$$Q_{sca} = \frac{C_{sca}}{\pi r^2} \quad , \tag{52}$$

and this quantity is sometimes called an efficiency factor. In practice, the computer programs are always set up to calculate Q_{sca} directly. The quantities i_1 and i_2 are calculated separately if they are desired.

In a similar way, we can define the absorption cross section C_{abs} as the total amount of light absorbed divided by the incident light irradiance, and the absorption efficiency is

$$Q_{abs} = \frac{C_{abs}}{\pi r^2} \quad . \tag{53}$$

The total amount of light both scattered and absorbed is given by the extinction cross section

$$C_{ext} = C_{sca} + C_{abs} \quad . \tag{54}$$

Also

$$Q_{ext} = \frac{C_{ext}}{\pi r^2} = Q_{sca} + Q_{abs} \quad . \tag{55}$$

The MIETBL algorithm calculates Q_{ext} and Q_{sca} from the Mie equations, then evaluates Q_{abs} by taking the difference. Therefore, in practice, it is possible for Q_{abs} to have negative values about the size of the round off error of the computer.

The book by Kerker (1969) gives an overview of light scattering by particles.

2.3.3 Accuracy of the Interpolated Results of Mie Calculations

One problem that had to be overcome to permit the separation of the Mie calculations from PLUVUE II is that the strength of the aerosol light scattering must be determined at each of the various scattering angles required by each of the sun-plume-observer geometries.

In MIETBL, the strength of the aerosol light scattering at the desired angles is determined by linear interpolation using data tabulated every 2°.

To calculate the light scattering properties of a log-normal size distribution of aerosol particles, it is necessary to perform Mie calculations for a number of different particle sizes in the size range of interest. These results are then averaged using weighting factors derived from the relative numbers of particles of each size in the log-normal particle size distribution.

For large particles, averaging over particle sizes is important because the angular distribution of light scattered by a single size of particles shows many peaks and valleys. When results for only a few sizes of particles are averaged, some of these peaks and valleys persist. However, when calculated results for many different particle sizes are weighted according to a log-normal distribution and averaged, the angular distribution of scattered light becomes quite smooth.

The default aerosol properties for PLUVUE II which are contained in the Mie default library are listed in Table 2. The data were obtained from a listing of input parameters presented in an earlier version of the PLUVUE II User's Manual (Seigneur et al., 1983). These six aerosol size distributions provide a compact data set that may be used when no better aerosol size distribution data are available. When using this default library, the only choice to be made is aerosol diameter (D) = 0.2 μm for the plume secondary aerosol in polluted or humid areas (e.g., east of the Mississippi) or D = 0.1 μm in clean or dry areas (e.g., the clean areas in the west or Alaska).

2.4 Comparison of Revised PLUVUE II with Original PLUVUE II

A comparison of the original version of PLUVUE II with the revised version for different stability classes is presented in Table A-1 in the Appendix. The example used is the same as that provided with the original version of the PLUVUE II User's Manual. The calculations are made at a downwind distance of 9 km. Four different visibility parameters: visual range reduction, blue-red ratio, plume contrast, and ΔE are compared for six different stability classes (SC = A, B, C, D, E, and F). Four different backgrounds are examined: sky, white, gray, and black. As shown in Table A-1, the differences between the two versions of PLUVUE II are minimal and are primarily due to the changes in the methods for calculating σ_y and σ_z (see explanation in Section 2.1.7). Due to numerical underflows associated with the calculation of σ_y and σ_z, the original version of the model did not run for a number of attempted tests.

TABLE 2

DEFAULT AEROSOL PROPERTIES FOR PLUVUE II

Particle Type	Size Parameters Radius (μm)	Diameter (μm)	Sigma	Density (g/cm^3)	Index of Refraction Real	Imaginary
Background Accumulation Mode	0.15	0.3	2.0	1.5	1.5	0.0
Background Coarse Mode	3.0	6.0	2.2	2.5	1.5	0.0
Plume Secondary	0.1	0.2	2.0	1.5	1.5	0.0
Plume Primary	1.0	2.0	2.0	2.5	1.5	0.0
Carbonaceous	0.05	0.1	2.0	2.0	2.0	1.0

3.0 USER INSTRUCTIONS

This section describes the basic computer requirements which are necessary to use the RUNPLUVU system, detailed operating instructions, and a Level-3 plume visibility example.

3.1 Computer Requirements

The basic computer requirements for using the RUNPLUVU software are as follows:

- 80386 or higher processor
- > 1 MB of RAM
- Hard Disk with sufficient storage space to handle the executable file, input data files, and output files (file sizes will vary depending on application)
- Math coprocessor (80 x 87 chip)

The amount of memory available on any particular PC will depend on the machine configuration including the amount of memory used by the operating system, memory used by any special device drivers, and any utility programs resident in memory. The amount of memory needed to actually run the software will be somewhat larger than 1 MB because additional memory is needed for buffers when the program opens files.

RUNPLUVU is compiled using Lahey F77L-EM/32 Version 5.0. This is the extended memory version for 32-bit computers. This will only run on 386 or higher PCs with more than 640K memory.

3.2 Operating Instructions for RUNPLUVU

In this section, shaded text denotes what will appear on the computer screen during the RUNPLUVU session. All the data files on the RUNPLUVU diskette should be loaded onto your personal computer's hard drive. It is recommended that a separate working directing be used. While using RUNPLUVU, you have the option of aborting the program at any time by pressing the control (Ctrl) and "C" key (e.g., Ctrl-C) at the same time.

To start a session, the user simply types RUNPLUVU:

RUNPLUVU

The following brief description of the run command system will immediately appear on the screen:

PLUVUE II Run Command System

A program designed to assist the user with the application
of the PLUVUE II visibility model by allowing the user to:

1) Prepare an input file or to specify a previously prepared file,

2) Select or create a library of Mie calculations for input to PLUVUE II,

3) Run PLUVUE II

Press ENTER to Continue

After the user presses the ENTER key, the following prompt will appear:

Do you wish to modify an existing PLUVUE II input file (Y or N)?

If the user responds no (using "N" or "n"), then the user will be prompted to enter the name of an existing PLUVUE II input file:

Do you wish to use an existing PLUVUE II input file (Y or N)?

If the user responds yes (using "Y" or "y"), then the user will be prompted for the name of a PLUVUE II input file to modify:

Enter the PLUVUE II input file name (up to 24 characters):
XXXXXXXXXXXXXXXXXXXXXXXX = 24 characters

The software will check to make sure the file exists. If the file does not exist, then the following message will appear:

Error opening file. File does not exist. Try again.

and the user will then be prompted again for the PLUVUE II input file name. Use the CONTROL-C command to abort the program if the file cannot be located.

If the user responds yes (using "Y") to the prompt concerning whether or not an existing PLUVUE II input file needs to be modified, then the code enters into the PLUIN2 section of RUNPLUVU. The following messages will appear on the screen:

08:39:12 09/15/92

PLUIN2

A program to assist in the preparation of input
data files for PLUVUE II.

Based on PLUIN1, Written by J.A. McDonald and L. W. Richards
for WEST Associates.

PLUIN2 written by R. G. M. Hammarstrand and L. W. Richards
for use on PC compatible computers.
Funding provided by the NPS and the EPA.

Enter drive and path where data files are located.
(Carriage return to select default directory).
XXXXXXXXXXXXXXXXXXXXXXXXXXXXXXXXXXXXXXXXXXXXXXXXXX
= 50 characters maximum.

Once the user has typed the full path name (e.g., C:\A248\RUNPLUVU) of where the data files are located, a listing of the files in that directory will appear as follows:

```
 Volume in drive C is VOL1
 Volume Serial Number is 0180-FC67
 Directory of C:\A248\RUNPLUVU

DEFAULT  MIE      43891 07-29-92   1:58p
DEFAULTM LST        605 07-29-92   1:58p
TEST               11479 09-08-92   4:33p
TEST1    INP        1084 09-14-92   5:27p
TEST1    OUT       11479 09-14-92   5:29p
TEST2    INP        1084 09-15-92   8:40a
F77L3    EER       40584 05-29-92  11:54a
LIST     OUT        9198 09-15-92   8:40a
LIST2    OUT           0 09-15-92   8:41a
MIETBL   EXE      281152 08-13-92   8:27a
PLUIN2   EXE      297708 09-08-92   4:31p
PLUVUE   INP        3218 09-15-92   8:40a
PLUVUE   OUT       11479 09-14-92   5:29p
PLUVUE7  BIN        1049 09-14-92   5:29p
PLUVUE8  BIN           1 09-08-92   4:25p
PV2NEW   EXE      685076 08-13-92   8:25a
README               449 08-13-92   5:07p
RUNPLUVU EXE      252044 08-13-92   9:26a
SCRATCH              115 09-15-92   8:40a
Press any key to continue . . .

(continuing C:\A248\RUNPLUVU)
SCRATCH2              65 09-15-92   8:40a
TEST3    INP        1011 08-07-92  11:13a
TEST3    OUT       11479 08-07-92  11:14a
TEST4    INP        1084 09-08-92   4:33p
       23 file(s)    1665334 bytes
                    58511360 bytes free
```

If there are more than 18 files in the directory, the user must press any key to continue listing the files. Once all the files in the directory have been listed, the user must then select the PLUVUE II input file to be modified and an output file which will contain the modifications. This output file will be the PLUVUE II input file which will later be used by RUNPLUVU.

Enter input filename, 12 characters maximum.
XXXXXXXX.XXX

Enter filename which contains revisions. 12 characters maximum.
(The filename can be the same as the input filename listed above.)
XXXXXXXX.XXX

If the name entered for the output file is already in use, the user is warned. If the user responds with "y" for yes in response to the warning, the new output file will overwrite the existing file. It is possible to use the same name for the both the input and output files, so it is possible to correct a minor error in an input file without the necessity of changing the file name.

The user will then be notified that a new file is being opened. The user is now ready to modify the file:

Opening new file c:\a248\runpluvu\test3.inp

NOTES:

A <RETURN> accepts the current value.

Entering "goto n" or "GOTO n" instead of any data value will cause a branch to ENTRY CODE n.

Each entry code corresponds to a line in the data file, but options in the input parameters make it so the nth entry code may not generate the nth line of data.

Press ENTER to continue ...

Once the user presses the enter key, each entry code of the PLUVUE II input file will appear, for example, as follows:

ENTRY CODE 1

Plant Name (up to 24 characters): Test Case
XXXXXXXXXXXXXXXXXXXXXXXX = 24 characters

ENTRY CODE 2

Wind speed: 10.0 mph

Stability index: 6.
For Pasquill-Gifford stability classes, use 1. for class A,
2. = B, 3. = C, 4. = D, 5. = E, 6. = F, AND 7. = G

Ambient temp. lapse rate:-4.00 deg F per 1000 ft.

Each line of data in the PLUVUE II input data file is identified with an entry code. It is possible to branch to any of these lines at any time during the modification of a file by typing GOTO nn where nn is the entry code number of the desired line. The values of the entry codes are summarized as follows:

Entry Code	Input Data Summary
1	Plant name
2	Wind speed, stability, lapse rate
3	Wind speed measurement height flag
4	Initial plume dimensions
5	Mixing height
6	Relative humidity
7	Diffusion parameter flag
8	Calculation flags
9	Print out flags
10	Downwind distances
11	Emission rates
12	Stack parameters
13	Stack height
14	Ambient air temperature
15	Ambient pollutant concentrations
16	Mass mean radii for aerosol size distributions
17	Geometric standard deviation of aerosol size distributions
18	Density of aerosol material
19	Carbonaceous aerosol information

Entry Code	Input Data Summary
20	Indices of refraction for background aerosol
21	Indices of refraction for primary and carbonaceous aerosols
22	Background coarse mode aerosol concentration
23	Background sulfate/nitrate flag
24	Ambient background visual range
25	Not in use
26	Deposition velocities
27	Sulfur dioxide to sulfate conversion flag
28	Rate of sulfur dioxide to sulfate conversion
29	Not in use
30	Calculation flag
31	Not in use
32	Observer coordinates
33	Stack coordinates
34	Time zone
35	Terrain elevation
36	Background object distances
37	Wind direction
38	Not in use
39	Save current values

Various options in PLUVUE II cause the number of lines in the input file to vary. Therefore, entry code 15 may not write the 15th line in the input file. The system will accept several formats for the GOTO nn command. The GOTO can be in either upper or lower case, but must not have a space between GO and TO. The number for the entry code can be entered with or without a decimal, but should be preceded by only one space. The entry code for the end of the program is 39. The system will branch to the end of the modification portion of the system for any value of nn equal to or greater than 39. Also, it is possible to branch to the end of the program, write the output file, then branch to an earlier entry code for continued data entry. This makes it possible to save intermediate stages of the data to guard against data loss. The new user may wish to enter GOTO 1 at the final prompt. This makes it possible to review all values to be written to the output file by entering a succession of carriage returns. Finally, the system will accept data entries with or without a decimal point, regardless of whether the variables are floating point numbers or integers in the input to PLUVUE II. The use of a decimal point is required only when there are digits following a decimal point.

As an example, if the user only wished to change the wind speed, then the user would: (1) type GOTO 2, (2) enter the new wind speed followed by the ENTER key, and (3) GOTO 39 to exit. The user is then notified that the PLUIN2 output file (which is the PLUVUE II input file) is being saved:

Writing output file.

Current values saved to output file

c:\a248\runpluvu\test3.inp

Carriage return to exit
or enter "goto n" to return to entry code n.

Program PLUIN2 terminating.

After the user has supplied the PLUVUE II input file name or has modified an existing PLUVUE II input file, the user will then be prompted regarding the use or creation of a Mie library file:

The default Mie library as input to PLUVUE II contains the following:

Radius	Sigma	Index of Refraction		Number of Wavelengths	Phase angles
		real	imag		
0.1500	2.0000	1.5000	0.000000	9	91
3.0000	2.2000	1.5000	0.000000	9	91
0.1000	2.0000	1.5000	0.000000	9	91
0.0500	2.0000	1.5000	0.000000	9	91
1.0000	2.0000	1.5000	0.000000	9	91
0.0500	2.0000	2.0000	1.000000	9	91

If the user wishes to use the default Mie library, then the following question should be answered as yes ("Y" or "y"):

Do you wish to use the default Mie library (Y or N)?

and the program will then proceed to the PLUVUE II portion of the run system. The default Mie library should be sufficient for the majority of visibility analyses. The use of other values for the sigma, radius, and indices of refraction should be approved by the local EPA regional office.

If the user wishes to supply a Mie library file, then the following question should be answered in the affirmative ("Y" or "y"):

Do you wish to supply a Mie library file (Y or N)?

and then the user will be prompted to enter the Mie library file name:

Enter the Mie library file name (up to 24 characters):
XXXXXXXXXXXXXXXXXXXXXXXX = 24 characters

Make sure to supply the full path name of the file, if the file resides in a directory other than the one you are working in.

If the user does not wish to use the default Mie library nor wishes to supply a Mie library file, then the final option is to create a Mie library file:

Do you wish to create a Mie library file (Y or N)?

If the user wishes to create a Mie library file, then the run command system will enter the MIETBL portion of the code. The following message will first appear:

CAUTION: The creation of a Mie Library file can take hours depending upon the computer being used.
Mie calculations for large particles take much longer than for small particles.
Therefore, the time required for the calculations for the first particle sizes in a given histogram are much shorter than for the last ones.

Press ENTER to Continue

After the user presses ENTER to continue, the user will be prompted for the output filename which will contain the Mie library data:

Enter output filename. Include drive and path.
30 characters maximum allowed.
XXXXXXXXXXXXXXXXXXXXXXXXXXXXXX = 30 characters

The user will be notified that a new file is being opened. The user will be asked to enter the geometric mean radius by volume (ROG) and the geometric standard deviation (SIGMA) of the log-normal aerosol. Then values of the real and imaginary part of the index of refraction (m and k) are requested:

Opening new file test.mie

Enter geometric mean radius (by volume) ROG
and geometric standard deviation SIGMA.
Separate the numbers by a blank space.
(A negative ROG terminates execution.):

Enter m and k for the index of refraction = m-i*k.
Separate the numbers by a blank space:

The input data are then echoed back to the screen and the screen will then display the progress of the calculations. The following is a sample run using a geometric mean radius of 0.16, a standard deviation of 1.5, and a m and k of 1.5 and 0.0:

```
ROG =  0.1600   SIGMA =  1.5000    m =  1.5000    k =0.000
Wavelength = 0.35    Size no.  1
Wavelength = 0.35    Size no.  2
          . . . .
          . . . .
          . . . .
Wavelength = 0.35    Size no. 101

 Wave-         Cross sections for                Average
length  Extinction  Scattering  Absorption       cosine
 0.35    12.40863    12.40863     0.00000        0.69446
          . . . .
          . . . .
          . . . .
Wavelength = 0.75    Size no.  1
Wavelength = 0.75    Size no.  2
          . . . .
          . . . .
          . . . .
Wavelength = 0.75    Size no. 101

 Wave-         Cross sections for                Average
length  Extinction  Scattering  Absorption       cosine
 0.75    3.01184     3.01184      0.00000        0.52909
```

To terminate the MIETBL calculations, the user must enter a negative value for the geometric mean radius when the following message appears:

```
Enter geometric mean radius (by volume) ROG
and geometric standard deviation SIGMA.
Separate the numbers by a blank space.
(A negative ROG terminates execution.):
```

Mie calculations for large particles take much longer than for small particles. Therefore, the time required for the calculations for the first particle sizes in a given histogram are much shorter than for the last ones.

The user is then asked if he or she would like to run PLUVUE II:

Do you wish to run PLUVUE II (Y or N)?

If the user responds in the affirmative ("Y" or "y"), then the PLUVUE II portion of the run command system is entered. The user is told that the algorithm is now running PLUVUE II:

Running PLUVUE II ...

When PLUVUE II is finished running, the user will be prompted for the name of the PLUVUE II output file:

Enter PLUVUE II output filename:

The user is warned if the output file is about to be overwritten with an existing file of the same name. Finally, the user is asked if he or she wishes to make another run:

Do you wish to make another run (Y or N)?

If the user answers in the affirmative ("Y" or "y"), then the user is prompted for a new input file or the name of a file to modify. Otherwise, the program terminates with the following message:

Exiting PLUVUE II Run Command System

3.3 Level-3 Visibility Modeling Example

This example is provided only for instructional purposes regarding the Level-3 visibility modeling methodology. Each visibility modeling study is different; therefore, the approach used must be discussed before the start of any study with the appropriate EPA regional office, state permitting agency, and/or Federal Land Manager.

3.3.1 Overview

This example outlines the steps performed in a Level 3 visibility analysis to analyze the visual impacts associated with the exploration, construction, and operation of a nuclear waste repository site at a canyon location near a national park. The PLUVUE-II model was applied to calculate the magnitude of plume visual effects, including visual range reduction, plume contrast, plume coloration, and plume perceptibility, associated with various orientations of the plume with respect to potential observers, the sun, and terrain viewing backgrounds. The visual impact magnitudes were then combined with frequency distributions of meteorological conditions to assess the frequency distribution of plume visual impact using the Level-3 analysis guidance in EPA's Workbook for Plume Visual Impact Screening and Analysis (Revised) (EPA, 1992).

The Level-1 and -2 screening criteria were exceeded, suggesting that the possibility of adverse visibility impairment could not be ruled out without more detailed analysis. As opposed to the more cursory and conservative assessment of potential, worst-case visual impacts performed for Level-1 and -2 visibility screening analyses, the Level-3 analysis is a more detailed assessment of plume visual impacts. The Level-3 analysis uses the more sophisticated plume visibility model, PLUVUE II, to calculate the magnitude of plume visibility impacts for a variety of meteorological conditions that might be encountered in a year. These magnitudes of impact are then combined with the frequency of occurrence of corresponding conditions to estimate the frequency of occurrence of plume visual impacts. Because computer software has not yet been developed to iterate through the hourly meteorological conditions encountered in a year, the Level-3 analysis is performed by sampling a variety of possible plume transport conditions.

This example is complex for the following reasons:

1) The potential emissions source, a proposed nuclear waste repository site, is to be located less than 2 km from the nearest Federal Class I PSD area for which visibility is an important value.

2) The emission source consists of emissions that are not continuous and that vary considerably (1) diurnally, due to variations in activity throughout the day, with maximum activities during daylight hours, (2) monthly due to different activity levels, and (3) over longer time frames corresponding to the exploratory shaft

facility (ESF) construction, repository construction (RC), and repository operation (RO). Because the emissions are considerably less at night, the opportunity for significant impacts resulting from long transport during nocturnal, stable, drainage flows is considerably less than for continuous emission sources such as power plants.

3) The emission source is not a point source, but is an area source, distributed over many acres with the areas changing depending on the phase of operation (ESF, RC, RO). Thus, emissions are initially diluted over a significant vertical and horizontal area.

4) A significant fraction of the emissions from the source are diesel exhaust emissions which are largely fine organic particulate (soot) which has a significant light absorbing effect. The Level-1 and -2 screening techniques are not capable of addressing this component; thus, the more sophisticated PLUVUE-II model was applied.

5) The area is characterized by very complex terrain. The emission source will be located in a canyon. All observation points in the national park are located either well above the location of the canyon site or at locations where the plume would need to travel a circuitous route, either up and over or around significant terrain obstacles such as ridges, canyon walls, and mountains. Such a complex terrain setting (1) limits the distance an observer can see in certain directions, (2) creates a viewing background of terrain (which can be snow covered, sunlit, or in shadow), (3) enhances dispersion due to mechanical mixing effects, and (4) blocks flows, particularly stable flows, in certain directions.

6) There is interest in the visual impact not only at the closest park boundary, as analyzed in the Level-1 and -2 screening calculations, but also at more distant, but more frequently visited, locations farther in the park.

The user needs to review a full range of possible conditions (i.e., time of day, season, meteorological conditions, and observer locations). Therefore, for this example, over 250 PLUVUE-II runs have been made to attempt to characterize the variety of plume visual impacts that might occur. For each of the over 250 PLUVUE-II runs, visual impact calculations were made for several azimuths of view corresponding to different distances of the plume downwind from the source. In addition, an attempt was made to model the effect of viewing background, that is, whether it is a sky or white, gray, or black terrain object.

3.3.2 Site Location and Receptors

The location of the proposed nuclear waste repository site is in a canyon near the eastern boundary of a national park. The repository site is located approximately 1.9 km east of the eastern park boundary at an elevation of approximately 5160 ft MSL. Three observer locations are used in this study. Observer #1 was selected to represent the impact at the closest park boundary to the repository site. This observer location is likely to have the worst visual impacts because it is only 1.9 km from the center of the proposed site and it has a relatively unobstructed view down the canyon toward the site. Although this site is likely to have the worst magnitude and frequency of visual impacts, in reality the site may rarely, if ever, be visited. Observer #2 was chosen at a location that is visited by 4 percent of the national park visitors. The site is approximately 4 km from Observer #1 and 6 km from the canyon site. Finally, the third observer (#3) is immediately adjacent to the ranger station on the entrance road to the national park. This site was chosen because, although it is further from the canyon site (approximately 9 km), it is visited quite often and has a relatively unobstructed view in several directions. This area is visited by 12 percent of the park visitors and more visitors drive past this location.

3.3.3 Model Inputs and Assumptions

Emissions

The three phases of construction and operation of the proposed nuclear waste repository include the following:

Exploratory Shaft Facility (ESF) Construction

Repository Construction (RC)

Repository Operation (RO)

The emissions data encompass all stationary and mobile emission sources used at the site during these three phases. Emissions data do not include estimates of natural wind-blown dust; thus, such natural dust sources are not considered in this visibility impact analysis. It may be likely that the construction and operation activities will disturb the natural soil conditions of the area, thereby increasing the quantity of wind-blown dust. However, as will be shown later, the maximum impacts estimated in this analysis occur with light winds (less than 3 m/s) which are not likely to be strong enough to raise wind-blown dust. To the extent wind-blown dust is added to the line of sight in which the sight emissions are located, visual impacts may be diminished due to the obscuring effect of the dust. Therefore, it is believed that the exclusion of wind-blown dust is a conservative assumption for this analysis.

The species of emissions include nitrogen oxides (NO_x), sulfur dioxide (SO_2), and particulate. There are two categories of particulate considered: (1) diesel engine exhaust and (2) fugitive dust. Because the SO_2 emissions are minute and because SO_2 requires several hours before it is converted to sulfate aerosol which interacts with light (thus potentially impairing visibility), this species was not modeled for this example. The particulate emission classes were modeled separately as two distinct aerosol modes. The diesel exhaust was assumed to be elemental carbon, which is an effective light absorber. The mass median diameter of the emitted elemental carbon (soot) from diesel engines was calculated from California Air Resources Board (CARB) emission factors to be at a mass median diameter of 0.4 μm, which is near the most effective size range for both light scattering and absorption. Fugitive dust emissions were also sized using CARB's emission factors with a mass median diameter of 5.2 μm, which is consistent with other estimates of coarse mode aerosol size distribution.

These emissions vary both diurnally (with maximum emissions generally during the daylight hours) and on a month-to-month basis during any given phase. Daily emission values for the month with highest emissions in the particular year of the given phase of operation with the highest emissions were used as the starting point for emissions calculations. The specific emissions used as PLUVUE II input for each of the three phases are listed in Table 3. Emissions are greatest during the repository construction phase, with NO_x emissions of 2.75 tons per day, diesel exhaust emissions of 0.28 tons per day, and fugitive dust emissions of 0.61 tons per day. These emission rates are more than three times the emissions during the ESF construction, the phase with the next highest emissions. Emissions during the repository operation are the lowest.

For this example, emissions are treated as area sources. ESF construction emissions were distributed over 60 acres and repository construction and operation emissions were distributed over the entire 400 acres of the site.

Terrain

The complex terrain surrounding the canyon site and the three observation sites selected for analysis in this study complicates the realistic analysis of the visual impacts in the following ways:

1) Complex terrain will tend to dramatically effect the transport and dispersion of emissions. Elevated terrain will block and channel the airflow, especially during stable conditions. Also, elevated, rugged terrain tends to enhance diffusion because of mechanical mixing effects and because plume parcels are more easily torn apart and transported in different directions.

TABLE 3

EMISSIONS USED AS PLUVUE II INPUT FOR THE THREE PHASES OF CONSTRUCTION (TONS/DAY)

Phase	NO_x	Diesel Exhaust	Fugitive Dust
ESF Construction	0.86	0.06	0.15
Repository Construction	2.75	0.28	0.61
Repository Operation	0.58	0.01	0.24

2) Complex terrain will limit the direction and distance an observer can see in a given direction. Terrain obstacles may prevent an observer from seeing plumes that would be readily visible to an observer located on flat terrain or on an elevated vantage point.

3) Complex terrain will become the viewing background for many plumes. Terrain is either a viewing obstruction or a viewing background depending on whether the plume material is in front of or behind a given terrain object.

Observer #1 has a direct view of the canyon site, unobstructed by intervening terrain. Observer #2's view is obstructed by elevated terrain at approximately 4 km, and Observer #3's view is obstructed by terrain approximately 9 km from the observer. Terrain obstructions in all directions from the three observer locations were considered in this analysis. If a plume would be located in a position that would be obstructed from view by intervening terrain, its visual impact was assigned to zero.

Meteorological Conditions

Since meteorological data were not available for the canyon site or for any of the three observer locations used in this example, meteorological data from the closest monitoring site was used to characterize the frequency of occurrence of various meteorological conditions. The worst year of the available annual meteorological data were used to calculate tables of joint frequency of wind direction and speed and atmospheric stability for specific time periods of interest. The worst-case dispersion conditions were ranked in order of decreasing severity and the frequency of occurrence of these conditions associated with the wind direction that could transport emissions toward the Class I area. Dispersion conditions were ranked by evaluating the product $\sigma_y\sigma_z u$, where σ_y and σ_z are the Pasquill-Gifford horizontal and vertical dispersion coefficients for the given stability class and downwind distance x along the stable plume trajectory, and u is the maximum wind speed for the given wind speed category in the joint frequency table. The frequency of occurrence analysis was conducted for the following worst-case meteorological conditions:

Pasquill-Gifford Stability Class	Wind Speed (m/s)
F	1,2,3
E	1,2,3,4,5
D	1,2,3,4,5,6,7,8

The dispersion conditions were ranked in ascending order of the value $\sigma_y\sigma_z u$. The joint-frequency tables were prepared for each observer location at three different downwind distances. The transport time from the emissions source to each observer location was calculated along the minimum trajectory distance based on the midpoint value of wind speed

for each wind speed category. For example, for the wind speed category 0-1 m/s, a wind speed of 0.5 m/s was used to evaluate the transport time.

It is unlikely that steady-state plume conditions will persist for more than 12 hours. Thus, if a transit time of more than 12 hours is required to transport a plume parcel from the emissions source to the observer locations for a given dispersion condition, it was assumed that plume material is more dispersed than a standard Gaussian plume model would predict. The frequencies associated with transport times longer than 12 hours were not included in the cumulative frequency summations.

To obtain the worst-case meteorological conditions, it was necessary to determine the dispersion condition (a given wind speed and stability class associated with the wind direction that would transport emissions toward the observer locations) that has a $\sigma_y\sigma_z u$ product with a cumulative probability of one percent. In other words, the dispersion condition was selected such that the sum of all frequencies of occurrence of conditions worse than this condition totals one percent (i.e., about four days per year). The one-percentile meteorology is assumed to be indicative of worst-day plume visual impacts when the probability of worst-case meteorological conditions is coupled with the probability of other factors being ideal for maximizing plume visual impacts. Dispersion conditions associated with transport times of more than 12 hours were not considered in this cumulative frequency for the reasons stated above.

Emissions due to repository construction and operation principally occur during daylight hours, thus nighttime dispersion conditions are irrelevant for this study. (This would not be the case for a continuous emission source whose nighttime emissions could be caught in very stable flows and transported intact to long distances, as occurs with power plant emissions, for example.) For this example, emissions from daytime activities start at 0800 so the daylight hours were divided into three-hour periods starting at 0800 for cumulative frequency calculations. The poorest daylight dispersion conditions were found to occur in the morning for the first 3-hour period (0800-1100). Therefore, the analysis of the frequency of impacts were conducted for the morning (0800-1100) period.

3.3.4 Model Results

Over 250 PLUVUE-II model calculations of plume visual impact were performed to attempt to characterize the ranges of potential visual impacts for a variety of times of day/season, observer positions, and meteorological and emissions conditions. PLUVUE II calculates a number of parameters that quantify the visual effect of a plume of given dimensions, position (relative to the observer, the sun, and viewing backgrounds), and concentration. These parameters are calculated for each downwind distance considered in the model. In this example, downwind distances of 1, 3, 5, 7, 10, and 15 km were considered. Visual impacts were calculated from the separate perspectives associated with the three observers. The four parameters used to characterize the visibility effects of the plume

included: visual range reduction, plume contrast, blue-red ratio, and ΔE. The importance of these parameters was discussed in Section 1.

Table 4 summarizes the results of the first PLUVUE-II calculations that were performed to determine which of the emitted species (NO_x, diesel exhaust, or fugitive dust) caused the most impact. This determination was made by first modeling all emissions and then modeling separately the impacts of each emitted species alone. As expected, the base case (with all emitted species considered) produced the maximum visual impacts. Visual range was reduced 15%, plume contrast was most negative (-0.016), blue-red ratio was the lowest (0.987), and, as a result of the contrast and color change, the plume ΔE was highest (0.641). The values of these parameters indicate that for this particular condition the plume would not be visible since ΔE is less than 1 but that it would be slightly darker (negative contrast) and yellower (blue-red ratio less than 1) than the assumed sky background.

Diesel exhaust considered alone caused the next largest impact, nearly as great as all species combined. The values of the parameters suggest a darkening effect of the plume. This is not surprising considering that diesel exhaust particulate is elemental carbon (soot) which is a very effective light absorber.

Nitrogen oxide (NO_x) emissions caused nearly as large an impact as the diesel exhaust, again a darkening effect due to the light absorbing nature of the nitrogen dioxide molecule.

Fugitive dust had a much lower impact than either diesel exhaust particulates or NO_x because the particulate is relatively large and therefore not an effective light scatterer. Fugitive dust, which acts to scatter light both into and out of the line of sight, when present with the light absorbing soot and NO_x, may actually tend to mask some of the effect of the other emitted species. Thus, for this example, we conclude that the diesel exhaust particulate (largely soot) and NO_x from the construction and operation activities at the site are the principal causes of plume visual impacts calculated in this study. However, it should be noted that visual impacts of fugitive dust would be most noticeable against a dark terrain viewing background (e.g., a terrain feature in shadow) in which case the particulate, especially when the sun is in front of the observer, would scatter light into the line of sight thereby appearing brighter than the terrain.

As discussed, over 250 PLUVUE-II runs were made. For each run, plume visual effects were made for the particular vantage point of one of the three observers in the national park. Each run was based on a particular plume position appropriate for the given wind direction. Calculations were performed for six downwind distances. An input file for one of the many runs is shown in Figure 10. The corresponding output is shown in Figure 11. In this example, Observer #1 would observe the indicated plume visual effect as the plume was scanned from the closest downwind distance to the most distant. Thus, the indicated effects at given distances along the plume can also be interpreted as effects for various azimuths of view.

TABLE 4

SENSITIVITY OF PLUME VISUAL IMPACT TO EMITTED SPECIES

Scenario	Visual Range Reduction (%)	Blue-Red Ratio	Plume Contrast	$\Delta E(L^*a^*b^*)$
Base Case	15.2	0.987	-0.016	0.641
Diesel Exhaust Only	9.8	0.988	-0.015	0.586
NO_x Only	5.7	0.998	-0.011	0.497
Fugitive Dust Only	1.7	0.996	-0.005	0.175

Run Description:

Spring 0800 AM

Wind Direction = 90°

Wind Speed = 2 m/s

Stability = D

Observer #1

Emissions: ESF Construction

Downwind Distance = 3 km

```
all.mie
pluvue7.bin
pluvue8.bin
Test Case
  4.5    4 0.00
 0
       64.         5.
   10000.0
    56.000
    0
 1 0 1 0 6 1 7 1 0 0 0
 0 0 0 0 0 0
       1.0        3.0        5.0        7.0       10.0       15.0
      0.01       0.86       0.21
      10.0       80.0        0.0       0.10
  1.0  0.0
      72.7
     0.000      0.000      0.040      0.000
     0.150      3.000      0.100      1.000
     2.000      2.200      2.000      2.000
     1.500      2.500      1.500      2.500
     0.050      2.000      2.000      0.000      0.000
     1.500      0.000      1.500      0.000
     1.500      0.000      2.000      1.000
    10.000
    2
   170.000
 1.00 1.00 0.10 0.10
    0
 0.0000000
    2    2
      -1.9        0.0     5400.0
       0.0        0.0     5200.0
   12    4    1 800.    7. 1988
       0.0        0.0        0.0        0.0        0.0        0.0
      50.0       50.0       50.0       50.0       50.0       50.0       50.0       0.0
      50.0       50.0       50.0       50.0       50.0       50.0       50.0       0.0
      50.0       50.0       50.0       50.0       50.0       50.0       50.0       0.0
     225.0
```

Figure 10. Sample PLUVUE II input file.

```
                    PLUVUE II (VERSION 92243)
                    AN AIR QUALITY DISPERSION MODEL IN
                    SECTION 2.  NON-GUIDELINE MODELS
                    SOURCE: FILE 13 ON UNAMAP MAGNETIC TAPE FROM NTIS.

VISUAL IMPACT ASSESSMENT FOR Test Case

    EMISSIONS SOURCE DATA

        ELEVATION OF SITE =       5200.  FEET MSL
                                  1585.  METERS MSL

        NO. OF UNITS =     1.

        STACK HEIGHT =    0.  FEET
                          0.  METERS

        FLUE GAS FLOW RATE =        10.  CU FT/MIN
                                  0.00  CU M/SEC

        FLUE GAS TEMPERATURE =       80.  F
                                    300.  K

        FLUE GAS OXYGEN CONTENT =        0.0  MOL PERCENT

        SO2 EMISSION RATE (TOTAL) =       0.01  TONS/DAY
                                      1.050E-01  G/SEC

        NOX EMISSION RATE (TOTAL,AS NO2) =       0.86  TONS/DAY
                                             9.030E+00  G/SEC

        PARTICULATE EMISSION RATE (TOTAL) =       0.21  TONS/DAY
                                             2.205E+00  G/SEC
```


Figure 11. Example PLUVUE II output file.

```
METEOROLOGICAL AND AMBIENT AIR QUALITY DATA

     WINDSPEED =    4.5  MILES/HR
                    2.0  M/SEC

     PASQUILL-GIFFORD-TURNER STABILITY CATEGORY D

     LAPSE RATE =  0.00  F/1000 FT
                   0.000E+00  K/M

     POTENTIAL TEMPERATURE LAPSE RATE =    9.800E-03  K/M

     AMBIENT TEMPERATURE =  72.7  F
                           295.8  K

     RELATIVE HUMIDITY =  56.0  %

     MIXING DEPTH =    10000.0  M

     AMBIENT PRESSURE =  0.83  ATM

     BACKGROUND NOX CONCENTRATION =      0.000  PPM

     BACKGROUND NO2 CONCENTRATION =      0.000  PPM

     BACKGROUND OZONE CONCENTRATION =      0.040  PPM

     BACKGROUND SO2 CONCENTRATION =      0.000  PPM

 ROG =  0.1500        SIGMA =  2.0000        REFRACTIVE INDEX = 1.5000 +  0.000000
LOG-NORMAL SIZE DISTRIBUTION (101 POINT HISTOGRAM)
 ROG =  3.0000        SIGMA =  2.2000        REFRACTIVE INDEX = 1.5000 +  0.000000
LOG-NORMAL SIZE DISTRIBUTION (101 POINT HISTOGRAM)
 ROG =  1.0000        SIGMA =  2.0000        REFRACTIVE INDEX = 1.5000 +  0.000000
LOG-NORMAL SIZE DISTRIBUTION (101 POINT HISTOGRAM)
 ROG =  0.0500        SIGMA =  2.0000        REFRACTIVE INDEX = 2.0000 +  1.000000
LOG-NORMAL SIZE DISTRIBUTION (101 POINT HISTOGRAM)

     BACKGROUND COARSE MODE CONCENTRATION =       10.0  UG/M3

     BACKGROUND SULFATE CONCENTRATION =        2.2  UG/M3

     BACKGROUND NITRATE CONCENTRATION =        0.0  UG/M3

     BACKGROUND VISUAL RANGE =      170.0  KILOMETERS

     SO2 DEPOSITION VELOCITY =       1.00  CM/SEC

     NOX DEPOSITION VELOCITY =       1.00  CM/SEC

     COARSE PARTICULATE DEPOSITION VELOCITY =       0.10  CM/SEC

     SUBMICRON PARTICULATE DEPOSITION VELOCITY =       0.10  CM/SEC
```

Figure 11. Example PLUVUE II output file (continued).

AEROSOL STATISTICS

	BACKGROUND		PLUME		
	ACCUMULATION MODE	COARSE MODE	ACCUMULATION MODE	COARSE MODE	CARBONACEOUS AEROSOLS
MASS MEDIAN RADIUS MICROMETERS	0.150	3.000	0.100	1.000	0.050
GEOMETRIC STANDARD DEVIATION	2.000	2.200	2.000	2.000	2.000
PARTICLE DENSITY G/(CM**3)	1.500	2.500	1.500	2.500	2.000

CARBONACEOUS FRACTION OF PARTICLATE MASS EMISSIONS = 0.000

BACKGROUND ATMOSPHERIC ELEMENTAL CARBON = 0.000 UG/M**3

GEOMETRY OF USER-SPECIFIED PLUME-OBSERVER-SUN ORIENTATION

WIND DIRECTION (DEGREES) =225.0

SIMULATION IS FOR 800. HOURS ON 4/ 1

SOLAR ZENITH ANGLE (DEGREES) = 61.5

SOLAR AZIMUTH ANGLE (DEGREES) = 95.5

GEOMETRIES FOR LINES-OF-SIGHT THROUGH PLUME PARCELS AT GIVEN DOWNWIND DISTANCES (X)

X (KM)	AZIMUTH	RP	ALPHA	BETA	THETA
1.0	74.8	2.7	29.8	-1.3	35.7
3.0	62.2	4.5	17.2	-0.7	43.2
5.0	57.0	6.5	12.0	-0.5	46.9
7.0	54.1	8.5	9.1	-0.4	49.0
10.0	51.8	11.4	6.8	-0.3	50.8
15.0	49.7	16.4	4.7	-0.2	52.3

Figure 11. Example PLUVUE II output file (continued).

BACKGROUND CONDITIONS

ACCUMULATION MODE			COARSE PARTICLE MODE			PRIMARY PARTICLE MODE		
MASS RADIUS	SIGMA	BSCAT.55/MASS	MASS RADIUS	SIGMA	BSCAT.55/MASS	MASS RADIUS	SIGMA	BSCAT.55/MASS
0.1500E+00	0.2000E+01	0.5215E-02	0.3000E+01	0.2200E+01	0.3219E-03	0.1000E+01	0.2000E+01	0.1045E-02

REFRACTION INDEXES

ACCUMULATION MODE	=	0.1500E+01 + I	0.0000E+00
COARSE MODE	=	0.1500E+01 + I	0.0000E+00
PRIMARY AEROSOLS	=	0.1500E+01 + I	0.0000E+00
CARBONACEOUS AEROSOLS	=	0.2000E+01 + I	0.1000E+01

COEFFICIENTS AT 0.55 MICROMETERS , 1./KM

BTARAY =0.9885E-02 BTAAER =0.1457E-01 ABSNO2 =0.0000E+00 BTABAC =0.2301E-01

Figure 11. Example PLUVUE II output file (continued).

CONCENTRATIONS OF AEROSOL AND GASES CONTRIBUTED BY

Test Case

DOWNWIND DISTANCE (KM) = 1.0
PLUME ALTITUDE (M) = 2.
SIGMA Y (M) = 78.
SIGMA Z (M) = 33.
SO2-SO4 CONVERSION RATE= 0.0000 PERCENT/HR
NOX-NO3 CONVERSION RATE= 0.0000 PERCENT/HR

ALTITUDE	NOX (PPM)	NO2 (PPM)	NO3- (PPM)	NO2/NTOT (MOLE %)	NO3-/NTOT (MOLE %)	SO2 (PPM)	SO4= (UG/M3)	SO4=/STOT (MOLE %)	O3 (PPM)	PRIMARY (UG/M3)	BSP-TOTAL (10-4 M-1)	BSPSN/BSP (%)
H+2S												
INCREMENT:	0.043	0.025	0.000	57.178	0.000	0.000	0.000	0.000	-0.025	19.695	0.206	0.000
TOTAL AMB:	0.043	0.025	0.000	57.178	0.000	0.000	2.176	60.737	0.015	31.872	0.352	32.283
H+1S												
INCREMENT:	0.202	0.037	0.000	18.521	0.000	0.002	0.000	0.000	-0.037	92.685	0.969	0.000
TOTAL AMB:	0.202	0.037	0.000	18.521	0.000	0.002	2.176	24.740	0.003	104.861	1.115	10.183
H												
INCREMENT:	0.350	0.039	0.000	11.011	0.000	0.003	0.000	0.000	-0.039	160.910	1.682	0.000
TOTAL AMB:	0.350	0.039	0.000	11.011	0.000	0.003	2.176	15.920	0.001	173.087	1.828	6.210
H-1S												
INCREMENT:	0.351	0.039	0.000	10.996	0.000	0.003	0.000	0.000	-0.039	161.138	1.684	0.000
TOTAL AMB:	0.351	0.039	0.000	10.996	0.000	0.003	2.176	15.901	0.001	173.314	1.830	6.202
H-2S												
INCREMENT:	0.351	0.039	0.000	10.996	0.000	0.003	0.000	0.000	-0.039	161.138	1.684	0.000
TOTAL AMB:	0.351	0.039	0.000	10.996	0.000	0.003	2.176	15.901	0.001	173.314	1.830	6.202
0												
INCREMENT:	0.351	0.039	0.000	10.996	0.000	0.003	0.000	0.000	-0.039	161.138	1.684	0.000
TOTAL AMB:	0.351	0.039	0.000	10.996	0.000	0.003	2.176	15.901	0.001	173.314	1.830	6.202

CUMULATIVE SURFACE DEPOSITION (MOLE FRACTIONOF INITIAL FLUX

SO2:	0.0000
NOX:	0.0000
PRIMARY PARTICULATE:	0.0000
SO4:	0.0000
NO3:	0.0000

Figure 11. Example PLUVUE II output file (continued).

VISUAL EFFECTS FOR HORIZONTAL SIGHT PATHS
Test Case

DOWNWIND DISTANCE (KM) = 1.0
PLUME ALTITUDE (M) = 2.
PLUME-OBSERVER DISTANCE (KM) = 2.7
AZIMUTH OF LINE-OF-SIGHT = 74.8
ELEVATION ANGLE OF LINE-OF-SIGHT = -1.3
SOLAR ZENITH ANGLE = 61.5 AT 800. ON 4/ 1
SIGHT PATH IS THROUGH PLUME CENTER

THETA	ALPHA	RP/RV0	RV	%REDUCED	YCAP	L	X	Y	DELYCAP	DELL	C(550)	BRATIO	DELX	DELY	E(LUV)	E(LAB)
36.																
	30.	0.02	167.0	1.79	102.10	100.81	0.3370	0.3497	-0.52	-0.20	-0.0050	0.9602	0.0023	0.0022	2.0998	1.3615

0

PLUME VISUAL EFFECTS FOR HORIZONTAL VIEWS
OF THE PLUME OF WHITE, GRAY, AND BLACK OBJECTS
FOR SPECIFIC OBSERVER-PLUME AND OBSERVER-OBJECT DISTANCES

Test Case

DOWNWIND DISTANCE (KM) = 1.0
PLUME-OBSERVER DISTANCE (KM) = 2.7
AZIMUTH OF LINE-OF-SIGHT = 74.8
ELEVATION ANGLE OF LINE-OF-SIGHT = -1.3
SOLAR ZENITH ANGLE = 61.5 AT 800. ON 4/ 1
THETA = 36.

REFLECT	RP/RV0	RO/RV0	YCAP	L	X	Y	DELYCAP	DELL	C(550)	BRATIO	DELX	DELY	E(LUV)	E(LAB)
1.0	0.02	0.29	93.27	97.34	0.3328	0.3453	0.15	0.06	0.0018	0.9544	0.0027	0.0026	2.4100	1.5431
0.3	0.02	0.29	77.86	90.73	0.3190	0.3352	1.34	0.61	0.0171	0.9270	0.0040	0.0038	3.4004	2.1555
0.0	0.02	0.29	71.26	87.62	0.3116	0.3298	1.85	0.90	0.0257	0.9074	0.0048	0.0045	3.9892	2.5334

Figure 11. Example PLUVUE II output file (continued).

CONCENTRATIONS OF AEROSOL AND GASES CONTRIBUTED BY

Test Case

DOWNWIND DISTANCE (KM) = 3.0
PLUME ALTITUDE (M) = 2.
SIGMA Y (M) = 195.
SIGMA Z (M) = 66.
SO2-SO4 CONVERSION RATE= 0.0019 PERCENT/HR
NOX-NO3 CONVERSION RATE= 0.0135 PERCENT/HR

ALTITUDE	NOX (PPM)	NO2 (PPM)	NO3- (PPM)	NO2/NTOT (MOLE %)	NO3-/NTOT (MOLE %)	SO2 (PPM)	SO4= (UG/M3)	SO4=/STOT (MOLE %)	O3 (PPM)	PRIMARY (UG/M3)	BSP-TOTAL (10-4 M-1)	BSPSN/BSP (%)
H+2S												
INCREMENT:	0.009	0.007	0.000	74.135	0.037	0.000	0.000	0.009	-0.007	4.157	0.043	0.003
TOTAL AMB:	0.009	0.007	0.000	74.135	0.037	0.000	2.176	87.995	0.033	16.333	0.189	60.007
H+1S												
INCREMENT:	0.042	0.024	0.000	57.897	0.001	0.000	0.000	0.001	-0.024	19.110	0.200	0.000
TOTAL AMB:	0.042	0.024	0.000	57.897	0.001	0.000	2.176	61.454	0.016	31.287	0.345	32.855
H												
INCREMENT:	0.070	0.031	0.000	44.018	0.000	0.001	0.000	0.001	-0.031	32.343	0.338	0.000
TOTAL AMB:	0.070	0.031	0.000	44.018	0.000	0.001	2.176	48.507	0.009	44.520	0.484	23.460
H-1S												
INCREMENT:	0.070	0.031	0.000	44.018	0.000	0.001	0.000	0.001	-0.031	32.343	0.338	0.000
TOTAL AMB:	0.070	0.031	0.000	44.018	0.000	0.001	2.176	48.507	0.009	44.520	0.484	23.460
H-2S												
INCREMENT:	0.070	0.031	0.000	44.018	0.000	0.001	0.000	0.001	-0.031	32.343	0.338	0.000
TOTAL AMB:	0.070	0.031	0.000	44.018	0.000	0.001	2.176	48.507	0.009	44.520	0.484	23.460
0												
INCREMENT:	0.070	0.031	0.000	44.018	0.000	0.001	0.000	0.001	-0.031	32.343	0.338	0.000
TOTAL AMB:	0.070	0.031	0.000	44.018	0.000	0.001	2.176	48.507	0.009	44.520	0.484	23.460

CUMULATIVE SURFACE DEPOSITION (MOLE FRACTIONOF INITIAL FLUX

SO2:	0.0000
NOX:	0.0000
PRIMARY PARTICULATE:	0.0000
SO4:	0.0000
NO3:	0.0000

Figure 11. Example PLUVUE II output file (continued).

VISUAL EFFECTS FOR HORIZONTAL SIGHT PATHS
Test Case

DOWNWIND DISTANCE (KM) = 3.0
PLUME ALTITUDE (M) = 2.
PLUME-OBSERVER DISTANCE (KM) = 4.5
AZIMUTH OF LINE-OF-SIGHT = 62.2
ELEVATION ANGLE OF LINE-OF-SIGHT = -0.7
SOLAR ZENITH ANGLE = 61.5 AT 800. ON 4/ 1
SIGHT PATH IS THROUGH PLUME CENTER

THETA	ALPHA	RP/RV0	RV	%REDUCED	YCAP	L	X	Y	DELYCAP	DELL	C(550)	BRATIO	DELX	DELY	E(LUV)	E(LAB)
43.	17.	0.03	167.5	1.48	82.54	92.82	0.3356	0.3481	-1.54	-0.67	-0.0176	0.9235	0.0047	0.0049	4.1465	2.7541

PLUME VISUAL EFFECTS FOR HORIZONTAL VIEWS
OF THE PLUME OF WHITE, GRAY, AND BLACK OBJECTS
FOR SPECIFIC OBSERVER-PLUME AND OBSERVER-OBJECT DISTANCES

Test Case

DOWNWIND DISTANCE (KM) = 3.0
PLUME-OBSERVER DISTANCE (KM) = 4.5
AZIMUTH OF LINE-OF-SIGHT = 62.2
ELEVATION ANGLE OF LINE-OF-SIGHT = -0.7
SOLAR ZENITH ANGLE = 61.5 AT 800. ON 4/ 1
THETA = 43.

REFLECT	RP/RV0	RO/RV0	YCAP	L	X	Y	DELYCAP	DELL	C(550)	BRATIO	DELX	DELY	E(LUV)	E(LAB)
1.0	0.03	0.29	79.27	91.36	0.3355	0.3467	-1.29	-0.58	-0.0151	0.9243	0.0047	0.0049	4.1169	2.7320
0.3	0.03	0.29	63.86	83.91	0.3188	0.3344	-0.11	-0.06	-0.0009	0.9022	0.0057	0.0061	4.8232	3.0601
0.0	0.03	0.29	57.25	80.34	0.3094	0.3275	0.40	0.22	0.0076	0.8842	0.0065	0.0069	5.2911	3.3115

Figure 11. Example PLUVUE II output file (continued).

CONCENTRATIONS OF AEROSOL AND GASES CONTRIBUTED BY

Test Case

DOWNWIND DISTANCE (KM) = 5.0
PLUME ALTITUDE (M) = 2.
SIGMA Y (M) = 303.
SIGMA Z (M) = 89.
SO2-SO4 CONVERSION RATE= 0.0154 PERCENT/HR
NOX-NO3 CONVERSION RATE= 0.1077 PERCENT/HR

ALTITUDE	NOX (PPM)	NO2 (PPM)	NO3- (PPM)	NO2/NTOT (MOLE %)	NO3-/NTOT (MOLE %)	SO2 (PPM)	SO4= (UG/M3)	SO4=/STOT (MOLE %)	O3 (PPM)	PRIMARY (UG/M3)	BSP-TOTAL (10-4 M-1)	BSPSN/BSP (%)
H+2S												
INCREMENT:	0.004	0.003	0.000	75.685	0.400	0.000	0.000	0.078	-0.003	1.998	0.021	0.028
TOTAL AMB:	0.004	0.003	0.000	75.685	0.400	0.000	2.176	93.851	0.037	14.174	0.167	68.138
H+1S												
INCREMENT:	0.020	0.014	0.000	69.324	0.040	0.000	0.000	0.010	-0.014	9.126	0.095	0.004
TOTAL AMB:	0.020	0.014	0.000	69.324	0.040	0.000	2.176	76.953	0.026	21.302	0.241	47.079
H												
INCREMENT:	0.033	0.021	0.000	62.371	0.013	0.000	0.000	0.005	-0.021	15.340	0.160	0.002
TOTAL AMB:	0.033	0.021	0.000	62.371	0.013	0.000	2.176	66.513	0.019	27.516	0.306	37.086
H-1S												
INCREMENT:	0.033	0.021	0.000	62.371	0.013	0.000	0.000	0.005	-0.021	15.340	0.160	0.002
TOTAL AMB:	0.033	0.021	0.000	62.371	0.013	0.000	2.176	66.513	0.019	27.516	0.306	37.086
H-2S												
INCREMENT:	0.033	0.021	0.000	62.371	0.013	0.000	0.000	0.005	-0.021	15.340	0.160	0.002
TOTAL AMB:	0.033	0.021	0.000	62.371	0.013	0.000	2.176	66.513	0.019	27.516	0.306	37.086
0												
INCREMENT:	0.033	0.021	0.000	62.371	0.013	0.000	0.000	0.005	-0.021	15.340	0.160	0.002
TOTAL AMB:	0.033	0.021	0.000	62.371	0.013	0.000	2.176	66.513	0.019	27.516	0.306	37.086

CUMULATIVE SURFACE DEPOSITION (MOLE FRACTIONOF INITIAL FLUX

SO2:	0.0000
NOX:	0.0000
PRIMARY PARTICULATE:	0.0000
SO4:	0.0000
NO3:	0.0000

Figure 11. Example PLUVUE II output file (continued).

VISUAL EFFECTS FOR HORIZONTAL SIGHT PATHS
Test Case

DOWNWIND DISTANCE (KM) = 5.0
PLUME ALTITUDE (M) = 2.
PLUME-OBSERVER DISTANCE (KM) = 6.5
AZIMUTH OF LINE-OF-SIGHT = 57.0
ELEVATION ANGLE OF LINE-OF-SIGHT = -0.5
SOLAR ZENITH ANGLE = 61.5 AT 800. ON 4/ 1
SIGHT PATH IS THROUGH PLUME CENTER

THETA	ALPHA	RP/RV0	RV	%REDUCED	YCAP	L	X	Y	DELYCAP	DELL	C(550)	BRATIO	DELX	DELY	E(LUV)	E(LAB)
47.																
	12.	0.04	167.3	1.57	75.13	89.46	0.3342	0.3474	-1.82	-0.84	-0.0227	0.9117	0.0056	0.0058	4.7989	3.1967
0																

PLUME VISUAL EFFECTS FOR HORIZONTAL VIEWS
OF THE PLUME OF WHITE, GRAY, AND BLACK OBJECTS
FOR SPECIFIC OBSERVER-PLUME AND OBSERVER-OBJECT DISTANCES

Test Case

DOWNWIND DISTANCE (KM) = 5.0
PLUME-OBSERVER DISTANCE (KM) = 6.5
AZIMUTH OF LINE-OF-SIGHT = 57.0
ELEVATION ANGLE OF LINE-OF-SIGHT = -0.5
SOLAR ZENITH ANGLE = 61.5 AT 800. ON 4/ 1
THETA = 47.

REFLECT	RP/RV0	RO/RV0	YCAP	L	X	Y	DELYCAP	DELL	C(550)	BRATIO	DELX	DELY	E(LUV)	E(LAB)
1.0	0.04	0.29	74.02	88.94	0.3364	0.3474	-1.71	-0.80	-0.0214	0.9152	0.0055	0.0057	4.6587	3.1248
0.3	0.04	0.29	58.73	81.16	0.3183	0.3341	-0.41	-0.22	-0.0056	0.8927	0.0065	0.0070	5.3316	3.4032
0.0	0.04	0.29	52.18	77.41	0.3079	0.3265	0.15	0.09	0.0041	0.8732	0.0073	0.0078	5.8078	3.6480

Figure 11. Example PLUVUE II output file (continued).

CONCENTRATIONS OF AEROSOL AND GASES CONTRIBUTED BY

Test Case

DOWNWIND DISTANCE (KM) = 7.0
PLUME ALTITUDE (M) = 2.
SIGMA Y (M) = 406.
SIGMA Z (M) = 110.
SO2-SO4 CONVERSION RATE= 0.0483 PERCENT/HR
NOX-NO3 CONVERSION RATE= 0.3382 PERCENT/HR

ALTITUDE	NOX (PPM)	NO2 (PPM)	NO3- (PPM)	NO2/NTOT (MOLE %)	NO3-/NTOT (MOLE %)	SO2 (PPM)	SO4= (UG/M3)	SO4=/STOT (MOLE %)	O3 (PPM)	PRIMARY (UG/M3)	BSP-TOTAL (10-4 M-1)	BSPSN/BSP (%)
H+2S												
INCREMENT:	0.003	0.002	0.000	75.710	1.166	0.000	0.000	0.221	-0.002	1.227	0.013	0.079
TOTAL AMB:	0.003	0.002	0.000	75.710	1.166	0.000	2.176	96.137	0.038	13.403	0.159	71.603
H+1S												
INCREMENT:	0.012	0.009	0.000	72.758	0.164	0.000	0.000	0.035	-0.009	5.585	0.058	0.012
TOTAL AMB:	0.012	0.009	0.000	72.758	0.164	0.000	2.176	84.514	0.031	17.761	0.204	55.618
H												
INCREMENT:	0.020	0.014	0.000	69.078	0.068	0.000	0.000	0.017	-0.014	9.355	0.098	0.006
TOTAL AMB:	0.020	0.014	0.000	69.078	0.068	0.000	2.176	76.511	0.026	21.532	0.243	46.616
H-1S												
INCREMENT:	0.020	0.014	0.000	69.078	0.068	0.000	0.000	0.017	-0.014	9.355	0.098	0.006
TOTAL AMB:	0.020	0.014	0.000	69.078	0.068	0.000	2.176	76.511	0.026	21.532	0.243	46.616
H-2S												
INCREMENT:	0.020	0.014	0.000	69.078	0.068	0.000	0.000	0.017	-0.014	9.355	0.098	0.006
TOTAL AMB:	0.020	0.014	0.000	69.078	0.068	0.000	2.176	76.511	0.026	21.532	0.243	46.616
0												
INCREMENT:	0.020	0.014	0.000	69.078	0.068	0.000	0.000	0.017	-0.014	9.355	0.098	0.006
TOTAL AMB:	0.020	0.014	0.000	69.078	0.068	0.000	2.176	76.511	0.026	21.532	0.243	46.616

CUMULATIVE SURFACE DEPOSITION (MOLE FRACTIONOF INITIAL FLUX

SO2:	0.0000
NOX:	0.0000
PRIMARY PARTICULATE:	0.0000
SO4:	0.0000
NO3:	0.0000

Figure 11. Example PLUVUE II output file (continued).

VISUAL EFFECTS FOR HORIZONTAL SIGHT PATHS
Test Case

DOWNWIND DISTANCE (KM) = 7.0
PLUME ALTITUDE (M) = 2.
PLUME-OBSERVER DISTANCE (KM) = 8.5
AZIMUTH OF LINE-OF-SIGHT = 54.1
ELEVATION ANGLE OF LINE-OF-SIGHT = -0.4
SOLAR ZENITH ANGLE = 61.5 AT 800. ON 4/ 1
SIGHT PATH IS THROUGH PLUME CENTER

THETA	ALPHA	RP/RV0	RV	%REDUCED	YCAP	L	X	Y	DELYCAP	DELL	C(550)	BRATIO	DELX	DELY	E(LUV)	E(LAB)
49.																
	9.	0.05	167.1	1.70	71.32	87.65	0.3332	0.3462	-1.89	-0.90	-0.0248	0.9112	0.0059	0.0060	4.9299	3.2771

0

PLUME VISUAL EFFECTS FOR HORIZONTAL VIEWS
OF THE PLUME OF WHITE, GRAY, AND BLACK OBJECTS
FOR SPECIFIC OBSERVER-PLUME AND OBSERVER-OBJECT DISTANCES

Test Case

DOWNWIND DISTANCE (KM) = 7.0
PLUME-OBSERVER DISTANCE (KM) = 8.5
AZIMUTH OF LINE-OF-SIGHT = 54.1
ELEVATION ANGLE OF LINE-OF-SIGHT = -0.4
SOLAR ZENITH ANGLE = 61.5 AT 800. ON 4/ 1
THETA = 49.

REFLECT	RP/RV0	RO/RV0	YCAP	L	X	Y	DELYCAP	DELL	C(550)	BRATIO	DELX	DELY	E(LUV)	E(LAB)
1.0	0.05	0.29	71.34	87.66	0.3367	0.3472	-1.87	-0.90	-0.0244	0.9164	0.0057	0.0058	4.7217	3.1747
0.3	0.05	0.29	56.15	79.72	0.3178	0.3333	-0.46	-0.26	-0.0069	0.8929	0.0067	0.0071	5.3901	3.4358
0.0	0.05	0.29	49.65	75.87	0.3069	0.3252	0.14	0.09	0.0041	0.8717	0.0075	0.0080	5.8887	3.6924

Figure 11. Example PLUVUE II output file (continued).

CONCENTRATIONS OF AEROSOL AND GASES CONTRIBUTED BY

Test Case

DOWNWIND DISTANCE (KM) = 10.0
PLUME ALTITUDE (M) = 2.
SIGMA Y (M) = 554.
SIGMA Z (M) = 136.
SO2-SO4 CONVERSION RATE= 0.0966 PERCENT/HR
NOX-NO3 CONVERSION RATE= 0.6763 PERCENT/HR

ALTITUDE	NOX (PPM)	NO2 (PPM)	NO3- (PPM)	NO2/NTOT (MOLE %)	NO3-/NTOT (MOLE %)	SO2 (PPM)	SO4= (UG/M3)	SO4=/STOT (MOLE %)	O3 (PPM)	PRIMARY (UG/M3)	BSP-TOTAL (10-4 M-1)	BSPSN/BSP (%)
H+2S												
INCREMENT:	0.002	0.001	0.000	74.635	3.061	0.000	0.000	0.572	-0.001	0.730	0.008	0.203
TOTAL AMB:	0.002	0.001	0.000	74.635	3.061	0.000	2.177	97.675	0.039	12.906	0.153	74.032
H+1S												
INCREMENT:	0.007	0.005	0.000	74.527	0.514	0.000	0.000	0.102	-0.005	3.312	0.035	0.036
TOTAL AMB:	0.007	0.005	0.000	74.527	0.514	0.000	2.176	90.206	0.035	15.488	0.180	62.950
H												
INCREMENT:	0.012	0.009	0.000	72.760	0.245	0.000	0.000	0.052	-0.009	5.530	0.058	0.019
TOTAL AMB:	0.012	0.009	0.000	72.760	0.245	0.000	2.176	84.645	0.031	17.707	0.204	55.775
H-1S												
INCREMENT:	0.012	0.009	0.000	72.760	0.245	0.000	0.000	0.052	-0.009	5.530	0.058	0.019
TOTAL AMB:	0.012	0.009	0.000	72.760	0.245	0.000	2.176	84.645	0.031	17.707	0.204	55.775
H-2S												
INCREMENT:	0.012	0.009	0.000	72.760	0.245	0.000	0.000	0.052	-0.009	5.530	0.058	0.019
TOTAL AMB:	0.012	0.009	0.000	72.760	0.245	0.000	2.176	84.645	0.031	17.707	0.204	55.775
0												
INCREMENT:	0.012	0.009	0.000	72.760	0.245	0.000	0.000	0.052	-0.009	5.530	0.058	0.019
TOTAL AMB:	0.012	0.009	0.000	72.760	0.245	0.000	2.176	84.645	0.031	17.707	0.204	55.775

CUMULATIVE SURFACE DEPOSITION (MOLE FRACTIONOF INITIAL FLUX

SO2:	0.0000
NOX:	0.0000
PRIMARY PARTICULATE:	0.0000
SO4:	0.0000
NO3:	0.0000

Figure 11. Example PLUVUE II output file (continued).

```
                    VISUAL EFFECTS FOR HORIZONTAL SIGHT PATHS
                    Test Case

 DOWNWIND DISTANCE (KM) =   10.0
 PLUME ALTITUDE (M)     =     2.
 PLUME-OBSERVER DISTANCE (KM) =   11.4
 AZIMUTH OF LINE-OF-SIGHT =   51.8
 ELEVATION ANGLE OF LINE-OF-SIGHT =   -0.3
 SOLAR ZENITH ANGLE =   61.5   AT  800. ON  4/ 1
 SIGHT PATH IS THROUGH PLUME CENTER

 THETA ALPHA  RP/RV0    RV  %REDUCED    YCAP       L       X       Y DELYCAP    DELL  C(550)  BRATIO    DELX    DELY  E(LUV)  E(LAB)

   51.
         7.    0.07   166.8    1.90   68.44   86.24  0.3321  0.3452   -1.90   -0.94 -0.0263  0.9163  0.0059  0.0058  4.8116  3.1852
0
         PLUME VISUAL EFFECTS FOR HORIZONTAL VIEWS
         OF THE PLUME OF WHITE, GRAY, AND BLACK OBJECTS
         FOR SPECIFIC OBSERVER-PLUME AND OBSERVER-OBJECT DISTANCES

         Test Case


 DOWNWIND DISTANCE (KM) =   10.0
 PLUME-OBSERVER DISTANCE (KM) =   11.4
 AZIMUTH OF LINE-OF-SIGHT =   51.8
 ELEVATION ANGLE OF LINE-OF-SIGHT =   -0.3
 SOLAR ZENITH ANGLE =   61.5   AT  800. ON  4/ 1
 THETA =   51.

 REFLECT  RP/RV0  RO/RV0    YCAP       L       X       Y DELYCAP    DELL  C(550)  BRATIO    DELX    DELY  E(LUV)  E(LAB)

     1.0    0.07    0.29   69.29   86.66  0.3367  0.3468   -1.97   -0.96 -0.0267  0.9234  0.0056  0.0055  4.5419  3.0571
     0.3    0.07    0.29   54.24   78.62  0.3171  0.3323   -0.43   -0.25 -0.0067  0.8981  0.0066  0.0068  5.2072  3.3035
     0.0    0.07    0.29   47.79   74.72  0.3058  0.3239    0.23    0.15  0.0059  0.8745  0.0075  0.0078  5.7388  3.5839
```


Figure 11. Example PLUVUE II output file (continued).

CONCENTRATIONS OF AEROSOL AND GASES CONTRIBUTED BY

Test Case

DOWNWIND DISTANCE (KM) = 15.0
PLUME ALTITUDE (M) = 2.
SIGMA Y (M) = 789.
SIGMA Z (M) = 170.
SO2-SO4 CONVERSION RATE= 0.1868 PERCENT/HR
NOX-NO3 CONVERSION RATE= 1.3077 PERCENT/HR

ALTITUDE	NOX (PPM)	NO2 (PPM)	NO3- (PPM)	NO2/NTOT (MOLE %)	NO3-/NTOT (MOLE %)	SO2 (PPM)	SO4= (UG/M3)	SO4=/STOT (MOLE %)	O3 (PPM)	PRIMARY (UG/M3)	BSP-TOTAL (10-4 M-1)	BSPSN/BSP (%)
H+2S												
INCREMENT:	0.001	0.001	0.000	72.217	6.498	0.000	0.000	1.208	-0.001	0.410	0.004	0.429
TOTAL AMB:	0.001	0.001	0.000	72.217	6.498	0.000	2.177	98.690	0.039	12.586	0.150	75.684
H+1S												
INCREMENT:	0.004	0.003	0.000	74.943	1.550	0.000	0.000	0.296	-0.003	1.854	0.019	0.105
TOTAL AMB:	0.004	0.003	0.000	74.943	1.550	0.000	2.177	94.281	0.037	14.030	0.165	68.762
H												
INCREMENT:	0.007	0.005	0.000	74.499	0.814	0.000	0.000	0.161	-0.005	3.088	0.032	0.057
TOTAL AMB:	0.007	0.005	0.000	74.499	0.814	0.000	2.177	90.811	0.035	15.264	0.178	63.777
H-1S												
INCREMENT:	0.007	0.005	0.000	74.499	0.814	0.000	0.000	0.161	-0.005	3.088	0.032	0.057
TOTAL AMB:	0.007	0.005	0.000	74.499	0.814	0.000	2.177	90.811	0.035	15.264	0.178	63.777
H-2S												
INCREMENT:	0.007	0.005	0.000	74.499	0.814	0.000	0.000	0.161	-0.005	3.088	0.032	0.057
TOTAL AMB:	0.007	0.005	0.000	74.499	0.814	0.000	2.177	90.811	0.035	15.264	0.178	63.777
0												
INCREMENT:	0.007	0.005	0.000	74.499	0.814	0.000	0.000	0.161	-0.005	3.088	0.032	0.057
TOTAL AMB:	0.007	0.005	0.000	74.499	0.814	0.000	2.177	90.811	0.035	15.264	0.178	63.777

CUMULATIVE SURFACE DEPOSITION (MOLE FRACTIONOF INITIAL FLUX

SO2:	0.0000
NOX:	0.0000
PRIMARY PARTICULATE:	0.0000
SO4:	0.0000
NO3:	0.0000

Figure 11. Example PLUVUE II output file (continued).

VISUAL EFFECTS FOR HORIZONTAL SIGHT PATHS
Test Case

DOWNWIND DISTANCE (KM) = 15.0
PLUME ALTITUDE (M) = 2.
PLUME-OBSERVER DISTANCE (KM) = 16.4
AZIMUTH OF LINE-OF-SIGHT = 49.7
ELEVATION ANGLE OF LINE-OF-SIGHT = -0.2
SOLAR ZENITH ANGLE = 61.5 AT 800. ON 4/ 1
SIGHT PATH IS THROUGH PLUME CENTER

THETA	ALPHA	RP/RVO	RV	%REDUCED	YCAP	L	X	Y	DELYCAP	DELL	C(550)	BRATIO	DELX	DELY	E(LUV)	E(LAB)
52.																
	5.	0.10	166.4	2.11	66.41	85.22	0.3306	0.3432	-1.72	-0.86	-0.0248	0.9366	0.0049	0.0045	3.9218	2.5805

PLUME VISUAL EFFECTS FOR HORIZONTAL VIEWS
OF THE PLUME OF WHITE, GRAY, AND BLACK OBJECTS
FOR SPECIFIC OBSERVER-PLUME AND OBSERVER-OBJECT DISTANCES

Test Case

DOWNWIND DISTANCE (KM) = 15.0
PLUME-OBSERVER DISTANCE (KM) = 16.4
AZIMUTH OF LINE-OF-SIGHT = 49.7
ELEVATION ANGLE OF LINE-OF-SIGHT = -0.2
SOLAR ZENITH ANGLE = 61.5 AT 800. ON 4/ 1
THETA = 52.

REFLECT	RP/RVO	RO/RVO	YCAP	L	X	Y	DELYCAP	DELL	C(550)	BRATIO	DELX	DELY	E(LUV)	E(LAB)
1.0	0.10	0.29	67.90	85.97	0.3359	0.3454	-1.86	-0.92	-0.0260	0.0045	0.0045	0.0042	3.6034	2.4296
0.3	0.10	0.29	52.95	77.87	0.3158	0.3305	-0.21	-0.13	-0.0034	0.9190	0.0055	0.0054	4.2062	2.6373
0.0	0.10	0.29	46.55	73.92	0.3041	0.3217	0.49	0.32	0.0110	0.8930	0.0064	0.0064	4.7546	3.9513

HISTORY OF PLUME PARCEL AT DOWNWIND DISTANCE = 1.0 KM

PARCEL AGE (HR)	LOCAL TIME	SO2-TO-SO4= CONVERSION RATE (%/HR)						NOX-TO-HNO3 CONVERSION RATE (%/HR)					
		H+2S	H+1S	H	H-1S	H-2S	0	H+2S	H+1S	H	H-1S	H-2S	0
0.1	700	0.00	0.00	0.00	0.00	0.00	0.00	0.00	0.00	0.00	0.00	0.00	0.00

HISTORY OF PLUME PARCEL AT DOWNWIND DISTANCE = 3.0 KM

PARCEL AGE (HR)	LOCAL TIME	SO2-TO-SO4= CONVERSION RATE (%/HR)						NOX-TO-HNO3 CONVERSION RATE (%/HR)					
		H+2S	H+1S	H	H-1S	H-2S	0	H+2S	H+1S	H	H-1S	H-2S	0
0.1	643	0.00	0.00	0.00	0.00	0.00	0.00	0.00	0.00	0.00	0.00	0.00	0.00
0.4	700	0.03	0.00	0.00	0.00	0.00	0.00	0.23	0.03	0.01	0.01	0.01	0.01

Figure 11. Example PLUVUE II output file (continued).

HISTORY OF PLUME PARCEL AT DOWNWIND DISTANCE = 5.0 KM

PARCEL AGE (HR)	LOCAL TIME	SO2-TO-SO4= CONVERSION RATE (%/HR)						NOX-TO-HNO3 CONVERSION RATE (%/HR)					
		H+2S	H+1S	H	H-1S	H-2S	0	H+2S	H+1S	H	H-1S	H-2S	0
0.1	626	0.00	0.00	0.00	0.00	0.00	0.00	0.00	0.00	0.00	0.00	0.00	0.00
0.4	643	0.02	0.00	0.00	0.00	0.00	0.00	0.17	0.02	0.01	0.01	0.01	0.01
0.7	700	0.26	0.03	0.02	0.02	0.02	0.02	1.82	0.24	0.11	0.11	0.11	0.11

HISTORY OF PLUME PARCEL AT DOWNWIND DISTANCE = 7.0 KM

PARCEL AGE (HR)	LOCAL TIME	SO2-TO-SO4= CONVERSION RATE (%/HR)						NOX-TO-HNO3 CONVERSION RATE (%/HR)					
		H+2S	H+1S	H	H-1S	H-2S	0	H+2S	H+1S	H	H-1S	H-2S	0
0.1	610	0.00	0.00	0.00	0.00	0.00	0.00	0.00	0.00	0.00	0.00	0.00	0.00
0.4	626	0.02	0.00	0.00	0.00	0.00	0.00	0.11	0.01	0.01	0.01	0.01	0.01
0.7	643	0.20	0.03	0.01	0.01	0.01	0.01	1.39	0.18	0.08	0.08	0.08	0.08
1.0	700	0.58	0.10	0.05	0.05	0.05	0.05	4.09	0.70	0.34	0.34	0.34	0.34

HISTORY OF PLUME PARCEL AT DOWNWIND DISTANCE = 10.0 KM

PARCEL AGE (HR)	LOCAL TIME	SO2-TO-SO4= CONVERSION RATE (%/HR)						NOX-TO-HNO3 CONVERSION RATE (%/HR)					
		H+2S	H+1S	H	H-1S	H-2S	0	H+2S	H+1S	H	H-1S	H-2S	0
0.1	545	0.00	0.00	0.00	0.00	0.00	0.00	0.00	0.00	0.00	0.00	0.00	0.00
0.4	602	0.01	0.00	0.00	0.00	0.00	0.00	0.07	0.01	0.00	0.00	0.00	0.00
0.7	618	0.14	0.02	0.01	0.01	0.01	0.01	0.99	0.12	0.05	0.05	0.05	0.05
1.0	635	0.45	0.08	0.04	0.04	0.04	0.04	3.13	0.53	0.25	0.25	0.25	0.25
1.4	700	0.98	0.18	0.10	0.10	0.10	0.10	6.88	1.29	0.68	0.68	0.68	0.68

HISTORY OF PLUME PARCEL AT DOWNWIND DISTANCE = 15.0 KM

PARCEL AGE (HR)	LOCAL TIME	SO2-TO-SO4= CONVERSION RATE (%/HR)						NOX-TO-HNO3 CONVERSION RATE (%/HR)					
		H+2S	H+1S	H	H-1S	H-2S	0	H+2S	H+1S	H	H-1S	H-2S	0
0.1	504	0.00	0.00	0.00	0.00	0.00	0.00	0.00	0.00	0.00	0.00	0.00	0.00
0.4	520	0.00	0.00	0.00	0.00	0.00	0.00	0.03	0.00	0.00	0.00	0.00	0.00
0.7	537	0.06	0.01	0.00	0.00	0.00	0.00	0.42	0.05	0.02	0.02	0.02	0.02
1.0	553	0.26	0.04	0.02	0.02	0.02	0.02	1.80	0.29	0.14	0.14	0.14	0.14
1.4	618	0.64	0.12	0.06	0.06	0.06	0.06	4.51	0.84	0.43	0.43	0.43	0.43
2.1	700	1.24	0.34	0.19	0.19	0.19	0.19	8.67	2.36	1.31	1.31	1.31	1.31

Figure 11. Example PLUVUE II output file (continued).

PLOT FILE VERIFICATION
OBSERVER-BASED DATA

SKY BACKGROUND						
NX	1	2	3	4	5	6
DISTANCE (KM)	1.	3.	5.	7.	10.	15.
REDUCTION OF VISUAL RANGE (%)	1.793	1.476	1.567	1.698	1.895	2.111
BLUE-RED RATIO	0.960	0.923	0.912	0.911	0.916	0.937
PLUME CONTRAST AT 0.55 MICRONS	-0.005	-0.018	-0.023	-0.025	-0.026	-0.025
PLUME PERCEPTIBILITY DELTA E(L*A*B*)	1.362	2.754	3.197	3.277	3.185	2.581
WHITE BACKGROUND						
NX	1	2	3	4	5	6
DISTANCE (KM)	1.	3.	5.	7.	10.	15.
REDUCTION OF VISUAL RANGE (%)	0.000	0.000	0.000	0.000	0.000	0.000
BLUE-RED RATIO	0.954	0.924	0.915	0.916	0.923	0.946
PLUME CONTRAST AT 0.55 MICRONS	0.002	-0.015	-0.021	-0.024	-0.027	-0.026
PLUME PERCEPTIBILITY DELTA E(L*A*B*)	1.543	2.732	3.125	3.175	3.057	2.430
GRAY BACKGROUND						
NX	1	2	3	4	5	6
DISTANCE (KM)	1.	3.	5.	7.	10.	15.
REDUCTION OF VISUAL RANGE (%)	0.000	0.000	0.000	0.000	0.000	0.000
BLUE-RED RATIO	0.927	0.902	0.893	0.893	0.898	0.919
PLUME CONTRAST AT 0.55 MICRONS	0.017	-0.001	-0.006	-0.007	-0.007	-0.003
PLUME PERCEPTIBILITY DELTA E(L*A*B*)	2.155	3.060	3.403	3.436	3.303	2.637
BLACK BACKGROUND						
NX	1	2	3	4	5	6
DISTANCE (KM)	1.	3.	5.	7.	10.	15.
REDUCTION OF VISUAL RANGE (%)	0.000	0.000	0.000	0.000	0.000	0.000
BLUE-RED RATIO	0.907	0.884	0.873	0.872	0.875	0.893
PLUME CONTRAST AT 0.55 MICRONS	0.026	0.008	0.004	0.004	0.006	0.011
PLUME PERCEPTIBILITY DELTA E(L*A*B*)	2.533	3.311	3.648	3.692	3.584	2.951

Figure 11. Example PLUVUE II output file (continued).

After the PLUVUE II runs were completed, a check was made to determine whether elevated terrain existed between the observer and the location of the plume. If the plume would not have been visible due to intervening terrain, visual effects were set to zero. Tables 5 and 6 summarize the maximum ΔE values for each of the PLUVUE II runs for Observers #1, #2, and #3. In Table 5, the first series of runs, shown by the matrix of calculations running across the top of the table, was done to determine the sensitivity of visual effects to sun angle (i.e., time of day and season). This sensitivity analysis indicated that visual impacts are not strong functions of sun angle; however, slightly higher magnitudes of effects were noted for the winter morning sun angle. Therefore, subsequent runs were performed for this time of day/year. The next set of runs were performed to test the sensitivity to atmospheric stability and wind speed. Because of the distributed nature of the area sources in this example, plume visual effects were relatively insensitive to stability. This is because the plume ΔE values occurred generally at the closest downwind distance where plume dimensions were defined by the initial dilution of the area source. However, visual effects were found to be sensitive to wind speed, with ΔE decreasing with increasing wind speed. The final set of calculations sampled the visual effects associated with various wind directions, wind speeds, and emissions corresponding to the three phases of operation: exploratory shaft facility construction (ESF), repository construction (RC), and repository operation (RO).

Table 6 shows the results of PLUVUE II runs performed to characterize the visual effects observed from the vantage points of Observers #2 and #3. For this example, calculations were performed for neutral (Stability Class D) conditions only because it is believed that elevated terrain would block the transport of stable plumes within view of these observers and, if stable flow did occur, mechanically induced turbulence caused by the flow over the rugged, elevated terrain would produce the equivalent of D stability conditions. Calculations were also performed for the winter morning (0800) sun angle, for a range of wind speeds and directions, and for each of the three phases of construction and operation.

Table 7 displays in descending order the calculated maximum plume ΔE values for each observer position and each phase of repository construction and operation. Generally, the maximum visual impact occurs when the winds are most light and the plume is carried to the observer.

The magnitudes of the plume visual impact, as characterized by the plume ΔE, were combined with meteorological data to estimate the frequency of occurrence of worst-case impacts for each of the three observers. This compilation is summarized in Table 8. For each of the three observers, the maximum and average (across all azimuths of view) plume visual impacts are summarized for five meteorological conditions and for each of the three phases. The five meteorological conditions for each observer were selected from the larger sample of meteorological conditions, as discussed in the meteorology discussion in Section 3.3.3, to provide a range of ΔE values and cumulative frequencies. All combinations of wind speed and wind direction that yielded ΔE values greater than the indicated values were summed to assign a cumulative frequency for each meteorological condition. The cumulative

TABLE 5

SUMMARY OF MAXIMUM CALCULATED ΔE VALUES ASSOCIATED WITH THE ESF FOR EACH OF THE PLUVUE II MODEL RUNS FOR OBSERVER #1

Stability	Wind Speed (m/s)	Wind Dir.	Winter 8 AM	Winter Noon	Winter 4 PM	Spring 8 AM	Spring Noon	Spring 4 PM	Summer 8 AM	Summer Noon	Summer 4 PM
D	2.0	E	1.2	0.9	1.2	1.1	0.9	1.0		0.9	0.9
D	2.0	WSW	3.1	2.3	3.0	2.7	2.2	2.5		2.1	2.3
D	2.0	W	3.2	2.3	3.0		2.2	2.5		2.1	2.3
D	2.0	ENE	1.3	0.9	1.2		0.9	1.0			0.9
D	2.0	WNW	1.1	0.8	1.0		0.8	0.9		0.7	0.8
D	1.0	W	5.0								
D	3.0	W	2.4								
D	5.0	W	1.6								
E	1.0	W	4.9								
E	2.0	W	3.0								
E	3.0	W	2.3								
E	5.0	W	1.6								
F	2.0	W	4.0								
F	3.0	W	3.0								
F	5.0	W	2.1								
D	1.0	ENE	2.1								
D	3.0	ENE	1.0								
D	5.0	ENE	0.7								
E	1.0	ENE	1.9								
E	2.0	ENE	1.2								
E	3.0	ENE	0.9								
E	5.0	ENE	0.7								
F	2.0	ENE	1.4								
F	3.0	ENE	1.1								
F	5.0	ENE	0.8								

TABLE 6

SUMMARY OF MAXIMUM CALCULATED ΔE VALUES FOR EACH OF THE PLUVUE II RUNS FOR OBSERVERS #2 AND #3

Stability	Wind Speed (m/s)	Wind Direction	Observer #2 ESF	RC	RO	Observer #3 ESF	RC	RO
D	2.0	NNW	0.5	1.0		0.5		
D	2.0	N	0.4			0.4		
D	2.0	NNE	0.4			0.4		0.2
D	2.0	NE	0.5			0.4		
D	2.0	ENE	1.0	2.1	0.5	0.4		
D	2.0	E				0.7		0.4
D	2.0	ESE	0.4			4.4	6.6	2.7
D	2.0	SE	0.2	0.9	0.2	0.5		
D	2.0	SSE	0.2			0.3		
D	2.0	S	0.2			0.2		
D	1.0	NNW	0.7	1.6	0.4			
D	1.0	NNE	5.4				1.2	
D	1.0	SE	3.2	17.1	17.3			
D	1.0	NNE				0.6		0.3
D	1.0	E				3.3	18.0	18.2
D	1.0	ESE				10.0	27.3	28.5
D	3.0	NNW	0.3	1.1	0.7			
D	3.0	ENE	0.7	1.7	0.5			
D	3.0	SE	0.2	7.9	0.4			
D	3.0	NNE				0.3	0.6	0.2
D	3.0	E				0.5	1.0	0.4
D	3.0	ESE				3.3	5.3	2.1
D	5.0	NNW	0.2	0.6	0.4			
D	5.0	ENE	0.5	2.0	1.6			
D	5.0	SE	0.1	1.2	1.0			
D	5.0	NNE				0.2	0.4	0.1
D	5.0	E				0.4	1.2	1.0
D	5.0	ESE				2.3	3.9	3.0
D	1.0	ENE		24.8	25.2			

TABLE 7

MAXIMUM PLUME ΔE VALUES FOR EACH OBSERVER LOCATION AND PHASE OF REPOSITORY CONSTRUCTION AND OPERATION

OBSERVER #1:

SC	WS	WD	ESF	SC	WS	WD	RC	SC	WS	WD	RO
D	1	W	5.0	D	1	W	8.4	D	1	WSW	2.0
E	1	W	4.9	D	1	WSW	8.2	D	1	W	2.0
F	2	W	4.0	D	2	W	5.9	D	2	WSW	1.3
D	2	W	3.2	D	2	WSW	5.7	D	2	W	1.3
D	2	WSW	3.1	D	3	W	4.6	D	3	W	1.0
F	3	W	3.0	D	3	WSW	4.5	D	3	WSW	1.0
E	2	W	3.0	D	1	WSW	3.9	D	1	WNW	0.9
D	3	W	2.4	D	1	ENE	3.8	D	1	E	0.8
E	3	W	2.3	D	1	E	3.6	D	1	ENE	0.8
F	5	W	2.1	D	5	W	3.3	D	5	WSW	0.7
D	1	ENE	2.1	D	5	WSW	3.3	D	5	W	0.7
E	1	ENE	1.9	D	2	WNW	2.6	D	2	WNW	0.6
E	5	W	1.6	D	2	ENE	2.5	D	2	E	0.5
D	5	W	1.6	D	2	E	2.4	D	2	ENE	0.5
F	2	ENE	1.4	D	3	ENE	2.0	D	3	WNW	0.4
D	2	ENE	1.3	D	3	WNW	2.0	D	3	E	0.4
D	2	E	1.2	D	3	E	1.9	D	3	ENE	0.4
E	2	ENE	1.2	D	5	ENE	1.4	D	5	ENE	0.3
F	3	ENE	1.1	D	5	WNW	1.4	D	5	E	0.3
D	2	WNW	1.1	D	5	E	1.3	D	5	WNW	0.3
D	3	ENE	1.0								
E	3	ENE	0.9								
F	5	ENE	0.8								
D	5	ENE	0.7								
E	5	ENE	0.7								

Note:

SC = Stability Class
WS = Wind Speed (m/s)
WD = Wind Direction
ESF = Exploratory Shaft Facility Construction
RC = Repository Construction
RO = Repository Operation

TABLE 7 (CONTINUED)

MAXIMUM PLUME ΔE VALUES FOR EACH OBSERVER LOCATION AND PHASE OF REPOSITORY CONSTRUCTION AND OPERATION

OBSERVER #2:

SC	WS	WD	ESF	SC	WS	WD	RC	SC	WS	WD	RO
D	1	NNE	5.4	D	1	ENE	25.2	D	1	ENE	24.8
D	1	SE	3.2	D	1	SE	17.3	D	1	SE	17.1
D	2	ENE	1.0	D	5	ENE	1.5	D	3	SE	7.9
D	1	NNW	0.7	D	5	SE	1.0	D	2	ENE	2.1
D	3	ENE	0.7	D	3	NNW	0.7	D	5	ENE	2.0
D	2	NE	0.5	D	2	ENE	0.5	D	3	ENE	1.7
D	5	ENE	0.5	D	3	ENE	0.5	D	1	NNW	1.6
D	2	NNW	0.5	D	3	SE	0.4	D	5	SE	1.2
D	2	ESE	0.4	D	1	NNW	0.4	D	3	NNW	1.1
D	2	N	0.4	D	5	NNW	0.4	D	2	NNW	1.0
D	2	NNE	0.4	D	2	SE	0.2	D	2	SE	0.9
D	3	NNW	0.3					D	5	NNW	0.6
D	2	S	0.2								
D	3	SE	0.2								
D	5	NNW	0.2								
D	2	SSE	0.2								
D	2	SE	0.2								
D	5	SE	0.1								

OBSERVER #3:

SC	WS	WD	ESF	SC	WS	WD	RC	SC	WS	WD	RO
D	1	ESE	10.0	D	1	ESE	27.3	D	1	ESE	28.5
D	2	ESE	4.4	D	1	E	18.0	D	1	E	18.2
D	3	ESE	3.3	D	2	ESE	6.6	D	5	ESE	3.0
D	1	E	3.3	D	3	ESE	5.3	D	2	ESE	2.7
D	5	ESE	2.3	D	5	ESE	3.9	D	3	ESE	2.1
D	2	E	0.7	D	5	E	1.2	D	5	E	1.0
D	1	NNE	0.6	D	1	NNE	1.2	D	3	E	0.4
D	2	SE	0.5	D	3	E	1.0	D	2	E	0.4
D	2	NNW	0.5	D	3	NNE	0.6	D	1	NNE	0.3
D	3	E	0.5	D	5	NNE	0.4	D	3	NNE	0.2
D	5	E	0.4					D	2	NNE	0.2
D	2	NE	0.4					D	5	NNE	0.1
D	2	NNE	0.4								
D	2	ENE	0.4								
D	2	N	0.4								
D	3	NNE	0.3								
D	2	SSE	0.3								
D	5	NNE	0.2								
D	2	S	0.2								

TABLE 8

CUMULATIVE FREQUENCY OF WORST-CASE MORNING ΔE VALUES
FOR OBSERVERS #1, #2, AND #3 IN THE NATIONAL PARK

Wind Speed (m/s)	Wind Direction	ESF Max.	ESF Avg.	RC Max.	RC Avg.	RO Max.	RO Avg.	Cumulative Frequency (%) Ann.	Win.	Spr.	Sum.	Fall
OBSERVER #1:												
1	WSW,W,NNW	5.0	4.8	8.2	8.0	2.0	1.9	9.8	17.6	3.4	3.7	13.6
1	NE...SE	4.9	4.7	3.6	3.6	0.8	0.8	31.4	49.6	12.9	15.4	45.9
2	NE...SE	3.0	2.8	2.4	2.4	0.5	0.5	65.0	80.3	42.5	59.8	77.4
3	NE...SE	1.0	0.9	1.9	1.9	0.4	0.4	77.8	84.0	60.3	80.8	87.0
5	NE...SE	0.7	0.6	1.3	1.3	0.3	0.3	86.1	86.9	74.3	93.0	91.4
OBSERVER #2:												
1	ENE,E,ESE	5.4	1.5	24.8	5.4	25.2	4.5	1.0	0.8	0.0	1.4	1.9
1	NE...SE	3.2	0.9	17.1	4.2	17.3	3.6	2.2	2.4	0.4	2.3	2.9
2	NNE...SSE	1.0	0.2	7.9	1.9	1.6	0.4	14.2	11.1	9.8	23.8	5.8
3	NNE...SSE	0.7	0.2	2.2	1.2	1.0	0.3	17.4	15.1	14.3	29.9	16.3
5	NNE...SSE	0.5	0.1	1.2	0.5	0.4	0.2	19.0	15.5	16.3	34.1	16.3
OBSERVER #3:												
1	SE,ESE,SSE	10.0	3.9	27.3	8.1	28.5	6.1	2.3	2.5	1.1	2.3	3.3
1	NE...SSE	4.4	1.5	18.0	4.0	18.2	3.3	3.2	2.6	1.1	4.7	4.1
2	NNE...S	3.3	1.0	6.6	3.0	2.7	1.0	18.3	12.8	12.4	29.0	20.3
3	NNE...S	0.5	0.2	0.6	0.5	0.2	0.2	22.2	14.0	17.3	36.9	22.2
5	NNE...S	0.2	0.2	0.4	0.4	0.1	0.1	24.0	15.2	19.2	41.1	22.5

frequencies were determined separately for each season as well as for the annual period. The cumulative frequency values shown in Table 8 are percentages of morning hours (0800-1100) which were found to be worst-case for this example.

For Observer #1 the maximum and azimuth-average plume visual impacts are essentially the same, because this observer's line of sight is limited to just the first few downwind distances modeled. Maximum plume ΔE values of about 8 occur nearly 10 percent of the morning hours from this vantage point during repository construction. During ESF construction and repository operation, impacts are much lower -- about 5 and 2, respectively. Nearly a third of the morning ΔE values of approximately 4 are calculated to occur from the Observer #1 vantage point during the construction of the ESF and the repository. During the repository operation, the plume ΔE values would be greater than 1 less than a third of the morning hours. If we use the range of ΔE between 1 and 4 as the approximate threshold of plume perceptibility, these results suggest that the plume would be visible from the vantage point of Observer #1 between a third and two-thirds of the mornings in the year. However, these impacts may not be perceptible this often if the viewing background is dark and/or nonuniform. Essentially all of these observations of plume impact would be of emissions located outside the park boundary while observed within the park boundary. Impacts vary with season with most frequent impacts occurring during the winter and least frequent impacts during the more windy spring and summer seasons. Impacts are much less frequent in the afternoon hours than in the morning for Observer #1. Values of ΔE greater than 8 occur only one percent of the afternoon hours (as opposed to 10 percent of the morning hours). Values of ΔE greater than 4 occur 8 percent of the afternoons as opposed to a third of the mornings.

For Observer #2, predicted frequencies of visible impacts are lower than for Observer #1, which is not surprising considering that this vantage point does not have a direct view of and is farther away from the canyon site. Somewhat more surprising, however, is the fact that for certain azimuths of view, maximum plume visual impacts are larger than maximum impacts for Observer #1. This results from the fact that this vantage point offers relatively unobstructed lines of sight along which the plume from the repository site can be seen. The maximum plume impacts occur when the wind carries the plume relatively close to the observer and when the observer is looking obliquely through the plume centerline. Unlike the case for Observer #1, the average plume impact, averaged over all azimuths of view for which the plume is unobstructed by intervening terrain, is considerably lower than the plume impact for the worst-case azimuth of view. Azimuth-averaged plume ΔE values are roughly a factor of five lower than the azimuth-maximum values. These calculations suggest that during repository construction and operation, about one percent of the mornings in a year may have maximum plume ΔE values as large or larger than 25, indicating a very dark, perceptible plume. These maximum impacts would be about five times larger than the average over all visible directions of view, which is a ΔE of about 5, still above the perceptibility threshold range of 1 to 4. Impacts during ESF construction are projected to be considerably lower. For about two percent of the morning hours, impacts would be greater than or equal to 17 (azimuth-maximum) and 4 (azimuth-average). During repository construction, maximum plume visual impacts would be greater than the just perceptible threshold range of 1 to 4

between 15 and 20 percent of the morning hours in the year. For this observation point, summer impacts would be almost twice as frequent as annual-average impacts due to the increased probability of transport winds of the right magnitude and direction.

Impacts for Observer #3 are somewhat similar to those for Observer #2, both in magnitude and frequency. Maximum impacts -- plume ΔE values of about 28 -- are calculated to occur about two percent of the mornings, while impacts above the perceptibility threshold are calculated to occur about 20 percent of the mornings. Again, impacts from the vantage point of Observer #3 are much more frequent in summer than in any other season. For example, above-threshold impacts occur nearly 30 percent of the summer mornings.

4.0 REFERENCES

Altshuller, A.P., 1979: Model Predictions of the Rates of Homogeneous Oxidation of Sulfur Dioxide to Sulfate in the Troposphere. *Atmos. Environ.*, 13:1653-1661.

Baulch, D.L., D.D. Drysdale, and D.G. Horne, 1973: *Evaluated Kinetic Data for High Temperature Reactions, Volume 2 -- Homogeneous Gas Phase Reactions of the H_2-N_2-O_2 System.* CRC Press, Cleveland, OH.

Briggs, G.A., 1969: *Plume Rise.* U.S. Atomic Energy Commission Critical Review Series, TID-25075, NTIS, Springfield, VA.

Briggs, G.A., 1971: Some Recent Analyses of Plume Rise Observations. *Proc. of 2nd Int. Clean Air Congress*, H.M. Englund and W.T. Berry, eds. Academic Press, New York, NY, 1029-1032.

Briggs, G.A., 1972: Discussion of Chimney Plumes in Neutral and Stable Surroundings. *Atmos. Environ.*, 6:507-610.

Calvert, J.G., F. Su, J.W. Bottenheim, and O.P. Strausz, 1978: Mechanism of the Homogeneous Oxidation of Sulfur Dioxide in the Troposphere. *Atmos. Environ.*, 12:197-226.

Chandrasekhar, S., 1960: *Radiative Transfer.* Dover Publications, New York, NY.

Davis, D.D., D.G. Smith, and J. Klauber, 1974: Trace Gas Analysis of Power Plant Plumes Via Aircraft Measurements: O_3, NO_x, and SO_2 Chemistry. *Science*, 186:733-736.

Ensor, D.S., L.E. Sparks, and M.J. Pilat, 1973: Light Transmittance across Smoke Plumes Downwind from Point Sources of Aerosol Emissions. *Atmos. Environ.*, 7:1267-1277.

EPA, 1977: User's Manual for a Single-Source (CRSTER) Model. EPA-450/2-77-013. U.S. Environmental Protection Agency, Research Triangle Park, NC.

EPA, 1984a: User's Manual for the Plume Visibility Model (PLUVUE). EPA-450/4-80-032. NTIS PB84-158302. U.S. Environmental Protection Agency, Research Triangle Park, NC.

EPA, 1984b: Addenda to the User's Manual for the Plume Visibility Model (PLUVUE II). EPA-600/8-84-005. NTIS PB84-158302. U.S. Environmental Protection Agency, Research Triangle Park, NC.

EPA, 1992: Workbook for Plume Visual Impact Screening and Analysis (Revised). EPA-454/R-92-023. U.S. Environmental Protection Agency, Research Triangle Park, NC.

Hampson, R.F. Jr. and D. Garvin, 1978: Reaction Rate and Photochemical Data for Atmospheric Chemistry-1977. NBS Special Pub. 513, National Bureau of Standards, Washington, D.C.

Hanson, J.E. and L.D. Travis, 1974: Light Scattering in Planetary Atmospheres. *Space Science Reviews*, 16:527-610.

Irvine, W.M., 1975: Multiple Scattering in Planetary Atmospheres *Icarus*, 25:175-204.

Isaacs, R.G., 1981: The Role of Radiative Transfer Theory in Visibility Modeling: Efficient Approximate Techniques. *Atmos. Environ.*, 15:1827-1833.

Isaksen, I., A., Hesstredt, and O. Hov, 1978: A Chemical Model for Urban Plumes: Test for Ozone and Particulate Sulfur Formation in St. Louis Urban Plume. *Atmos. Environ.*, 12:599-604.

Kerker, M., 1969: *The Scattering of Light and Other Electromagnetic Radiation.* Academic Press, New York, NY.

Latimer, D.A. and G.S. Samuelsen, 1975: Visual Impact of Plumes from Power Plants. UCI-ARTR-75-3. UCI Air Quality Laboratory, School of Engineering, University of California, Irvine, CA.

Latimer, D.A. and G.S. Samuelsen, 1978: Visual Impact of Plumes from Power Plants. *Atmos. Environ.*, 12:1455-1465.

Latimer, D.A., R.W. Bergstrom, S.R. Hayes, M.K. Liu, J.H. Seinfeld, G.Z. Whitten, M.A. Wojcik, and M.J. Hillyer, 1978: The Development of Mathematical Models for the Prediction of Anthropogenic Visibility Impairment. EPA-450/3-78-110a,b,c. U.S. Environmental Protection Agency, Research Triangle Park, NC.

Leighton, P.A., 1961: *Photochemistry of Air Pollution.* Academic Press, New York, NY.

Miller, D.F., 1978: Precursor Effects on SO_2 Oxidation. *Atmos. Environ.*, 12:273-280.

Niki, H., 1974: Reaction Kinetics Involving O and N Compounds. *Can. J. Chem.*, 52:1397-1404.

Nixon, J.K., 1940: Absorption Coefficient of Nitrogen Dioxide in the Visible Spectrum. *J. Chem. Phys.*, 8:157-160.

Richards, L.W. and R.G.M. Hammarstrand, 1988: User's Manual for Running PLUVUE and Performing Mie Calculations on a Personal Computer. Sonoma Technology Inc., Santa Rosa, CA.

SAI, 1989: Addenda User's Manual for the Plume Visibility Model (PLUVUE II). SYSAPP-89/045. Systems Applications, Inc., San Rafael, CA.

Schere, K.L. and K.L Demerjian, 1977: Calculation of Selected Photolytic Rate Constants over a Diurnal Range. EPA-600/4-77-015. U.S. Environmental Protection Agency, Research Triangle Park, NC.

Seigneur, C., R.W. Bergstrom, C.D. Johnson, and L.W. Richards, 1983: Measurements and Simulations of the Visual Effects of Particulate Plumes. Systems Applications, Inc., San Rafael, CA.

van de Hulst, H.C., 1957: *Light Scattering by Small Particles.* John Wiley & Sons, New York, NY.

Wallace, J.M. and P.V. Hobbs, 1977: *Atmospheric Science.* Academic Press, New York, NY.

White, W.H., 1977: NO_x-O_3 Photochemistry in Power Plant Plumes: Comparison of Theory with Observation. *Environ. Sci. Technol.*, 11:995-1000.

Winkler, P., 1973: The Growth of Atmospheric Aerosol Particles as a Function of the Relative Humidity--II. An Improved Concept of Mixed Nuclei. *Aerosol Sci.*, 4:373-387.

Appendix

Comparison of the Original Version of PLUVUE II with the Revised Version

TABLE A-1

COMPARISON OF THE ORIGINAL VERSION OF PLUVUE II WITH THE REVISED VERSION FOR DIFFERENT STABILITY CLASSES

Visibility Parameter	SC = A		SC = B		SC = C		SC = D		SC = E		SC = F	
	Old	New	Old	New	Old	New	Old	New	Old	New	Old	New
Sky Background:												
Visual Range Reduction	.008	.008	.045	.046	.100	.102	.215	.222	.347	.359	.537	.547
Blue-Red Ratio	1.000	1.000	1.000	1.000	.999	.999	.999	.999	.999	.998	.999	.999
Plume Contrast	.000	.000	-.001	-.001	-.001	-.001	-.003	-.003	-.004	-.005	-.006	-.006
ΔE	.004	.004	.025	.026	.055	.058	.114	.122	.174	.187	.226	.235
White Background:												
Visual Range Reduction	.000	.000	.000	.000	.000	.000	.000	.000	.000	.000	.000	.000
Blue-Red Ratio	1.000	1.000	1.000	1.000	1.000	1.000	1.001	1.001	1.002	1.002	1.005	1.004
Plume Contrast	.000	.000	-.001	-.001	-.002	-.002	-.004	-.004	-.006	-.006	-.009	-.009
ΔE	.004	.004	.027	.028	.060	.063	.127	.134	.197	.209	.280	.287

TABLE A-1 (Continued)

COMPARISON OF THE ORIGINAL VERSION OF PLUVUE II WITH THE REVISED VERSION FOR DIFFERENT STABILITY CLASSES

Visibility Parameter	SC = A		SC = B		SC = C		SC = D		SC = E		SC = F	
	Old	New	Old	New	Old	New	Old	New	Old	New	Old	New
Gray Background:												
Visual Range Reduction	.000	.000	.000	.000	.000	.000	.000	.000	.000	.000	.000	.000
Blue-Red Ratio	1.000	1.000	1.000	1.000	.999	.999	.998	.998	.998	.998	.997	.997
Plume Contrast	.000	.000	.000	.000	.000	.000	-.001	-.001	-.001	-.001	-.001	-.002
ΔE	.002	.002	.014	.015	.032	.034	.067	.072	.102	.110	.130	.136
Black Background:												
Visual Range Reduction	.000	.000	.000	.000	.000	.000	.000	.000	.000	.000	.000	.000
Blue-Red Ratio	1.000	1.000	.999	.999	.997	.997	.994	.994	.991	.990	.985	.985
Plume Contrast	.000	.000	.000	.000	.001	.001	.001	.001	.002	.002	.004	.004
ΔE	.003	.003	.021	.022	.048	.049	.102	.105	.164	.170	.251	.256

TECHNICAL REPORT DATA
(Please read Instructions on the reverse before completing)

1. REPORT NO.	2.	3. RECIPIENT'S ACCESSION NO.
EPA-454/B-92-008		

4. TITLE AND SUBTITLE	5. REPORT DATE
User's Manual for the Plume Visibility Model (PLUVUE II) (Revised)	October 1992
	6. PERFORMING ORGANIZATION CODE
7. AUTHOR(S)	8. PERFORMING ORGANIZATION REPORT NO.
9. PERFORMING ORGANIZATION NAME AND ADDRESS Sigma Research Corporation 196 Baker Avenue Concord, MA 01742	10. PROGRAM ELEMENT NO.
	11. CONTRACT/GRANT NO. EPA Contract No. 68 D90067 Work Assignment 3-3
12. SPONSORING AGENCY NAME AND ADDRESS U.S. Environmental Protection Agency Office of Air Quality Planning and Standards Technical Support Division Research Triangle Park, NC 27711	13. TYPE OF REPORT AND PERIOD COVERED Final Report
	14. SPONSORING AGENCY CODE

15. SUPPLEMENTARY NOTES

EPA Work Assignment Manager: Jawad S. Touma

16. ABSTRACT

This document provides a description for the restructured and revised version of the Plume Visibility Model (PLUVUE II). The model was restructured in order to improve the user interface and computing requirements and revised to remove several errors in the original code. The objective of the PLUVUE II model is to calculate visual range reduction and atmospheric discoloration caused by plumes consisting of primary particles, nitrogen oxides, and sulfur oxides emitted by a single emission source.

17. KEY WORDS AND DOCUMENT ANALYSIS

a. DESCRIPTORS	b. IDENTIFIERS/OPEN ENDED TERMS	c. COSATI Field/Group
Air Pollution Meteorology Air Quality Dispersion Model Visibility Aerosols Nitrogen Dioxide	New Source Review Air Pollution Control	13B

18. DISTRIBUTION STATEMENT	19. SECURITY CLASS *(This Report)*	21. NO. OF PAGES
Release Unlimited	Unclassified	114
	20. SECURITY CLASS *(This page)*	22. PRICE
	Unclassified	

EPA Form 2220-1 (Rev. 4-77) PREVIOUS EDITION IS OBSOLETE